Synthesis and Characterization of Ruthenium(II) Complexes with 2,2':6',2''-Terpyridine and 2-(Phenylazo)pyridine Ligands

Uraiwan Saeteaw

Master of Science Thesis in Inorganic Chemistry

Prince of Songkla University

2000

Thesis Title	Synthesis and Characterization of Ruthenium(II) Complexes with 2,2':6',2"-Terpyridine and 2-(Phenylazo)pyridine Ligands
Author	Miss Uraiwan Saeteaw
Major Program	Inorganic Chemistry

Advisory Committee

Kanidtha Hansongnern .....Chairman

(Dr. Kanidtha Hansongnern)

.....Committee

(Dr. Walailak Puetpaiboon)

Orawan Sirichote .....Committee

(Asst. Prof. Dr. Orawan Sirichote)

Examining Committee

Kanidtha Hansongnern .....Chairman

(Dr. Kanidtha Hansongnern)

.....Committee

(Dr. Walailak Puetpaiboon)

Orawan Sirichote .....Committee

(Asst. Prof. Dr. Orawan Sirichote)

.....Committee

(Asst. Prof. Dr. Damrongsak Faroongsarng)

The Graduate School, Prince of Songkla University, has approved this thesis as partial fulfillment of the requirement for the Master of Science degree in Inorganic Chemistry.

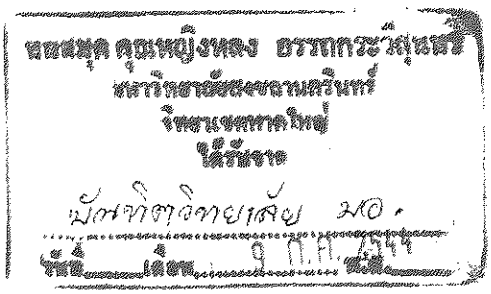

.....

(Assoc. Prof. Dr. Piti Trisdikoon)

Dean, Graduate School

ชื่อวิทยานิพนธ์	การสังเคราะห์และศึกษาคุณสมบัติของสารประกอบเชิงซ้อนของโลหะรูทีเนียม(II) กับลิแกนด์ 2,2':6',2"-Terpyridine และ 2-(Phenylazo)pyridine
ผู้เขียน	นางสาวอุไรวรรณ แซ่เตียว
สาขาวิชา	เคมีอนินทรีย์
ปีการศึกษา	2543

บทคัดย่อ

ทำการสังเคราะห์สารประกอบเชิงซ้อนของ $[Ru(tpy)(azpy)(X)]^+$ (เมื่อ tpy = 2,2':6',2"-Terpyridine azpy = 2-(Phenylazo)pyridine และ X = Cl^-, Br^-, I^-, NO_2^- และ NCS^-) และทำการศึกษาคุณสมบัติพื้นฐานทางเคมีโดยใช้เทคนิคทางสเปกโทรสโกปีและเทคนิคทางเคมีไฟฟ้า นอกจากนี้ยังทำการศึกษาด้วยวิธีการเลี้ยวเบนของรังสีเอกซ์โดยผลึกเดี่ยว จากข้อมูลโครงสร้างทางเอกซเรย์พบว่าสารประกอบเชิงซ้อนดังกล่าวสามารถเกิดได้เป็น 2 ไอโซเมอร์ คือ ไอโซเมอร์ 1 และ 2 ดังรูป

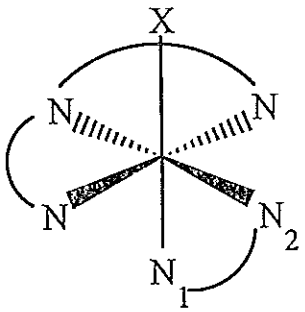

ไอโซเมอร์ 1

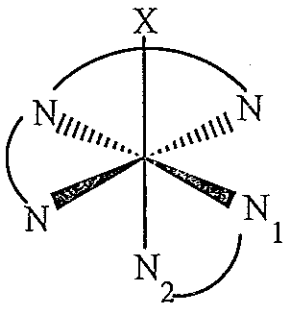

ไอโซเมอร์ 2

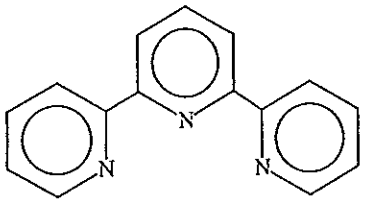

= N N N

2,2':6',2"-Terpyridine

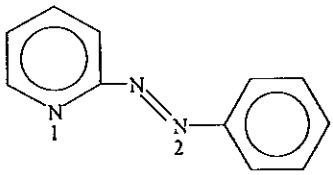

= N_1 N_2

2-(Phenylazo)pyridine

โครงสร้างของสารประกอบเชิงซ้อนที่ได้มี 4 ชนิด คือ [Ru(tpy)(azpy)(Cl)]Cl (1) [Ru(tpy)(azpy)(Cl/I)](BF_4) (2) [Ru(tpy)(azpy)(NO_2)](BF_4) (3) และ [Ru(tpy)(azpy)-(NCS)](BF_4) (4) ซึ่งโครงสร้างที่ (1) เป็นไอโซเมอร์แบบที่ 1 ส่วนโครงสร้างที่ (2)-(4) เป็นไอโซเมอร์แบบที่ 2 การศึกษาคุณสมบัติทางเคมีด้วยวิธีการทางสเปกโทร-สโกปีและเคมีไฟฟ้าจะเป็นการศึกษาเฉพาะไอโซเมอร์แบบที่ 2 เท่านั้น เนื่องจากไอโซเมอร์แบบที่ 2 ให้ผลิตภัณฑ์ที่มากกว่าไอโซเมอร์แบบที่ 1 มาก จากข้อมูลทางเคมีไฟฟ้าของสารประกอบเชิงซ้อนในกลุ่มนี้พบว่าสารประกอบเชิงซ้อนของ [Ru(tpy)-(azpy)(NO_2)](BF_4) ให้ค่าศักย์ไฟฟ้าออกซิเดชันของ รูทีเนียม(II)/รูทีเนียม(III) มีค่าเป็นบวกมากที่สุด(1.103 V) แสดงให้เห็นว่าลิแกนด์ไนโตรมีคุณสมบัติเป็นตัวรับไพอิเลค-ตรอนที่ดี สามารถทำให้โลหะอะตอมกลางคือรูทีเนียม(II) เสถียรที่สุดในสารประกอบเชิงซ้อนกลุ่มนี้ นอกจากนี้พบว่าข้อมูลจากอินฟราเรดสเปกโทรสโกปีช่วยสนับสนุนข้อความข้างต้นกล่าวคือ แถบการสั่นแบบยืดของหมู่ฟังก์ชันเอโซ($\nu_{(N=N)}$)ใช้ในการตรวจวัดความสามารถในการเป็นตัวรับไพอิเลคตรอนของลิแกนด์ X ได้ โดยที่ลิแกนด์ X ที่เป็นตัวรับไพอิเลคตรอนที่ดีจะให้ค่าแถบการสั่นของหมู่ฟังก์ชันเอโซเพิ่มขึ้น ผลจากการทดลองสามารถเรียงลำดับความสามารถในการเป็นตัวรับไพอิเลคตรอนของลิแกนด์ X ในสารประกอบเชิงซ้อนดังกล่าวได้ดังนี้ NO_2^- > NCS^- > halide (Cl^-, Br^-, I^-) ซึ่งสอดคล้องกับข้อมูลในสเปกโทรเคมีกัลซีรี่ส์ (spectrochemical series)

Thesis Title	Synthesis and Characterization of Ruthenium(II) Complexes with 2,2':6',2"-Terpyridine and 2-(Phenylazo)pyridine Ligands
Author	Miss Uraiwan Saeteaw
Major Program	Inorganic Chemistry
Academic Year	2000

Abstract

$[Ru(tpy)(azpy)(X)]^+$ (tpy = 2,2':6',2"-Terpyridine, azpy = 2-(Phenylazo)-pyridine and X = Cl^-, Br^-, I^-, NO_2^- and NCS^-) have been prepared and their properties were investigated by spectroscopic, electrochemical and single crystal X-ray diffraction techniques. Results from X-ray data revealed that the complexes have 2 isomers, the 1 and 2 isomer, as shown below. The crystal structures of 4 complexes, $[Ru(tpy)(azpy)(Cl)]Cl$ (1), $[Ru(tpy)(azpy)(Cl/I)](BF_4)$ (2), $[Ru(tpy)(azpy)(NO_2)](BF_4)$ (3) and $[Ru(tpy)(azpy)(NCS)](BF_4)$ (4) have been studied by X-ray crystallography.

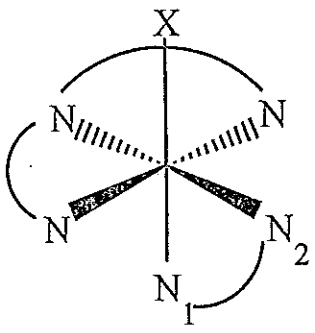

1 isomer

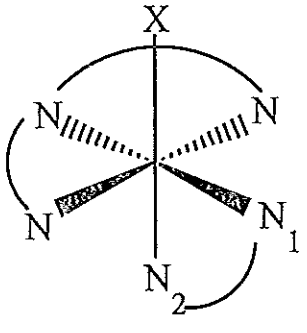

2 isomer

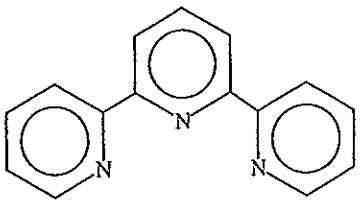

= N N N

2,2':6',2"-Terpyridine

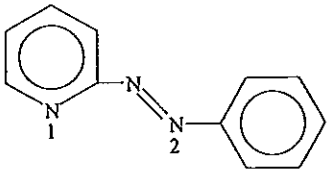

= N_1 N_2

2-(Phenylazo)pyridine

Crystals of (1) are 1 isomer and crystals of (2)-(4) are 2 isomer. The complexes of the 2 isomer are obtained in much greater yield than the 1 isomer, and are described in detail. The spectroscopic and electrochemical data show that the chemistry of $[Ru(tpy)(azpy)(X)]^+$ complexes are varied with the nature of X ligand. It is found that the Ru^{II}/Ru^{III} oxidation potential of $[Ru(tpy)(azpy)(NO_2)]^+$ complex, 1.103 V, is the highest in this series, it indicates that the NO_2^- ligand is better π-acceptor to stabilize Ru(II) center than other X ligand in these complexes. Furthermore, results from infrared spectra confirmed this property, i.e., the azpy azo stretching mode ($\nu_{(N=N)}$) was used to be diagnostic of the X ligand π-accepting behavior, which the strongly π-accepting X ligands increased the azpy N=N(azo) stretching vibration. Ligands may be arranged in order of their π-acceptor ability as; $NO_2^- > NCS^- >$ halide (Cl^-, Br^-, I^-), corresponded to the ligand field strength of ligand (X) in the spectrochemical series.

Acknowledgment

I would like to express my deep sense of gratitude and sincere appreciation to my supervisor, Dr. Kanidtha Hansongnern of the Department of Chemistry, Faculty of Science, Prince of Songkla University, for her suggestions, comments, and also her valuable advice through my master degree study.

I also would like to extend my warm and sincere appreciation to my co-supervisor, Dr. Walailak Puetpaiboon and Asst. Prof. Dr. Orawan Sirichote of the Department of Chemistry, Faculty of Science, Prince of Songkla University, for their helpful suggestions, comments on my thesis and critical review of this manuscript.

Special thanks go to the examing committee : Asst. Prof. Dr. Damrongsak Faroongsarng of the Department of Pharmaceutical Technology, Faculty of Pharmaceutical Sciences, Prince of Songkla University, for his helpful suggestions and efforts to thesis examination.

Special thanks are extended to Asst. Prof. Dr. Chaveng Pakawatchai and Sirintip Tanchatchawal of the Department of Chemistry, Faculty of Science, Prince of Songkla University, for their suggestions and valuable guidance in the part of X-ray crystallography.

I would like to direct my appreciation to Prof. Dr. Alan M. Bond and Dr. Gary Fallon of the Department of Chemistry, Faculty of Science, Monash University, Australia, for electrochemical measurements and X-ray crystallographic data.

I would like to thank Prof. Dr. A. G. Orpen of School of Chemistry, University of Bristol, U.K. and Prof. Dr. Tian-Huey Lu of Department of Physics, National Tsing Hua University, Taiwan, R.O.C., for obtaining X-ray crystallographic data.

I also would like to thank Dr. Paul A. Keller for obtaining ES-MS data.

My deeply gratitude is also extended to all of my friends and teaching staff who gave me their help and shared a hard time with me during my study.

I am grateful to Ministry of University Affairs, the Royal Thai Government for the scholarship from June 1999 to May 2000.

I also thank the Graduate School for partial support of this work.

I am very grateful to the Postgraduate Education and Research Program in Chemistry (PERCH) for partial support of my thesis.

Finally, I am indebted and grateful to all members in my family for their love, patience, understanding and support throughout my life.

Uraiwan Saeteaw

Contents

	Page
Abstract	(5)
Acknowledgment	(7)
Contents	(9)
List of Tables	(11)
List of Figures	(13)
Abbreviations and Symbols	(16)
Chapter	
1. INTRODUCTION	1
Introduction	1
Review of Literatures	3
Objective	5
2. METHOD OF STUDY	6
Materials	6
Chemical substances	6
Solvents	7
Preparation of Complexes	7
Melting Point Apparatus	12
Electrospray Mass Spectroscopy	12
UV-Visible Absorption Spectroscopy	12
Infrared Spectroscopy	13
Nuclear Magnetic Resonance Spectroscopy (^{1}H NMR)	13
Cyclic Voltammetry	13
Single Crystal X-ray Diffraction	14

Contents (continued)

	Page
3. RESULTS	15
Preparation of Complexes	15
Electrospray Mass Spectroscopy	17
UV-Visible Absorption Spectroscopy	17
Infrared Spectroscopy	17
Nuclear Magnetic Resonance Spectroscopy (^{1}H NMR)	18
Cyclic Voltammetry	18
Single Crystal X-ray Diffraction	49
4. DISCUSSION	87
Preparation of Complexes	87
Electrospray Mass Spectroscopy	90
UV-Visible Absorption Spectroscopy	92
Infrared Spectroscopy	96
Nuclear Magnetic Resonance Spectroscopy (^{1}H NMR)	100
Cyclic Voltammetry	104
Single Crystal X-ray Diffraction	110
5. CONCLUSION	114
Bibliography	116
Appendix	122
Appendix A	123
Vitae	124

List of Tables

Table		Page
1	The physical properties of ligand and compounds.	15
2	Solubility of ligand and compounds.	16
3	The crystallographic data for [Ru(tpy)(azpy)Cl]Cl.	49
4	Non-hydrogen interatomic distances of [Ru(tpy)(azpy)Cl]Cl.	51
5	Non-hydrogen interbond angles of [Ru(tpy)(azpy)Cl]Cl.	53
6	The crystallographic data for [Ru(tpy)(azpy)(Cl/I)](BF_4).	58
7	Non-hydrogen interatomic distances of [Ru(tpy)(azpy)(Cl/I)](BF_4).	59
8	Non-hydrogen interbond angles of [Ru(tpy)(azpy)(Cl/I)](BF_4).	62
9	The crystallographic data for [Ru(tpy)(azpy)(NO_2)](BF_4).	67
10	Non-hydrogen interatomic distances of [Ru(tpy)(azpy)(NO_2)](BF_4).	69
11	Non-hydrogen interbond angles of [Ru(tpy)(azpy)(NO_2)](BF_4).	72
12	The crystallographic data for [Ru(tpy)(azpy)(NCS)](BF_4).	77
13	Non-hydrogen interatomic distances of [Ru(tpy)(azpy)(NCS)](BF_4).	79
14	Non-hydrogen interbond angles of [Ru(tpy)(azpy)(NCS)](BF_4).	82
15	Electrospray mass spectroscopic data of [Ru(tpy)(azpy)(X)](BF_4) complexes, where X = Cl^-, Br^-, I^-, NO_2^-, and NCS^-.	90
16	UV-Visible absorption spectroscopic data of [Ru(tpy)(azpy)(X)](BF_4) complexes, where X = Cl^-, Br^-, I^-, NO_2^-, and NCS^-.	94
17	Summarized infrared spectroscopic data of azpy ligand and $[Ru(tpy)(azpy)(X)]^+$, where X = Cl^-, Br^-, I^-, NO_2^- and NCS^-.	99
18	Selected vibrational frequencies of azpy ligand and $[Ru(tpy)(azpy)(X)]^+$ complexes.	100
19	^1H NMR spectroscopic data of [Ru(tpy)(azpy)(X)](BF_4) complexes, where X = Cl^-, I^-, Br^-, NCS^- and NO_2^-.	101

List of Tables (continued)

Table		Page
20	Summarized H_{6A} NMR spectroscopic data of [Ru(tpy)(azpy)(X)](BF_4) complexes, where X = Cl^-, I^-, Br^-, NCS^- and NO_2^-.	104
21	Cyclic voltammetric data of [Ru(tpy)(azpy)(X)](BF_4) complexes, where X = Cl^-, Br^-, I^-, NO_2^- and NCS^-.	105
22	Summarized reduction potentials data of [Ru(tpy)(azpy)(X)](BF_4) complexes, where X = Cl^-, Br^-, I^-, NO_2^- and NCS^-.	108
23	Summarized Ru^{II}/Ru^{III} oxidation potential data of [Ru(tpy)(azpy)(X)(BF_4) complexes, where X = Cl^-, Br^-, I^-, NO_2^- and NCS^-.	108
24	Summarized Ru^{II}/Ru^{III} oxidation potential data of [Ru(tpy)(N-N)(Cl)](BF_4) complexes, where N-N = 2,2'-bipyridine (bpy) and 1,10-phenanthroline (phen).	109
25	Selected bond distances of $[Ru(tpy)(azpy)(X)]^+$, where X = Cl^-, Cl^-/I^-, NO_2^- and NCS^-.	113

List of Figures

Figure		Page
1	The structures of 2-(phenylazo)pyridine and 2,2':6',2"-terpyridine.	2
2	Electrospray mass spectrum of [Ru(tpy)(azpy)(Cl)](BF_4).	19
3	Electrospray mass spectrum of [Ru(tpy)(azpy)(Br)](BF_4).	20
4	Electrospray mass spectrum of [Ru(tpy)(azpy)(I)](BF_4).	21
5	Electrospray mass spectrum of [Ru(tpy)(azpy)(NO_2)](BF_4).	22
6	Electrospray mass spectrum of [Ru(tpy)(azpy)(NCS)](BF_4).	23
7	Electrospray mass spectrum of [Ru(tpy)(azpy)(Cl/I)](BF_4).	24
8	UV-Visible absorption spectrum of [Ru(tpy)(azpy)(Cl)](BF_4) in acetonitrile.	25
9	UV-Visible absorption spectrum of [Ru(tpy)(azpy)(Br)](BF_4) in acetonitrile.	26
10	UV-Visible absorption spectrum of [Ru(tpy)(azpy)(I)](BF_4) in acetonitrile.	27
11	UV-Visible absorption spectrum of [Ru(tpy)(azpy)(NCS)](BF_4) in acetonitrile.	28
12	UV-Visible absorption spectrum of [Ru(tpy)(azpy)(NO_2)](BF_4) in acetonitrile.	29
13	Infrared spectrum of 2-(phenylazo)pyridine. (range 400-1,700 cm^{-1})	30
14	Infrared spectrum of [Ru(tpy)(azpy)(Cl)]Cl complex. (range 400-1,700 cm^{-1})	31
15	Infrared spectrum of [Ru(tpy)(azpy)(Br)](BF_4) complex. (range 400-1,700 cm^{-1})	32
16	Infrared spectrum of [Ru(tpy)(azpy)(I)](I) complex. (range 400-1,700 cm^{-1})	33

List of Figures (continued)

Figure		Page
17	Infrared spectrum of [Ru(tpy)(azpy)(NCS)](BF_4) complex. (range 400-2,500 cm^{-1})	34
18	Infrared spectrum of [Ru(tpy)(azpy)(NO_2)](BF_4) complex. (range 400-1,700 cm^{-1})	35
19	^{1}H NMR spectrum of 2-(phenylazo)pyridine ligand in d_6-DMSO.	36
20	^{1}H NMR spectrum of 2,2':6',2"-terpyridine ligand in d_6-DMSO.	37
21	^{1}H NMR spectrum of [Ru(tpy)(azpy)(Cl)](BF_4) complex in d_6-DMSO.	38
22	^{1}H NMR spectrum of [Ru(tpy)(azpy)(Br)](BF_4) complex in d_6-DMSO.	39
23	^{1}H NMR spectrum of [Ru(tpy)(azpy)(I)](BF_4) complex in d_6-DMSO.	40
24	^{1}H NMR spectrum of [Ru(tpy)(azpy)(NCS)](BF_4) complex in d_6-DMSO.	41
25	^{1}H NMR spectrum of [Ru(tpy)(azpy)(NO_2)](BF_4) complex in d_6-DMSO.	42
26	Cyclic voltammogram of 2-(phenylazo)pyridine in acetonitrile. (scan rate 50 mV/s)	43
27	Cyclic voltammogram of [Ru(tpy)(azpy)(Cl)](BF_4) in acetonitrile. (scan rate 50 mV/s)	44
28	Cyclic voltammogram of [Ru(tpy)(azpy)(Br)](BF_4) in acetonitrile. (scan rate 50 mV/s)	45
29	Cyclic voltammogram of [Ru(tpy)(azpy)(I)](BF_4) in acetonitrile. (scan rate 50 mV/s)	46
30	Cyclic voltammogram of [Ru(tpy)(azpy)(NCS)](BF_4) in acetonitrile. (scan rate 50 mV/s)	47
31	Cyclic voltammogram of [Ru(tpy)(azpy)(NO_2)](BF_4) in acetonirile. (scan rate 50 mV/s)	48

List of Figures (continued)

Figure		Page
32	The structure of [Ru(tpy)(azpy)(Cl)]Cl. (H-atoms omitted)	57
33	The structure of [Ru(tpy)(azpy)(Cl/I)](BF_4). (H-atoms omitted)	66
34	The structure of [Ru(tpy)(azpy)(NO_2)](BF_4). (H-atoms omitted)	76
35	The structure of [Ru(tpy)(azpy)(NCS)](BF_4). (H-atoms omitted)	86
36	The two isomeric forms of $[Ru(tpy)(azpy)(X)]^+$.	88
37	Schematic diagram of a general electrochemical cell.	123

Abbreviations and Symbols

Å	=	Angstrom unit (1 Å = 10^{-10} meter)
A.R. grade	=	Analytical reagent grade
azpy	=	2-(phenylazo)pyridine
bpy	=	2,2'-bipyridine
cm^{-1}	=	wave number
DMF	=	*N,N*-Dimethylformamide
DMSO	=	Dimethylsulfoxide
g	=	gram
g/cm^3	=	gram per cubic centimeter
h	=	hour
K	=	Kelvin
L.R. grade	=	Laboratory reagent grade
MLCT	=	metal-to-ligand charge transfer
mg/mL	=	milligram per milliliter
mL	=	milliliter
mmol	=	millimole
mV/s	=	millivolt per second
nm	=	nanometer
phen	=	1,10-phenanthroline
Rel. Abun.	=	relative abundance
tpy	=	2,2':6',2"-terpyridine
°	=	degree
λ	=	wavelength
ε	=	molar extinction coefficient

Chapter 1

INTRODUCTION

1.1 Introduction

Ruthenium(II) is well recognized as a metal ion capable of entering into $d\pi$-$p\pi$ back-bonding with π-acceptor ligands such as polypyridyl and α-diimine ligands. This interaction results in the more stability of ruthenium(II) center. There has been considerable interest in ruthenium complexes that contain polypyridyl and α-diimine ligands such as 2,2'-bipyridine (Sullivan, *et al.*, 1980). The polypyridine complexes of ruthenium(II) have generated considerable interest in areas such as photochemistry, photophysics, and electrochemistry, particularly as a result of the interesting excited-state and redox properties of the $[Ru(bpy)_3]^{2+}$ (bpy = 2,2'-bipyridine) and related complexes. There are many advantages of polypyridine complexes of ruthenium(II) such as the ruthenium(II) complexes of 2,2'-bipyridine (bpy) and its derivatives act as photosensitizers in solar cells (Nazeeruddin, *et al.*, 1993).

In terms of structure and synthesis, the use of bidentate ligands in complexes such as $Ru(LL)_2Cl_2$, where LL = bidentate ligand, afforded many isomers. Therefore tridentate ligand such as 2,2':6',2''-terpyridine (tpy) has been used to avoid the structural problem. Results from previous studies have shown that complexes of the type $[Ru(tpy)(bpy)X]^{n+}$, where X = Cl^-, H_2O, NO_2^-, pyridine (py), have some interesting properties. For example the $[Ru^{IV}(tpy)(bpy)(O)]^{2+}$ complex, the oxidized form of $[Ru^{II}(tpy)(bpy)(OH_2)]^{2+}$, is capable of DNA cleavage agent (Thorp and Grover, 1991).

In this research, 2-(phenylazo)pyridine (azpy) was chosen as the bidentate ligand. The azpy ligand is a strong π-acid, stronger than 2,2'-bipyridine (bpy) and other familiar N-N donor ligands, and is recognized as a stabilizer of the lower oxidation states of ruthenium (Krause and Krause, 1980).

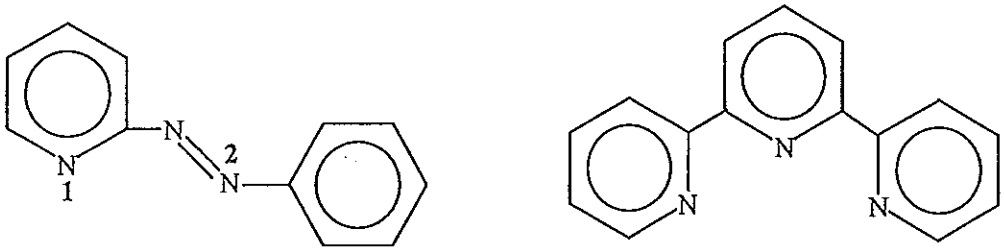

2-(phenylazo)pyridine (azpy) 2,2':6',2''-terpyridine (tpy)

Figure 1 Structures of 2-(phenylazo)pyridine and 2,2':6',2''-terpyridine.

Therefore, in this work, it is our of interest to investigate the chemistry of complexes of the type $[Ru(tpy)(azpy)X]^+$, where X = Cl^-, Br^-, I^-, NO_2^- and NCS^-. These complexes have been synthesized and characterized by UV-Visible absorption spectroscopy, ^1H NMR spectroscopy, infrared spectroscopy and cyclic voltammetry. In addition, X-ray diffraction methods have been used to determine the crystal structures of complexes which single crystals are available. Efforts are being made to study the chemistry of these complexes by varying the nature of the X ligand.

Furthermore, we hope that results from characterization of these complexes will be advantages for other researches.

1.2 Review of Literatures

Synthesis and characterization of ruthenium(II) with tpy ligand have been studied since 1970s ;

Balzani and Tokel-Takvoryan studied the electrochemistry and electrogenerated chemiluminescence (ecl) of four ruthenium(II) chelates, $Ru(L)_x^{n+}$ (x = 3, n = 2, L = 2,2′-bipyridine(bpy); x = 3, n = 2, L = 1,10-phenanthroline (phen); x = 2, n = 2, L = 2,2′:6′,2″-terpyridine (tpy). All compounds showed evidence of several one-electron reduction and oxidation steps to form products stable during cyclic voltammetric scans. The bpy, phen and tpy complexes produce ecl via redox reactions of oxidized and reduced forms to form emitting species, which have been identified as the triplet state by comparison with their lumninescence spectra; the ecl of the bpy complex is the most intense. (Tokel-Takvoryan, *et al.*, 1973)

Meyer and Sullivan studied the isomers of $[Ru(tpy)(PPh_3)Cl_2]$ complexes. They have been characterized by infrared spectroscopy, UV-Visible absorption spectroscopy, ^1H and ^{31}P NMR spectroscopy and cyclic voltammetry. (Sullivan, *et al.*, 1980)

Thorp and Grover studied the $[Ru(tpy)(bpy)O]^{2+}$ complex with electrochemistry, UV-Visible absorption spectroscopy and electrophoresis. This complex showed DNA cleavage agent property. (Thorp and Grover, 1991)

Thorp and Gupta studied the new DNA cleavage agents based on $[Ru(tpy)(bpy)O]^{2+}$ complex, oxoruthenium(IV), which 1,10-phenanthroline (phen), 2,4,6-tripyridyl-triazine (tpt) and N,N,N',N'-tetramethylethylenediamine (tmen) replace 2,2'-bipyridine (bpy). These complexes were investigated by electrochemistry, UV-Visible absorption spectroscopy, electrophoresis and single crystal X-ray diffraction. (Gupta, *et al.*, 1993)

Pramanik, *et al.* studied the chemistry of $[Ru(tpy)(azpy)Cl]^{+}$ complex and the monodentate ligand was varied. In addition, $[Ru(tpy)(azpy)(OH_2)]^{2+}$complex acts as a catalyst for the oxidation of water to oxygen via $[Ru(tpy)(azpy)(O)]^{2+}$ complex. (Pramanik, *et al.*, 1998)

Synthesis and characterization of the ruthenium(II) complexes with azpy ligand have been investigated since 1980s ;

Krause and Krause studied the three isomers of $[Ru(azpy)_2Cl_2]$ complex, i.e. two of *cis*-isomers (α and β) and a *trans*-isomer (γ). They were characterized by infrared spectroscopy, ^{13}C NMR spectroscopy, UV-Visible absorption spectroscopy and cyclic voltammetry. The results show that azpy ligand has the potential to be better π-acceptor than bpy ligand to stabilize ruthenium(II) center. (Krause and Krause, 1980)

Chakravarty and Goswami studied the complex of $[Ru(azpy)_2(P)_2]^{n+}$, where P = tertiary phosphine, which was synthesized via $[Ru(azpy)_2(OH_2)_2]^{2+}$. The results show that the bulkiness of phosphine ligand result in decrease the rate of reaction. The important role of aquo-complex, $[Ru(azpy)_2(OH_2)_2]^{2+}$, is precursor to synthesize the derivative complexes of ruthenium(II) with azpy ligand. (Goswami, *et al.*, 1982)

Goswami, Chakravarty and Chakravorty studied the isomers of $[Ru(azpy)_2(OH_2)(C_6H_5N)]^{2+}$ and $[Ru(azpy)_2(OH_2)(py)]^{2+}$ complexes, which were synthesized via $[Ru(azpy)_2(OH_2)_2]^{2+}$. The solvolysis of $[Ru(azpy)_2(OH_2)_2]^{2+}$ showed that the solution of the *tc* isomer (N(py), N(py) span *trans* positions, N(azo), N(azo) *cis* positions) in donor solvent (S) such as benzonitrile (C_6H_5N), the MLCT band energy undergoes significant shifts from acidic aqueous solution values due to substitution of coordinated water by solvent molecules. In acetonitrile and benzonitrile, the shifts are hypsochromic as expected from the Dq order ($RCN > H_2O$). (Goswami, *et al.*, 1983)

Goswami, Mukherjee and Chakravorty studied the $[Ru(L)_2(bpy)]^{2+}$complexes, where L = 2-(phenylazo)pyridine (azpy) and 2-(*m*-tolylazo)pyridine (tap). The electrochemical data show the highly positive metal oxidation potentials. A correlation of MLCT transition energy with the difference between the formal potentials of the ruthenium(III)-ruthenium(II) couple and the first ligand reduction couple is noted. From this correlation one can predict the energy of the MLCT band to be within ± 1000 cm^{-1} of experimental value. (Goswami, *et al.*, 1983)

The $[Ru(tpy)(azpy)(X)]^+$ complexes, where X = Cl^-, Br^-, I^-, NO_2^- and NCS^-, were synthesized and characterized by spectroscopic, electrochemical and single crystal X-ray diffraction techniques. Results from this work provide us some insight information on chemistry of those complexes.

1.3 Objective

1. To synthesize $[Ru(tpy)(azpy)(X)]^+$ complexes, where X = Cl^-, Br^-, I^-, NO_2^-, and NCS^-.
2. To investigate the chemistry of $[Ru(tpy)(azpy)(X)]^+$ complexes by spectroscopic and electrochemical techniques.
3. To analyze and to summarize the chemistry of $[Ru(tpy)(azpy)(X)]^+$ complexes.

Chapter 2

METHOD OF STUDY

2.1 Materials

2.1.1 Chemical substances

Products of Fluka Chemical, Buchs, Switzerland

1. 2-aminopyridine, $C_5H_6N_2$, A.R. grade
2. nitrosobenzene, C_6H_5NO, A.R. grade
3. 2,2':6',2"-terpyridine, $C_{15}H_{11}N_3$, A.R. grade

Products of E. Merck, Darmstadt, Germany

1. Potassium thiocyanate, KSCN, A.R. grade
2. Silica gel 60 GF_{254}

Products of BDH Chemical Ltd., England

1. Lithium bromide, LiBr, A.R. grade
2. Sodium iodide, NaI, A.R. grade
3. Sodium nitrite, $NaNO_2$, A.R. grade
4. Silver nitrate, $AgNO_3$, A.R. grade

Products of Aldrich Chemical Cl., Inc., USA

Ruthenium(III) trichloride hydrate, $RuCl_3 \cdot 3H_2O$, A.R. grade

Products of Farmitalia Carlo Erba, Miland

Sodium hydroxide, NaOH, A.R. grade

Products of Riedel-de Haen

Lithium chloride, LiCl, A.R. grade

Products of Hopkin & Williams

Ammonium tetrafluoroborate, NH_4BF_4, A.R. grade

2.1.2 Solvent (all other chemicals were reagent grade and used without further purification.)

Products of Lab-Scan Analytical Science

1. Hexane, C_6H_{12}, A.R. grade
2. Methanol, CH_3OH, A.R. grade
3. Dimethylsulfoxide, $(CH_3)_2SO$, A.R. grade
4. Acetonitrile, CH_3CN, A.R. grade

Products of E. Merck, Darmstadt, Germany

1. Absolute ethanol, C_2H_5OH, A.R. grade
2. Acetone, C_3H_6O, A.R. grade
3. Dichloromethane, CH_2Cl_2, A.R. grade

Products of J.T. Baker

1. Benzene, C_6H_6, A.R. grade
2. Ether, $(C_2H_5)_2O$, A.R. grade

Products of Farmitalia Carlo Erba, Miland

1. Ethylacetate, $C_4H_8O_2$, L.R. grade
2. *N,N*-Dimethylformamide, C_3H_7NO, A.R. grade

2.2 Preparation of Complexes

The 2-(phenylazo)pyridine ligand was prepared by modified literature methods (Krause and Krause, 1980). $Ru^{III}(tpy)Cl_3$ complex was synthesized by modified published procedures (Sullivan, *et al.*,1980). The [Ru(tpy)(azpy)(Cl)]Cl and [Ru-

(tpy)(azpy)(Cl)](BF$_4$) complexes were prepared by modified literature methods (Takeuchi, *et al.*, 1984). The [Ru(tpy)(azpy)(X)](BF$_4$) complexes, where X = Br$^-$, I$^-$, NCS$^-$ and NO$_2^-$, were prepared by modified published procedures (Hecker, *et al.*, 1991).

2.2.1 Preparation of 2-(phenylazo)pyridine ligand, azpy.

2-aminopyridine (3.88 g , 41.2 mmol) reacted with nitrosobenzene (4.03 g, 37.6 mmol) in 13.5 mL NaOH (25 M) and 2 mL benzene. The green solution was changed to brown color. The reaction mixture was heated for 30-45 min with stirring, then extracted with 5 x 50-mL of benzene. The benzene solution was heated in water bath and the activated carbon was added, with stirring and then filtered off. The red-orange filtrate was obtained. The solvent was evaporated and the residue was purified by silica gel column chromatography (Ethylacetate : Hexane 1:1) to give a red-orange oily solution. The yield was 28 %.

2.2.2 Preparation of Trichloro(2,2':6',2"-terpyridine)ruthenium(III) complex, Ru^{III}(tpy)Cl$_3$.

To 38 mL of absolute ethanol in a 100-mL round-bottom flask was added 0.399 g (1.53 mmol) of $RuCl_3 \cdot 3H_2O$ and 0.349 g (1.50 mmol) of tpy. The mixture was heated at reflux for 4 h while vigorous magnetic stirring was maintained. Then the reaction was cooled to room temperature, and the fine brown powder which had appeared was filtered from the reddish yellow solution. The product was washed with 3 x 30-mL of absolute ethanol followed by 3 x 30-mL of ether and air-dried. The yield was 88 %.

2.2.3 Preparation of Chloro(2-(phenylazo)pyridine)(2,2':6',2"-terpyridine)-ruthenium(II) chloride complex, [Ru(tpy)(azpy)(Cl)]Cl.

A 203 mg (0.454 mmol) of $Ru^{III}(tpy)Cl_3$ and 83 mg (0.454 mmol) of 2-(phenylazo)pyridine were heated at reflux for 4 h in 28 mL of 3:1 absolute ethanol : H_2O containing 65 mg (1.53 mmol) of LiCl and 0.7 mL of Et_3N as reductant with vigorous stirring. Then the reaction mixture was filtered while hot. The dark red solution was allowed to evaporate for a few days, then the black solid came out. The black solid then was isolated by filtration and washed with 2 x 10-mL of 3 M HCl, 2 x 10-mL of acetone, 2 x 10-mL of ether and air-dried. The yield was 63 %.

2.2.4 Preparation of Chloro(2-(phenylazo)pyridine)(2,2':6',2"-terpyridine)-ruthenium(II) tetrafluoroborate complex, [Ru(tpy)(azpy)(Cl)](BF_4).

A 50 mg sample of [Ru(tpy)(azpy)(Cl)]Cl (0.0847 mmol) was dissolved in 15 mL of 4 : 1 acetone : H_2O. Then the solution of 45 mg of NH_4BF_4 (0.43 mmol) was added to the red solution. The red solution was allowed to stand for 2 days at room temperature. The black solid was collected by vacuum filtration and washed with 20 mL of cooled water, 30 mL of ether and air-dried. The yield was 85 %.

2.2.5 Preparation of Isothiocyanato(2-(phenylazo)pyridine)(2,2':6',2"-terpyridine)-ruthenium(II) tetrafluoroborate complex, [Ru(tpy)(azpy)(NCS)](BF_4).

A 52 mg sample of [Ru(tpy)(azpy)(Cl)]Cl (0.0881 mmol) and 30 mg of $AgNO_3$ (0.1762 mmol) were heated together at reflux for 1 h in 12 mL of 3:1 acetone/H_2O solvent mixture. AgCl was filtered off. The dark orange solution was heated for 15 min and 52 mg of KSCN (0.5286 mmol) was added to the solution. The mixture was

heated at reflux with stirring for 1 h then cooled to room temperature. A 45 mg of NH_4BF_4 (0.43 mmol) was added to the red solution. The small black crystals precipitated after 5 days. The solid was collected by vacuum filtration and washed with 20 mL of cooled water followed by 30 mL of ether and air-dried. The yield was 79 %.

2.2.6 Preparation of Nitro(2-(phenylazo)pyridine)(2,2':6',2"-terpyridine)ruthenium-(II) tetrafluoroborate complex, $[Ru(tpy)(azpy)(NO_2)](BF_4)$.

A 52 mg sample of [Ru(tpy)(azpy)(Cl)]Cl (0.0881 mmol) and 30 mg of $AgNO_3$ (0.1762 mmol) were heated at reflux for 1 h in 12 mL of 3:1 acetone : H_2O. AgCl was filtered off. The dark orange solution was heated for 15 min and adding 40 mg of $NaNO_2$ (0.579 mmol) in the solution. The mixture was refluxed for 1 h the color was changed from dark brown to red. After the solution was cooled to room temperature then 45 mg of NH_4BF_4 (0.43 mmol) was added to the red solution. The small black solid precipitated after 5 days. The solid was collected on a frit and washed with 20 mL of cooled water followed by 30 mL of ether and air-dried. The yield was 89 %.

2.2.7 Preparation of Bromo(2-(phenylazo)pyridine)(2,2':6',2"-terpyridine)-ruthenium(II) tetrafluoroborate complex, $[Ru(tpy)(azpy)(Br)](BF_4)$.

A 52 mg of [Ru(tpy)(azpy)(Cl)]Cl (0.0881 mmol) and 30 mg of $AgNO_3$ (0.1762 mmol) were dissolved in 12 mL of 3:1 acetone : H_2O. The solution was heated at reflux and stirred for 1 h, whereupon it changed from deep red to dark orange. AgCl was filtered off. The solution was heated for 15 min and adding 42 mg of LiBr (0.4836 mmol) in solution. The mixture was heated at refluxed for 1 h and cooled to room temperature. Then 45 mg of NH_4BF_4 (0.43 mmol) was added in the red

solution. Keep the red solution opened air until the small black solid had appeared (5 days). The solid was collected by suction filtration and washed with 20 mL of cooled water followed by 30 mL of ether before it was dried in air. The yield was 94 %.

2.2.8 Preparation of Iodo(2-(phenylazo)pyridine)(2,2':6',2"-terpyridine)ruthenium-(II) tetrafluoroborate complex, [Ru(tpy)(azpy)(I)](BF_4).

A 52 mg of [Ru(tpy)(azpy)(Cl)]Cl (0.0881 mmol) in a 50-mL round bottom flask was dissolved in 3:1 mixture of acetone : H_2O and adding 30 mg of $AgNO_3$ (0.1762 mmol). The solution was heated at reflux with stirring for 1 h. The reaction was halted after the solution changed from deep red too dark orange. AgCl was filtered off. The solution was heated for 15 min and added 271 mg of NaI (1.808 mmol). The mixture was heated for 1 h and cooled to room temperature. A 45 mg of NH_4BF_4 (0.43 mmol) was added in the red solution. The red solution was allowed to stand for 5 days until the small black solid came out. Then it was collected by suction filtration, washed with 20 mL of cooled water followed by 30 mL of ether and air-dried. The yield was 92 %.

2.2.9 Preparation of Chloro/Iodo(2-(phenylazo)pyridine)(2,2':6',2"-terpyridine)-ruthenium(II) tetrafluoroborate complex, [Ru(tpy)(azpy)(Cl/I)](BF_4).

A 207 mg (0.469 mmol) of $Ru^{III}(tpy)Cl_3$ and 85 mg (0.464 mmol) of 2-(phenylazo)pyridine were heated at reflux for 5.30 h in 28 mL of 3:1 absolute ethanol : H_2O containing 5.224 g of NaI and 0.4 mL of Et_3N as reductant with vigorous stirring. The solution was filtered while hot, the obtained black solid was unreacted $Ru^{III}(tpy)Cl_3$. A 177 mg of the black solid and 85 mg (0.464 mmol) of 2-(phenylazo)-

pyridine were refluxed with sitrring for 1.30 h in 30 mL of 3:1 absolute ethanol/H_2O containing 182 mg (1.36 mmol) of LiCl and 0.6 mL of triethylamine. Then the dark red solution was filtered. A 15 mL of saturated aqueous NH_4BF_4 solution was added to the dark red solution. The solution was allowed to evaporate for 7 days in darkness, then the black solid came out. The black solid then was isolated by filtration and washed with 2 x 10-mL of H_2O, 2 x 10-mL of ether and air-dried. The clear red crystals were selected from the black solid. Then X-ray single crystal diffraction of this complex was done.

2.3 Melting Point Apparatus

Melting point of the complexes were measured on Thomas Hoover Capillary melting point apparatus, range in 30 - 300^{o}C.

2.4 Electrospray Mass Spectroscopy

Electrospray mass spectra were measured on a VG Quattro triple quardrupole system mass spectrometer with alcohol mobile phase.

2.4 UV-Visible Absorption Spectroscopy

Ultraviolet and visible absorption spectra were recorded by using a Hewlett-Packard 8452A diode array spectrophotometer.

2.5 Infrared Spectroscopy

Infrared spectra were obtained by using a Perkin Elmer Spectrum GX FT-IR spectrophotometer from 370 to 4,000 cm^{-1}, and Perkin Elmer 783 Infrared Spectrophotometer from 200 to 400 cm^{-1}, all samples were prepared in KBr pellets.

2.6 Nuclear Magnetic Resonance Spectroscopy

^1H NMR spectra were recorded in d_6-DMSO with a FT-NMR Varian UNITY SNOVA 500-MHz with Me_4Si as an internal standard.

2.7 Cyclic Voltammetry

Electrochemical experiments were performed using a CS-2000 (Cypress). A standard three-electrode configuration was used, with platinum wire working , platinum gauze counter and a $Ag/AgNO_3$ reference electrode. Electrochemical measurements were done in CH_3CN and 10 mM tetra-n-butylammonium-hexafluorophosphate ($[NBu_4]PF_6$) was used as the supporting electrolyte. Ferrocene was added at the end of each experiment as an internal standard; all potentials are quoted vs the ferrocene/ferrocenium couple (Fc/Fc^+). The solvent was used as received. N_2 was bubbled through the solutions prior to measurement. The electrochemical cell was shown in Appendix A.

2.8 Single Crystal X-ray Diffraction

Some X-ray structures of [Ru(tpy)(azpy)(Cl)]Cl and [Ru(tpy)(azpy)(NO_2)]BF_4 were determined by CCD X-ray diffractometer with SHELXL program (Department of Physics, National Tsing Hua University, Taiwan, R.O.C.).

The X-ray structure of [Ru(tpy)(azpy)(Cl/I)]BF_4 complex was determined by CCD X-ray diffractometer with SHELXL program (School of Chemistry, University of Bristol, U.K.).

The X-ray structure of [Ru(tpy)(azpy)(NCS)]BF_4 complex was determined by CCD X-ray diffractometer with teXsan program (Department of Chemistry, Faculty of Science, Monash University, Clayton, Victoria, Australia).

Chapter 3

RESULTS

3.1 Preparation of Complexes

The [Ru(tpy)(azpy)Cl](Cl) complex was synthesized by reaction of the free azpy ligand with $[Ru(tpy)Cl_3]$. This complex was used as a precursor to prepare ruthenium complexes containing various ligands other than Cl, $[Ru(tpy)(azpy)X]^+$ complexes (where $X = Br^-$, I^-, NO_2^-, and NCS^-). These complexes were obtained by the reaction of $[Ru(tpy)(azpy)Cl]^+$ with $AgNO_3$ in acetone : H_2O (3 : 1) solution followed by reaction with LiBr, NaI, $NaNO_2$ or KSCN and were precipitated by BF_4^- salt. Some of the physical properties of these complexes are summarized in Table 1 and 2.

Table 1 The physical properties of ligand and compounds.

Compounds	Physical properties		
	Appearance	Color	Melting point ($^{\circ}C$)
Azpy ligand	Liquid (oily)	Red	30
$[Ru(tpy)(azpy)(Cl)](BF_4)$	Rod like	Black	More than 250
$[Ru(tpy)(azpy)(Br)](BF_4)$	Rod like	Red crystal	More than 250
$[Ru(tpy)(azpy)(I)](BF_4)$	Needle	Black	More than 250
$[Ru(tpy)(azpy)(NCS)](BF_4)$	Plate	Black	More than 250
$[Ru(tpy)(azpy)(NO_2)](BF_4)$	Cubic	Red crystal	More than 250

Table 2 Solubility of ligand and compounds.

Solvent	Compounds					
	Azpy	Ru-Cl	Ru-Br	Ru-I	Ru-NO_2	Ru-NCS
H_2O	+++	-	-	-	-	-
Methanol	+++	++	++	++	++	++
Ethanol	+++	+	+	+	+	+
Acetonitrile	+++	+++	+++	+++	+++	+++
Acetone	+++	+++	+++	+++	+++	+++
DMSO	+++	+++	+++	+++	+++	+++
DMF	+++	+++	+++	+++	+++	+++
$CHCl_3$	+++	-	-	-	-	-
CH_2Cl_2	+++	-	-	-	-	-
Hexane	+++	-	-	-	-	-

Ru-Cl = [Ru(tpy)(azpy)(Cl)](BF_4)

Ru-Br = [Ru(tpy)(azpy)(Br)](BF_4)

Ru-I = [Ru(tpy)(azpy)(I)](BF_4)

Ru-NO_2 = [Ru(tpy)(azpy)(NO_2)](BF_4)

Ru-NCS = [Ru(tpy)(azpy)(NCS)](BF_4)

+++ = soluble (well), in the range 2.0 – 5.0 mg/mL

++ = soluble (fair) , in the range 0.5 – 2.0 mg/mL

+ = soluble (poor) , less than 0.5 mg/mL

- = insoluble

The solubility of ligand and compounds were quanlitative analysis. Azpy ligand can be soluble much greater than Ru(II) complexes. Then the solubility scale is focused on Ru(II) complexes.

3.2 Electrospray Mass Spectroscopy

The electrospray mass spectroscopy is important technique to study the molecular weight of the complexes. The electrospray mass spectra (ES-MS) of [Ru-(tpy)(azpy)X](BF_4) complexes, where X = Cl^-, Br^-, I^-, NO_2^-, NCS^- and Cl^-/I^-, are shown in Figure 2-7, respectively. The parent peak, which gives 100% relative abundance, is the molecular weight of each complex ion. So the expected structure will be confirmed by this method.

3.3 UV-Visible Absorption Spectroscopy

UV-Visible absorption spectroscopy is the technique to study the electronic transitions of the ligand and complexes. The UV-Visible absorption spectra of The [Ru(tpy)(azpy)X](BF_4) complexes, where X = Cl^-, Br^-, I^-, NCS^- and NO_2^-, in acetonitrile solution are shown in Figure 8-12, respectively. These complexes give intense bands in the visible region, which λ_{max} are in the 506-520 nm range.

3.4 Infrared Spectroscopy

Infrared spectroscopy is important technique to study the molecular structures of the complexes. The infrared spectra of azpy ligand, [Ru(tpy)(azpy)(Cl)](Cl) complex, and [Ru(tpy)(azpy)X](BF_4) complexes, where X = Br^-, I^-, NCS^-, and NO_2^-, are shown in Figure 13-18, respectively. The interesting intense vibration frequencies of azpy

ligand around the ruthenium(II) central metal atom are C=C, C=N, N=N(azo) stretching vibration and C-H out of plane bending in monosubstituted benzene. The intense N=N(azo) stretching frequencies are in 1,421-1,312 cm^{-1} range.

3.5 Nuclear Magnetic Resonance Spectroscopy (^{1}H NMR)

^{1}H NMR spectroscopy is one important technique to determine molecular structure because the different proton in the molecular structure will show the different chemical shift. The ^{1}H NMR spectra of azpy, tpy ligands and [Ru(tpy)(azpy)X](BF_4) complexes, where X = Cl^-, Br^-, I^-, NO_2^-, and NCS^-, are recorded in d_6-DMSO as shown in Figure 19-25, respectively. The ^{1}H NMR spectra of ligands and complexes show seven signals for nine hydrogens of azpy and six signals for eleven hydrogens of tpy ligands.

3.6 Cyclic Voltammetry

The cyclic voltammetry is important technique to study the electrochemistry of the ligand and complexes. The cyclic voltammogram of azpy ligand and [Ru(tpy)-(azpy)X](BF_4) complexes, where X = Cl^-, Br^-, I^-, NCS^-, and NO_2^-, are recorded in acetonitrile solution as shown in Figure 26-31, respectively. Ferrocene was added at the end of each experiment as an internal standard.

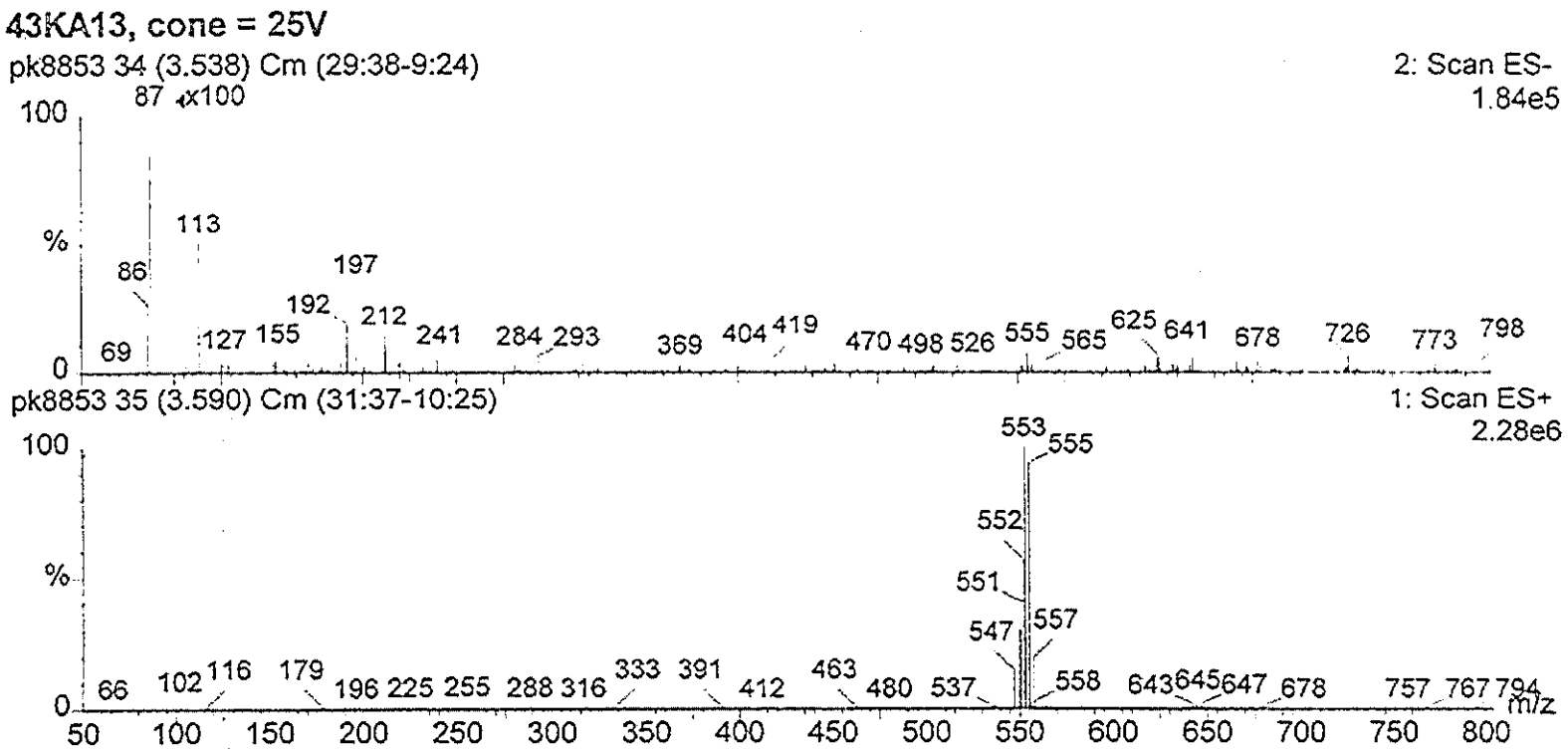

Figure 2 Electrospray mass spectrum of [Ru(tpy)(azpy)(Cl)](BF_4)

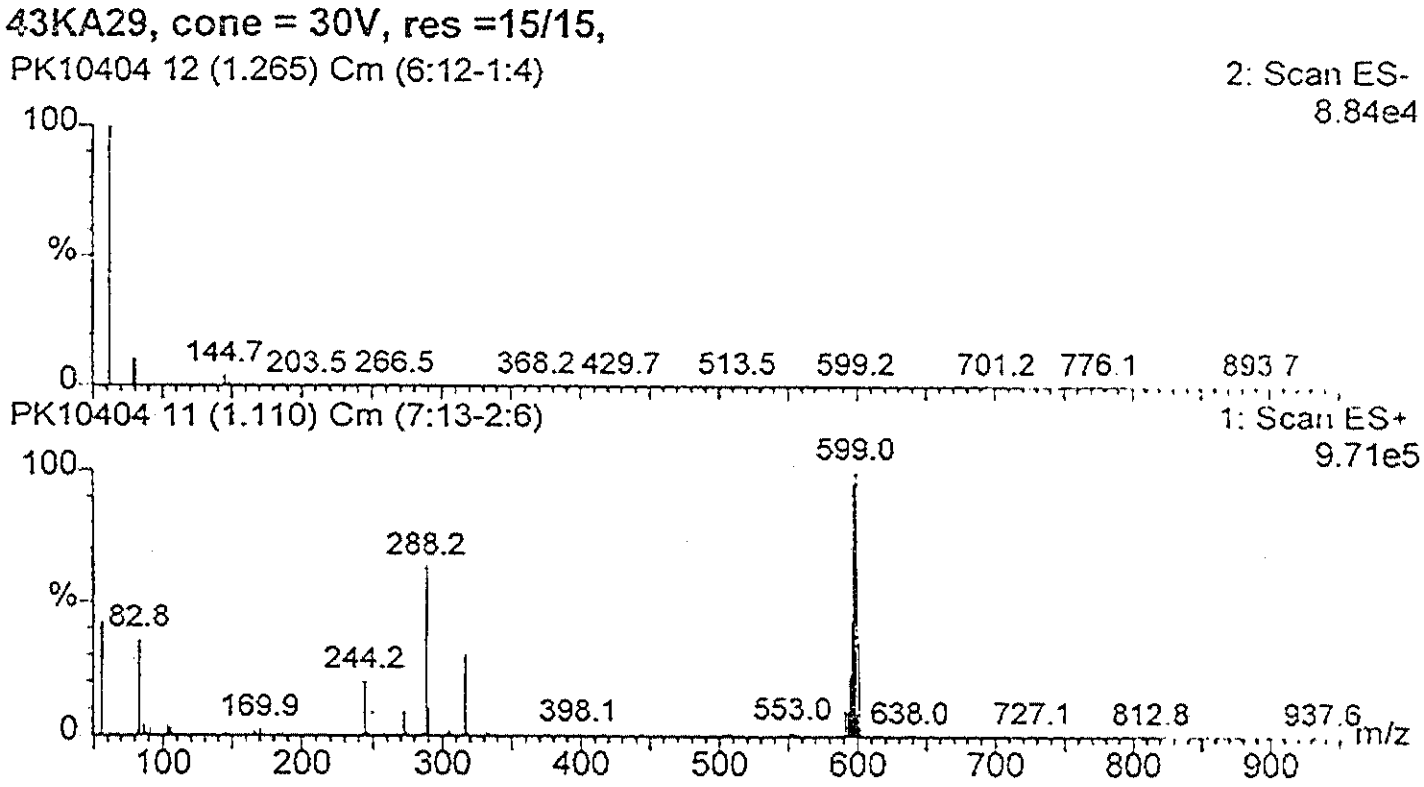

Figure 3 Electrospray mass spectrum of $[Ru(tpy)(azpy)(Br)](BF_4)$

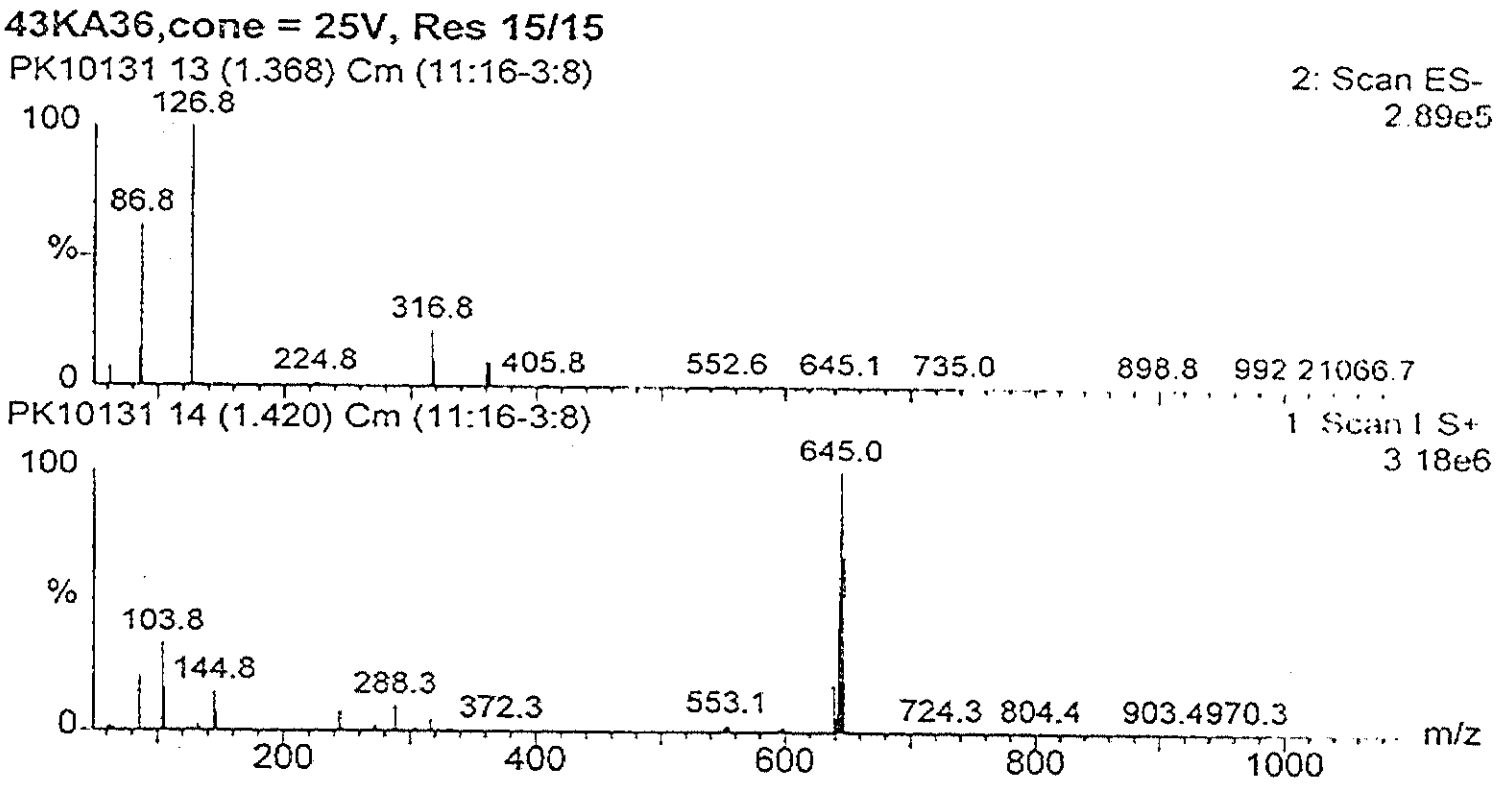

Figure 4 Electrospray mass spectrum of $[Ru(tpy)(azpy)(I)](BF_4)$

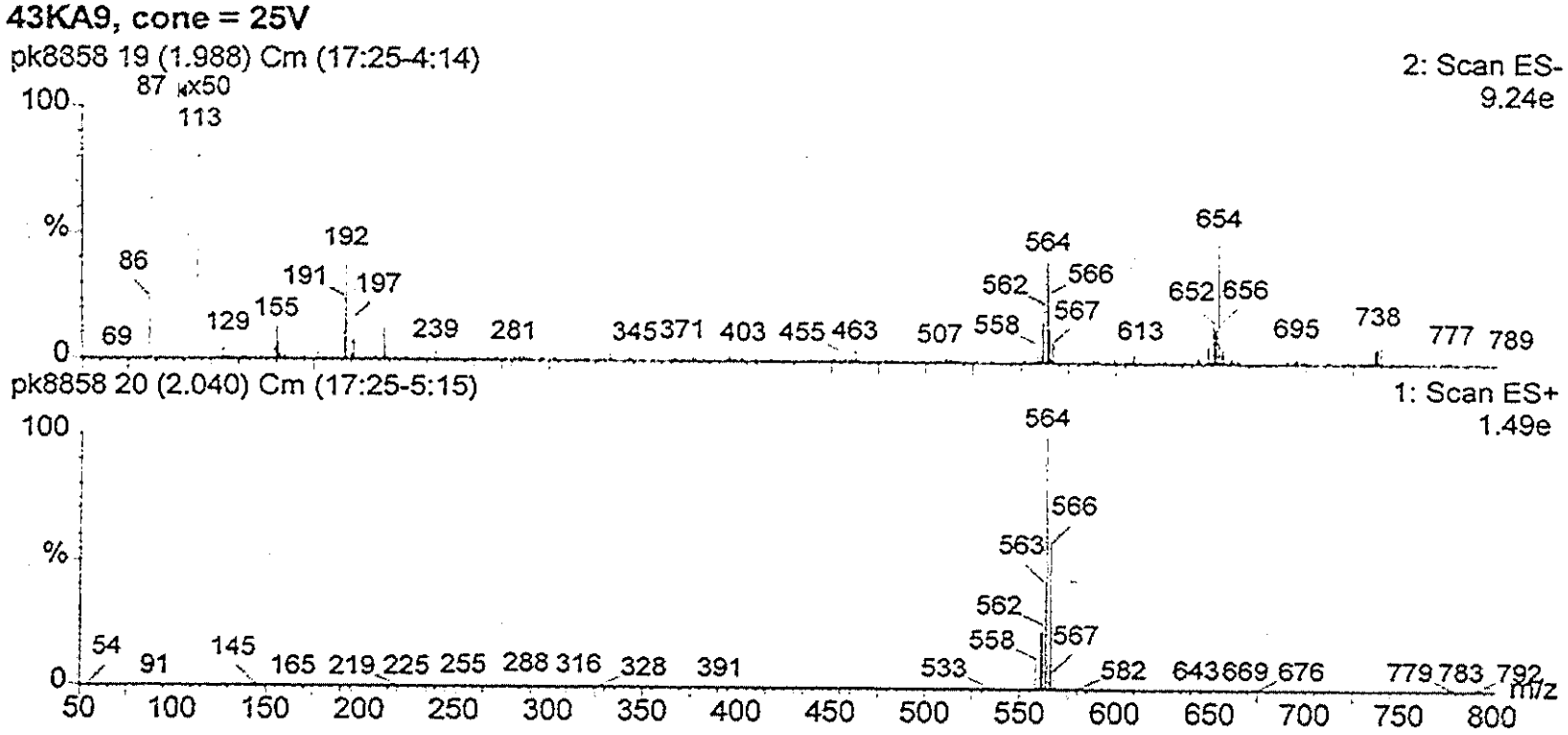

Figure 5 Electrospray mass spectrum of $[Ru(tpy)(azpy)(NO_2)](BF_4)$

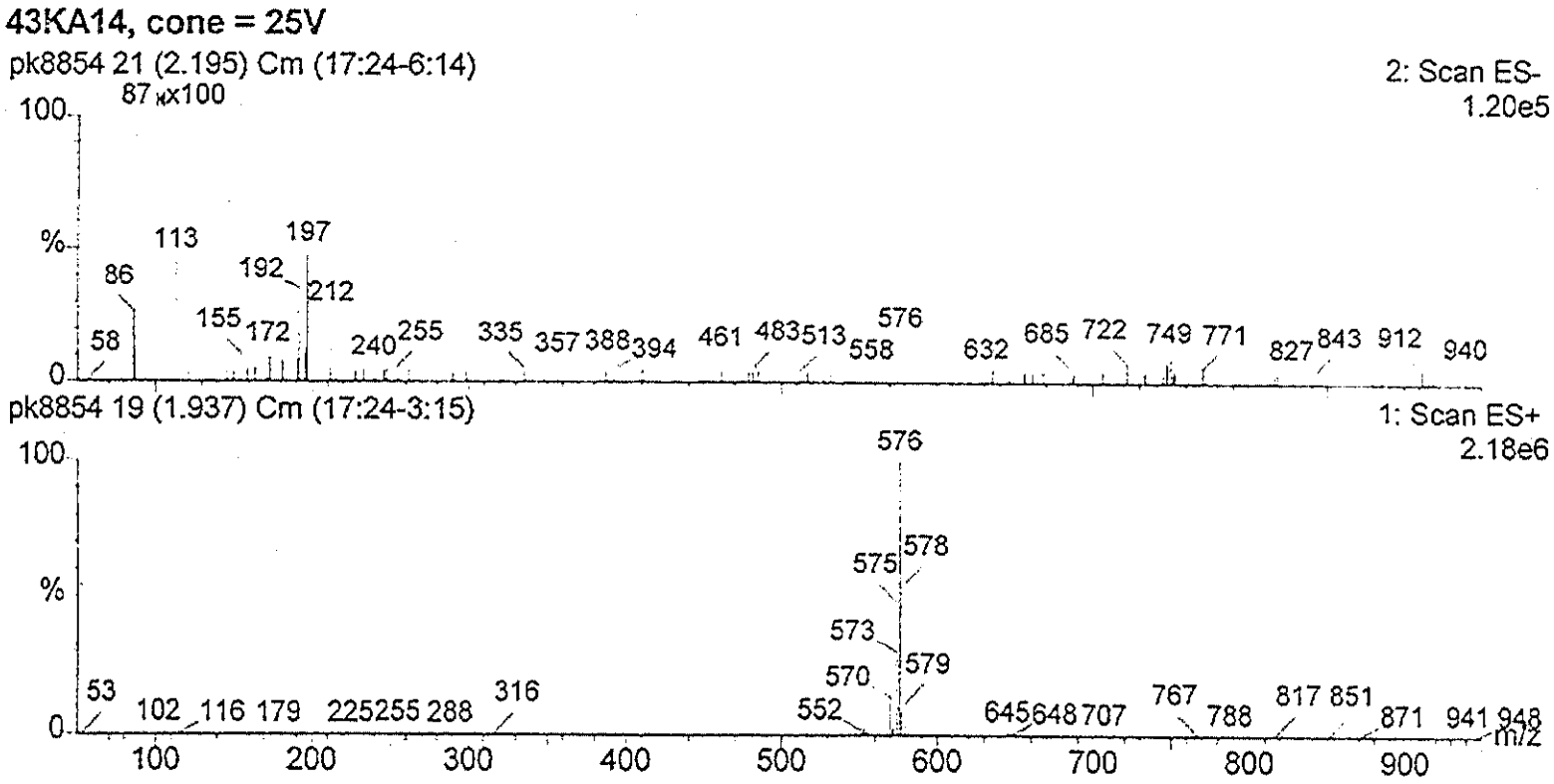

Figure 6 Electrospray mass spectrum of $[Ru(tpy)(azpy)(NCS)](BF_4)$

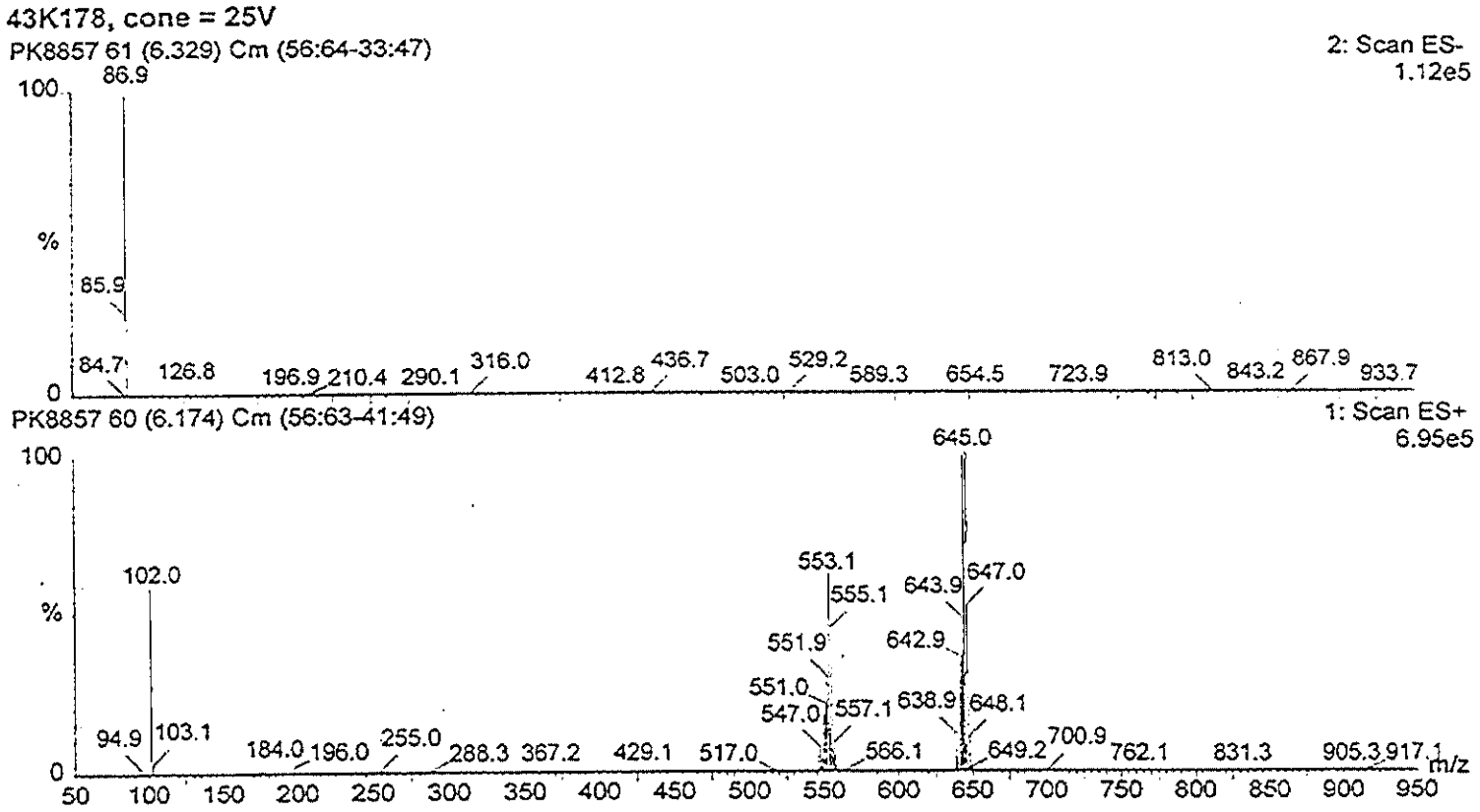

Figure 7 Electrospray mass spectrum of $[Ru(tpy)(azpy)(Cl/I)](BF_4)$

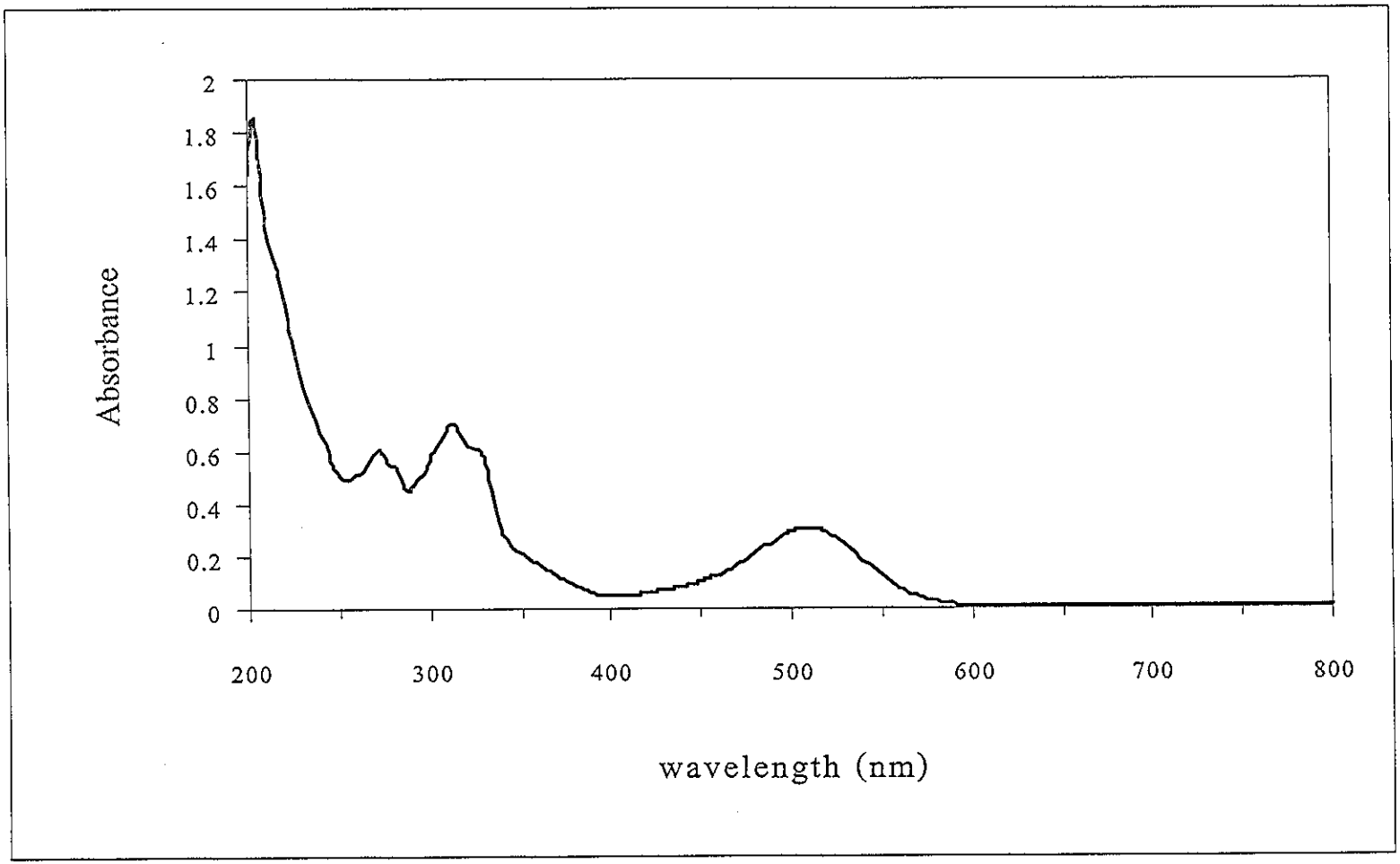

Figure 8 UV-Visible absorption spectrum of [Ru(tpy)(azpy)(Cl)](BF_4) in acetonitrile.

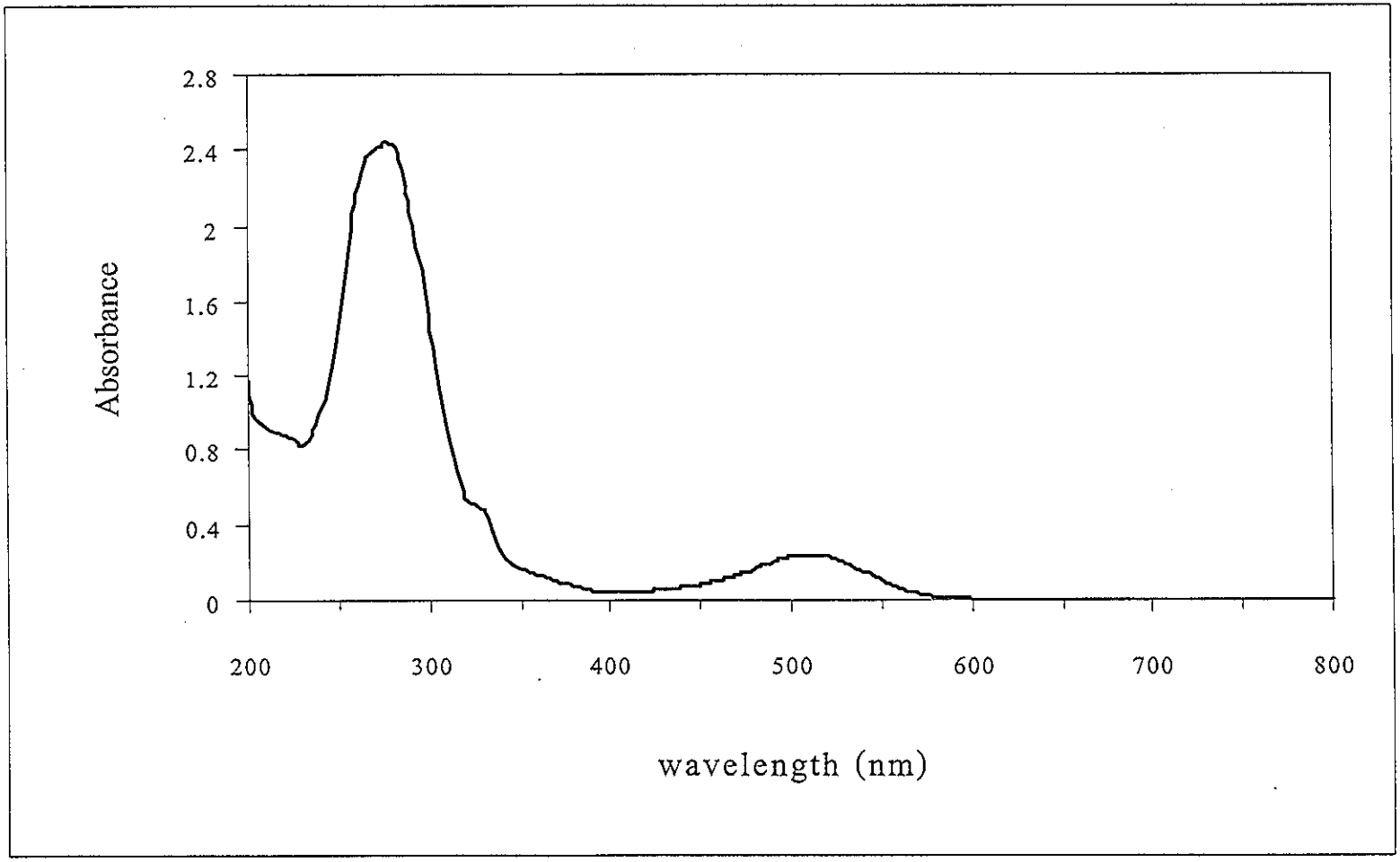

Figure 9 UV-Visible absorption spectrum of [Ru(tpy)(azpy)(Br)](BF_4) in acetonitrile.

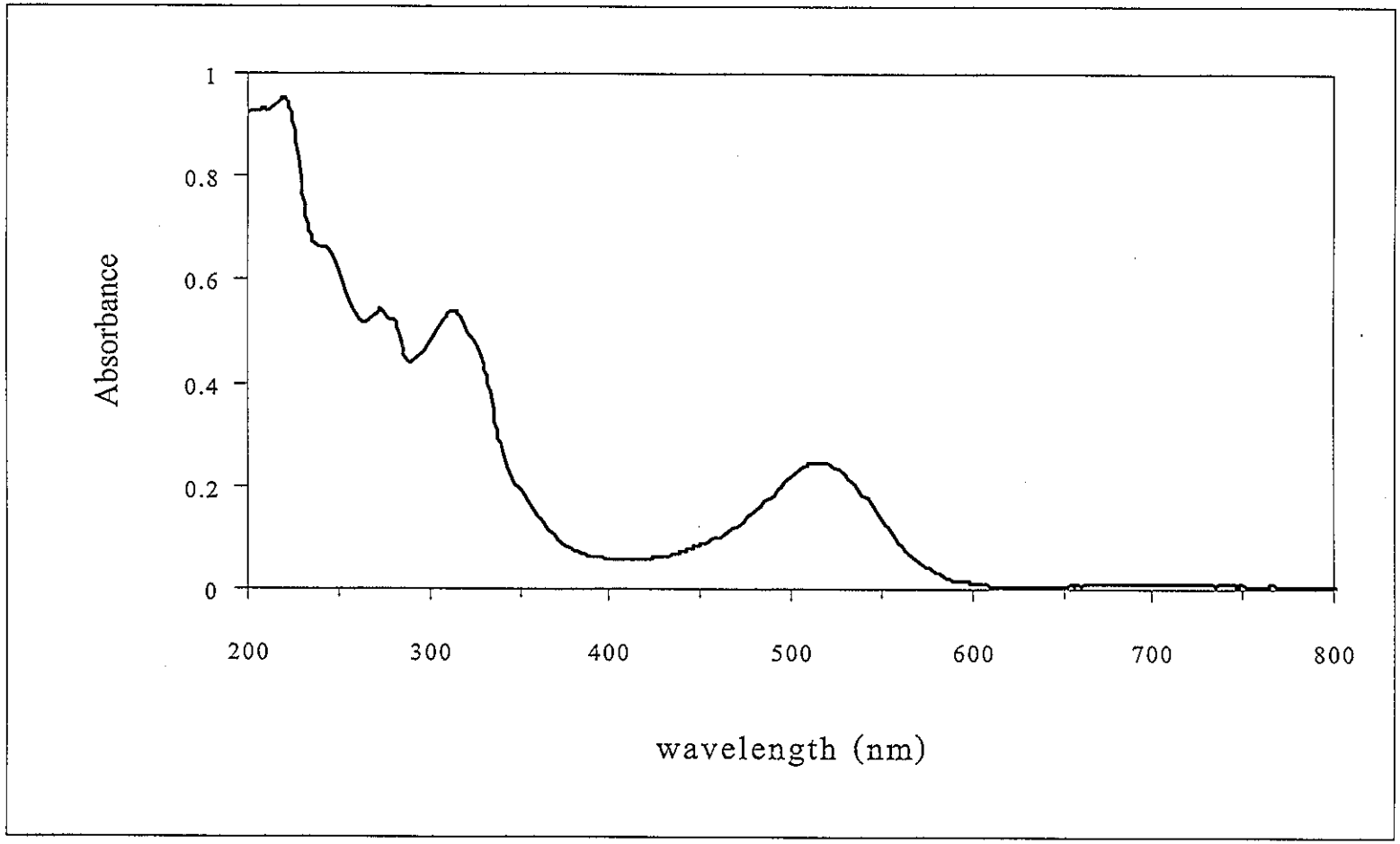

Figure 10 UV-Visible absorption spectrum of [Ru(tpy)(azpy)(I)](BF_4) in acetonitrile.

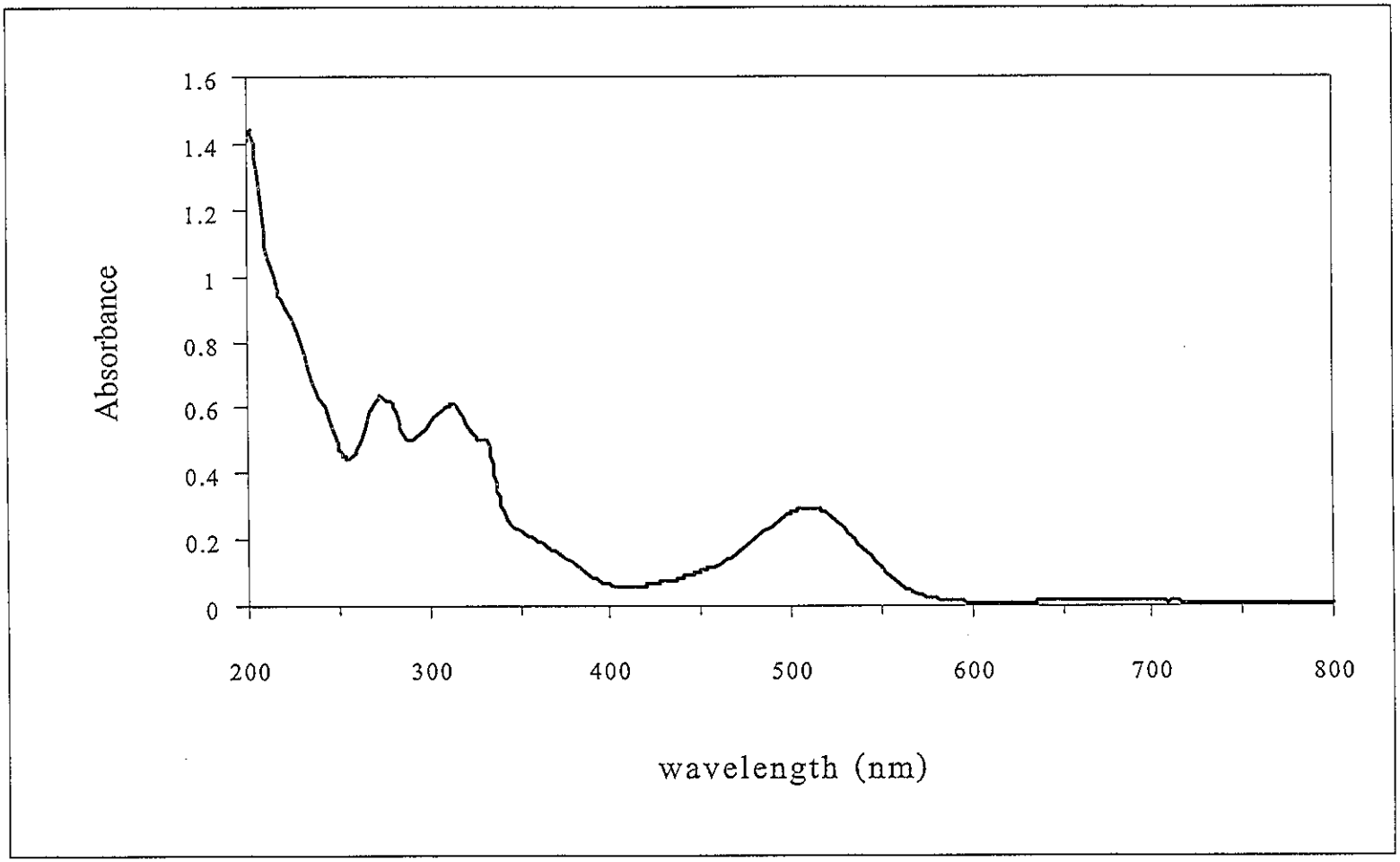

Figure 11 UV-Visible absorption spectrum of [Ru(tpy)(azpy)(NCS)](BF_4) in acetonitrile.

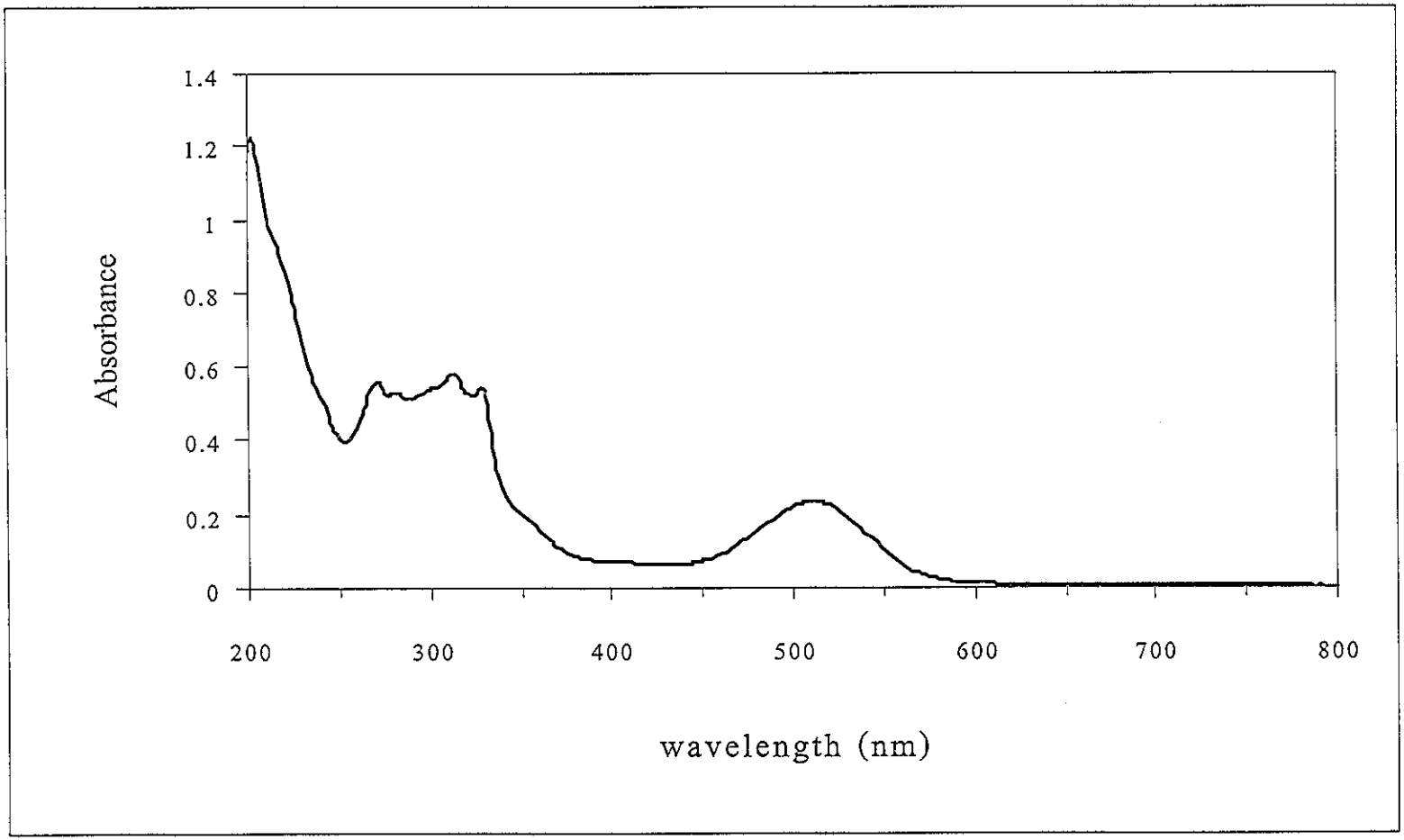

Figure 12 UV-Visible absorption spectrum of $[Ru(tpy)(azpy)(NO_2)](BF_4)$ in acetonitrile.

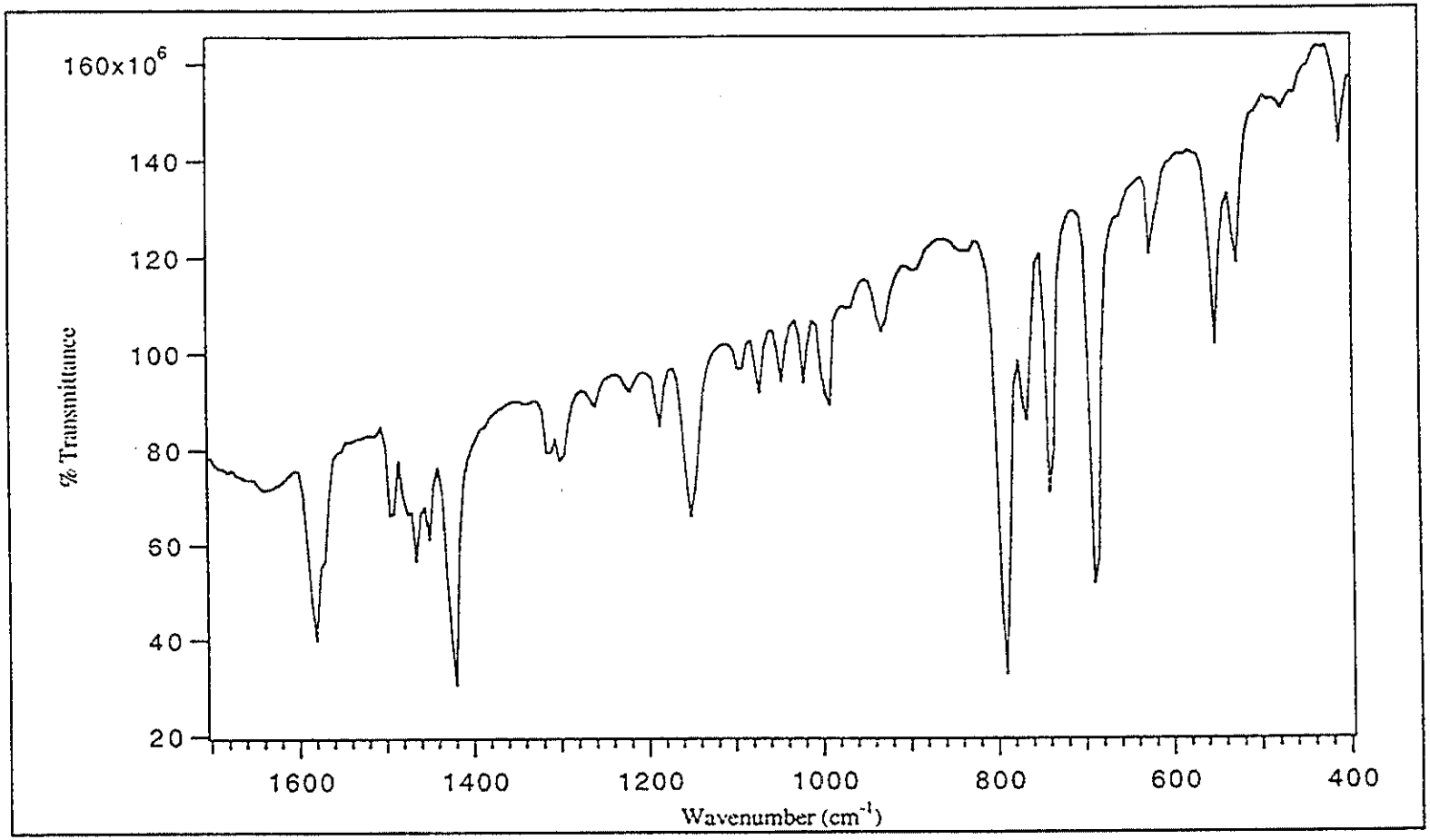

Figure 13 Infrared spectrum of 2-(phenylazo)pyridine. (range 400-1,700 cm^{-1})

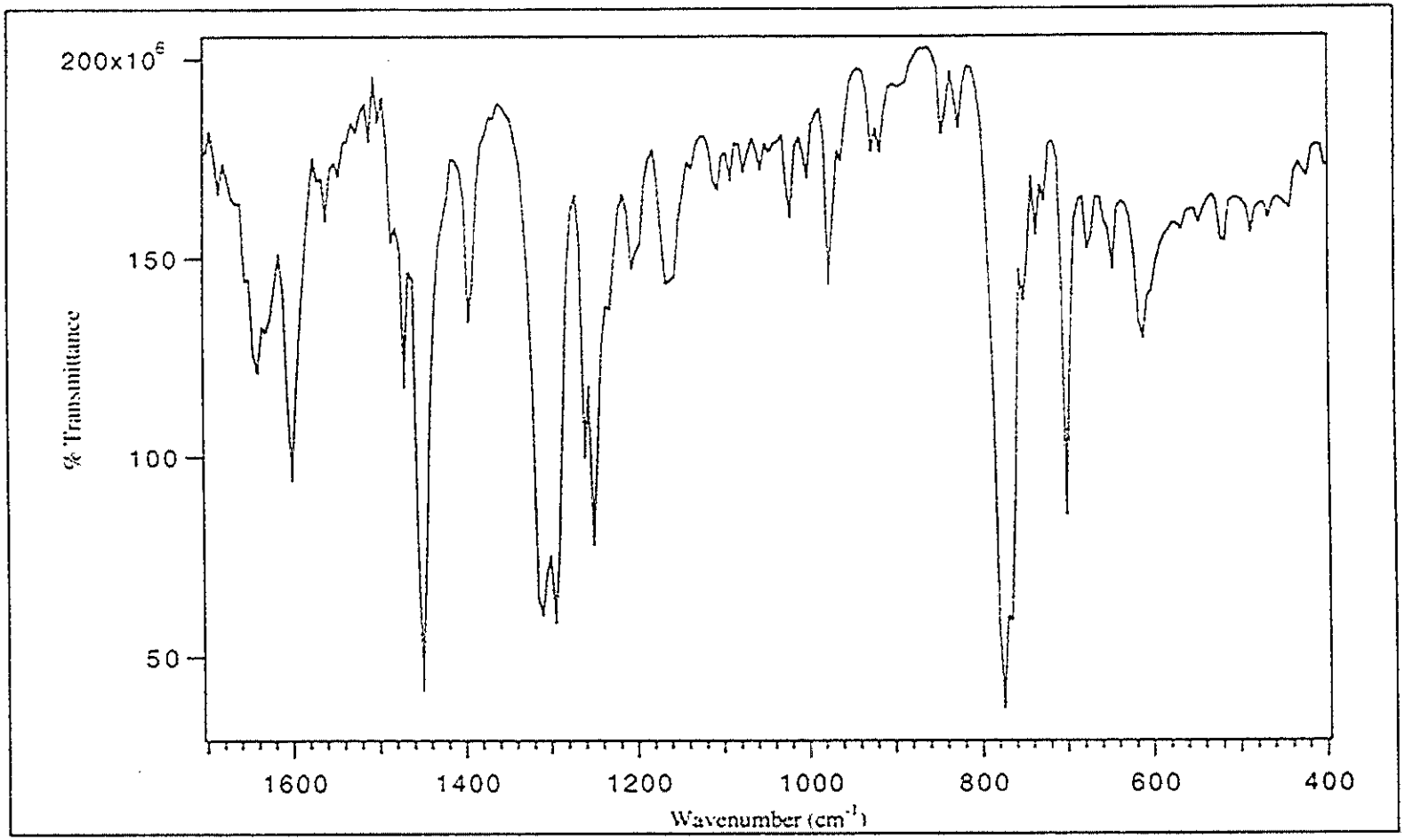

Figure 14 Infrared spectrum of [Ru(tpy)(azpy)(Cl)]Cl complex. (range 400-1,700 cm^{-1})

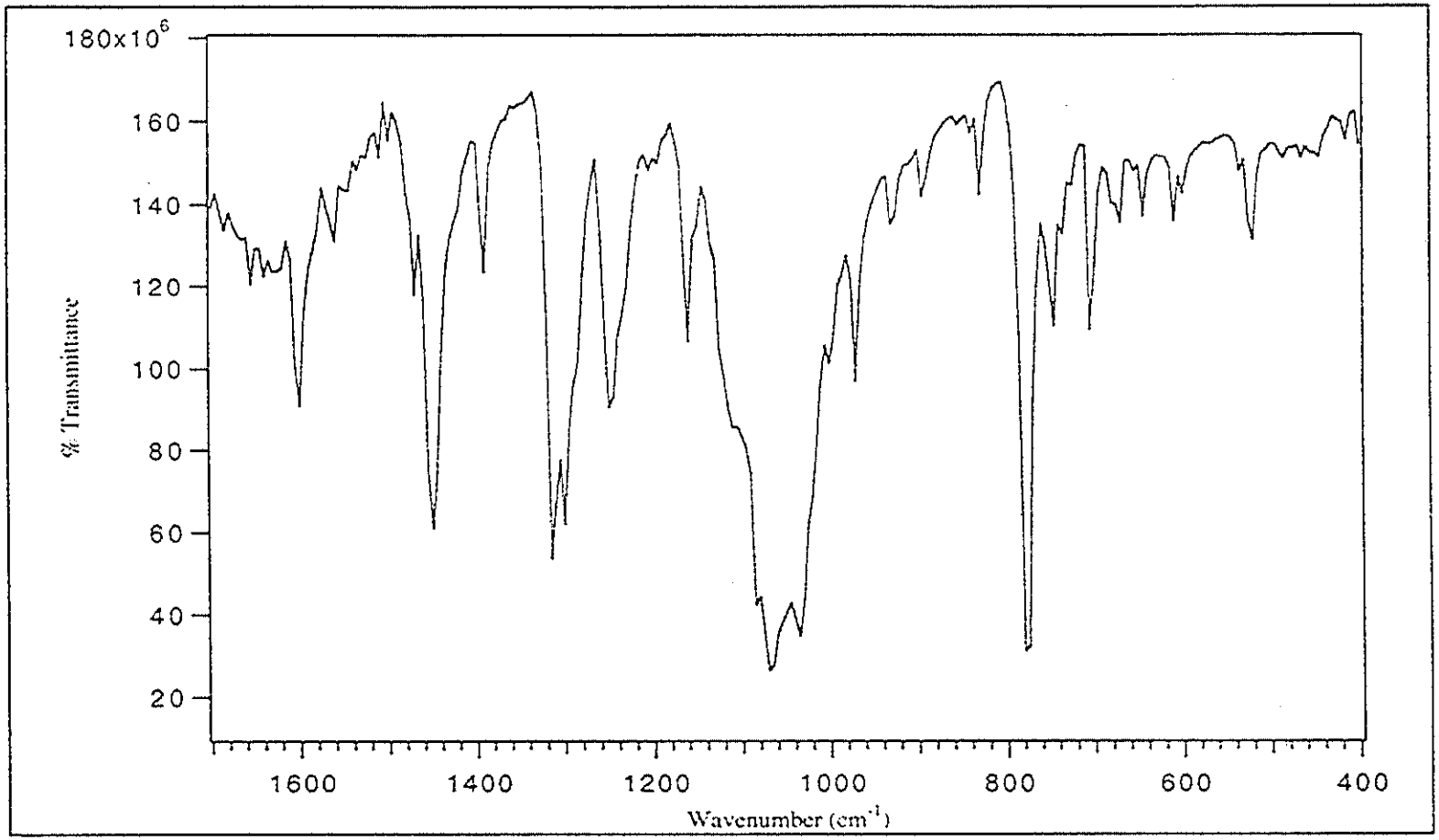

Figure 15 Infrared spectrum of [Ru(tpy)(azpy)(Br)](BF_4) complex. (range 400-1,700 cm^{-1})

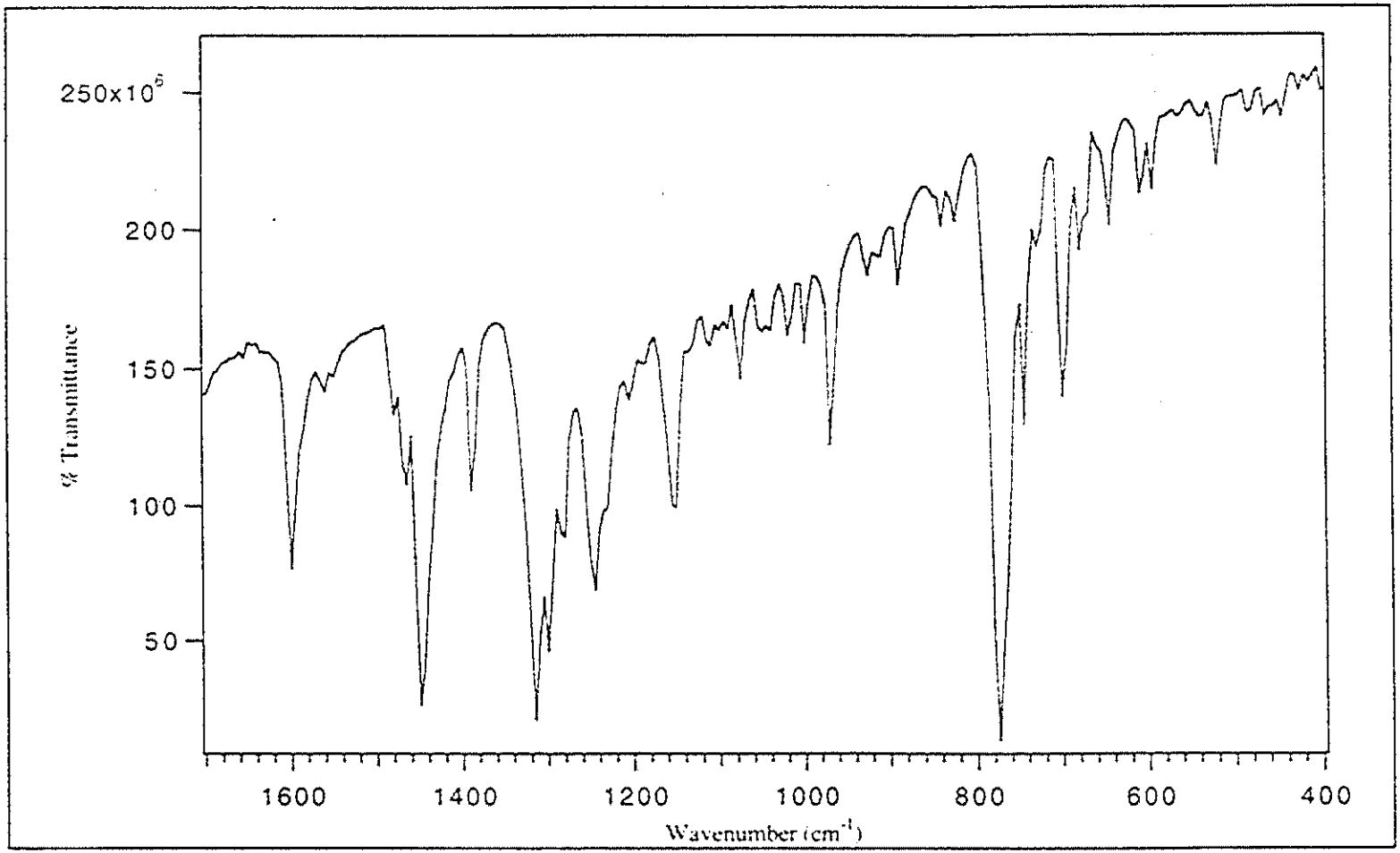

Figure 16 Infrared spectrum of [Ru(tpy)(azpy)(I)](I) complex. (range 400-1,700 cm^{-1})

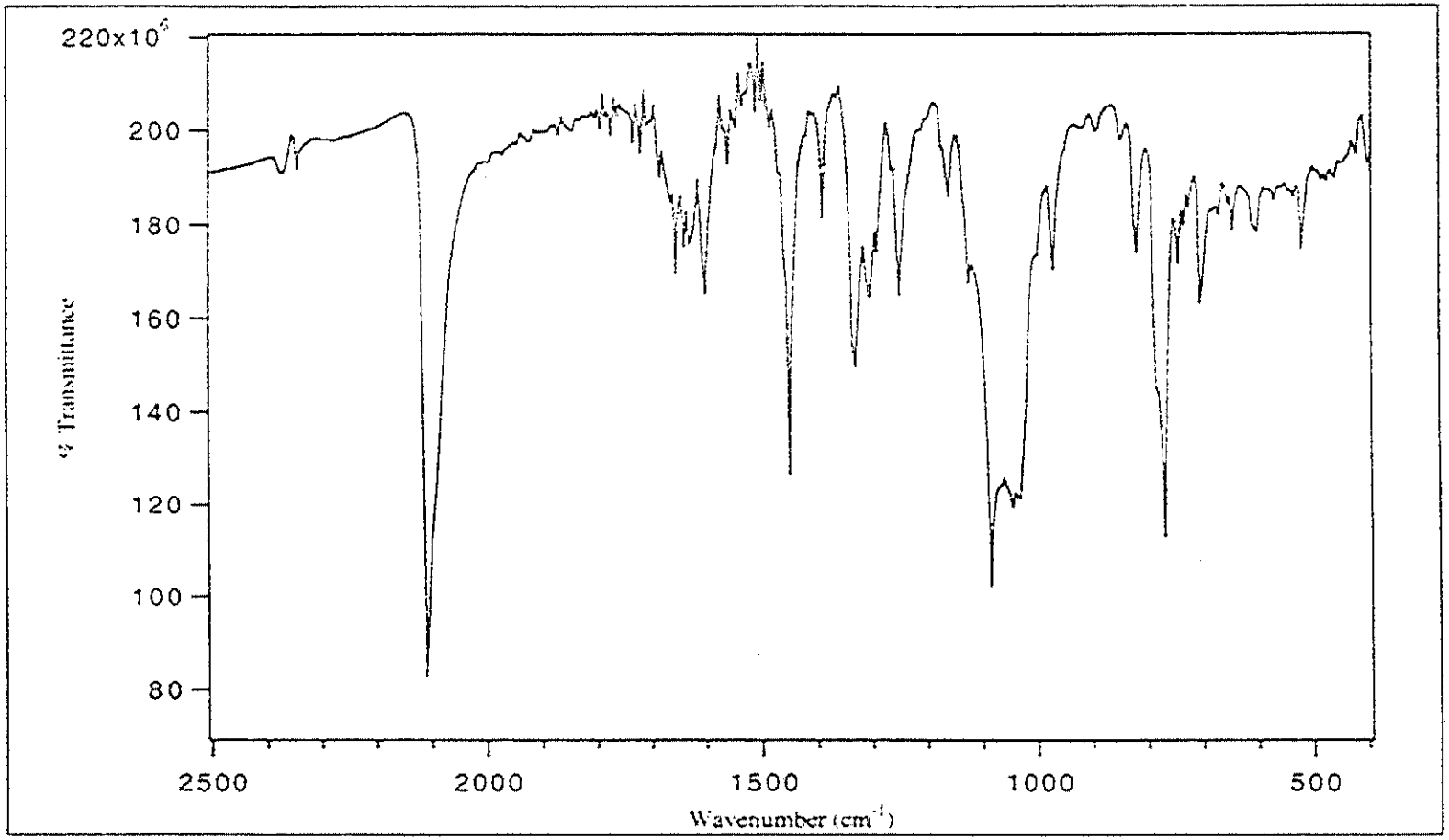

Figure 17 Infrared spectrum of [Ru(tpy)(azpy)(NCS)](BF_4) complex. (range 400-2,500 cm^{-1})

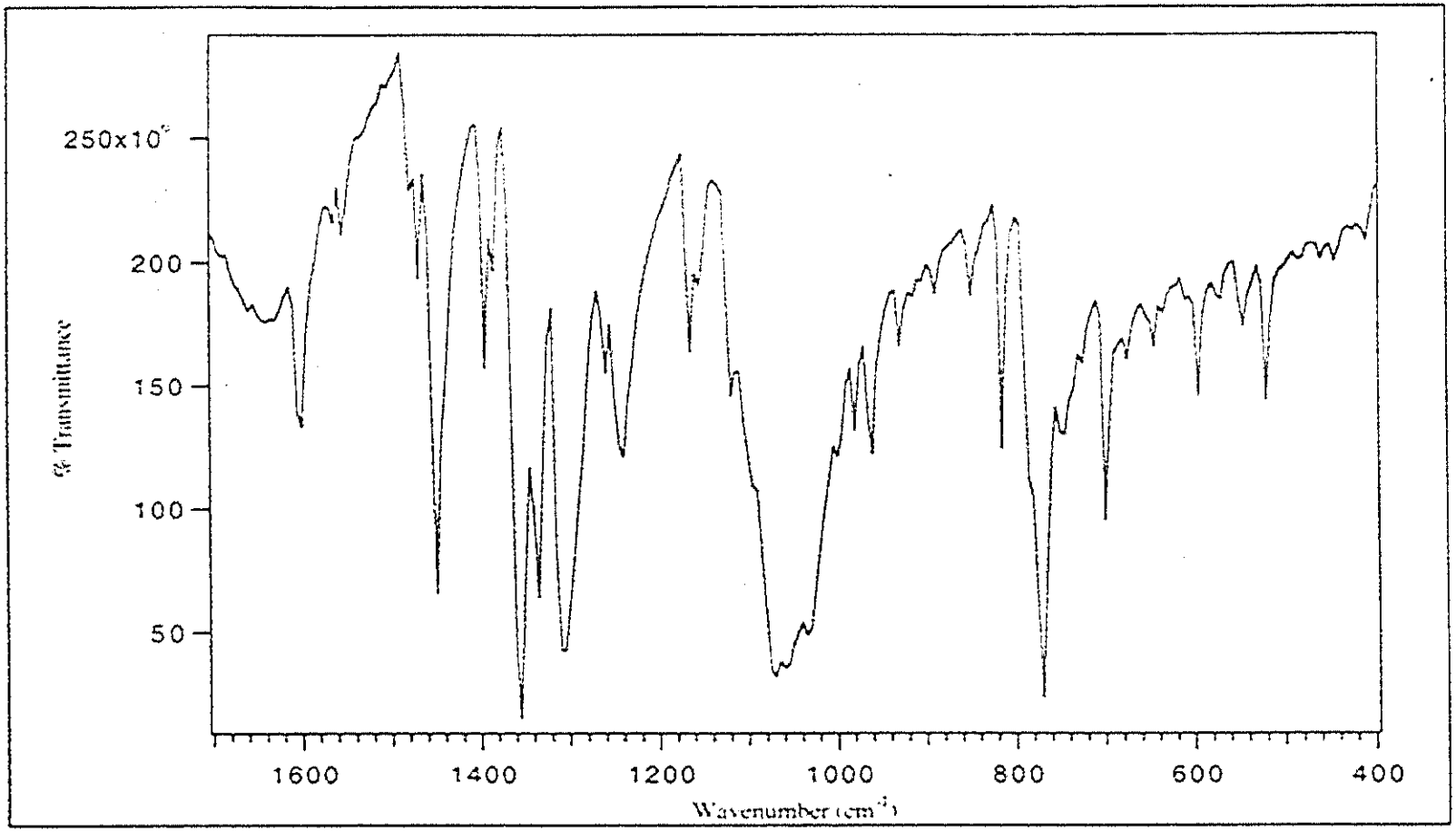

Figure 18 Infrared spectrum of $[Ru(tpy)(azpy)(NO_2)](BF_4)$ complex. (range 400-1,700 cm^{-1})

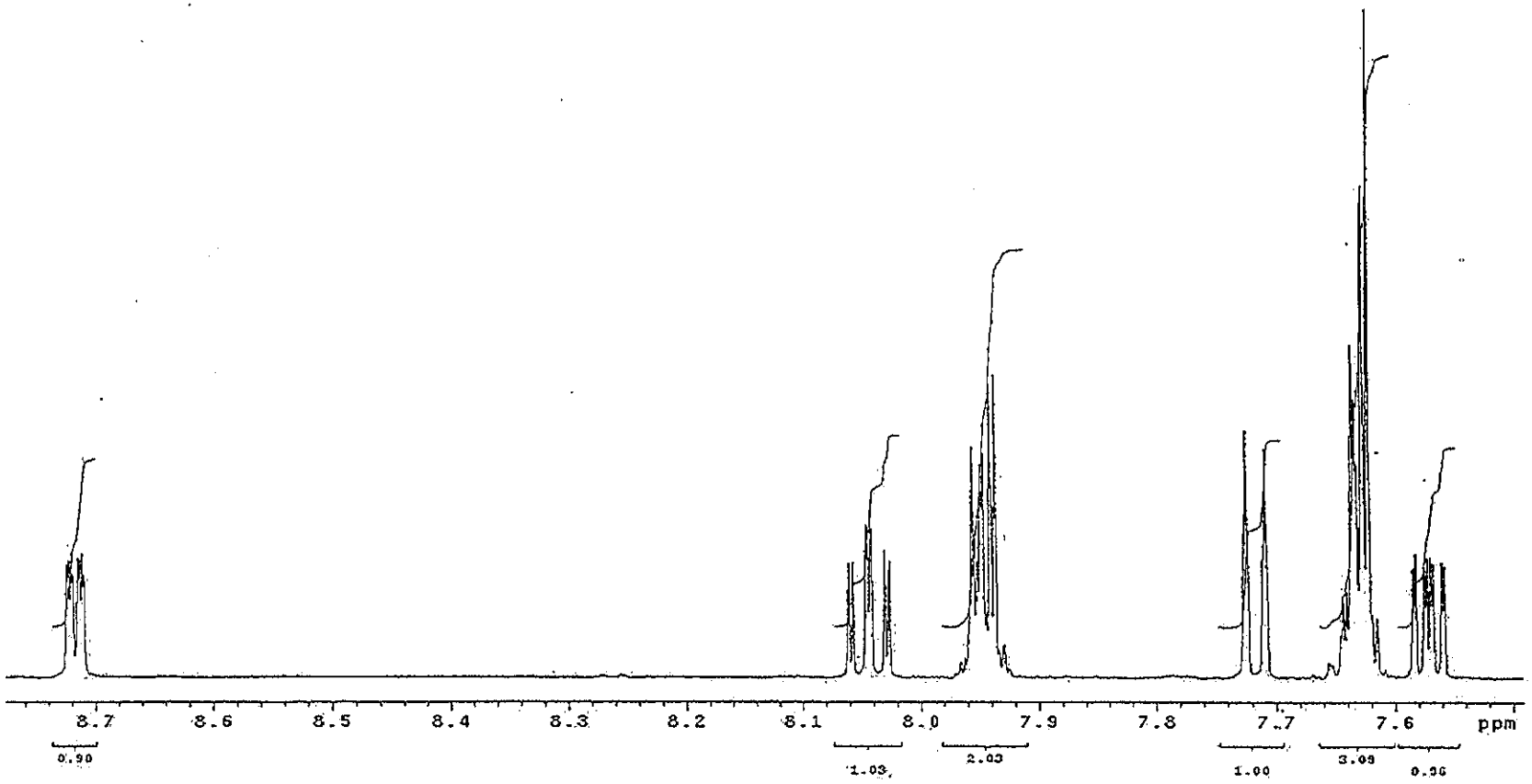

Figure 19 ^{1}H NMR spectrum of 2-(phenylazo)pyridine ligand in d_6-DMSO.

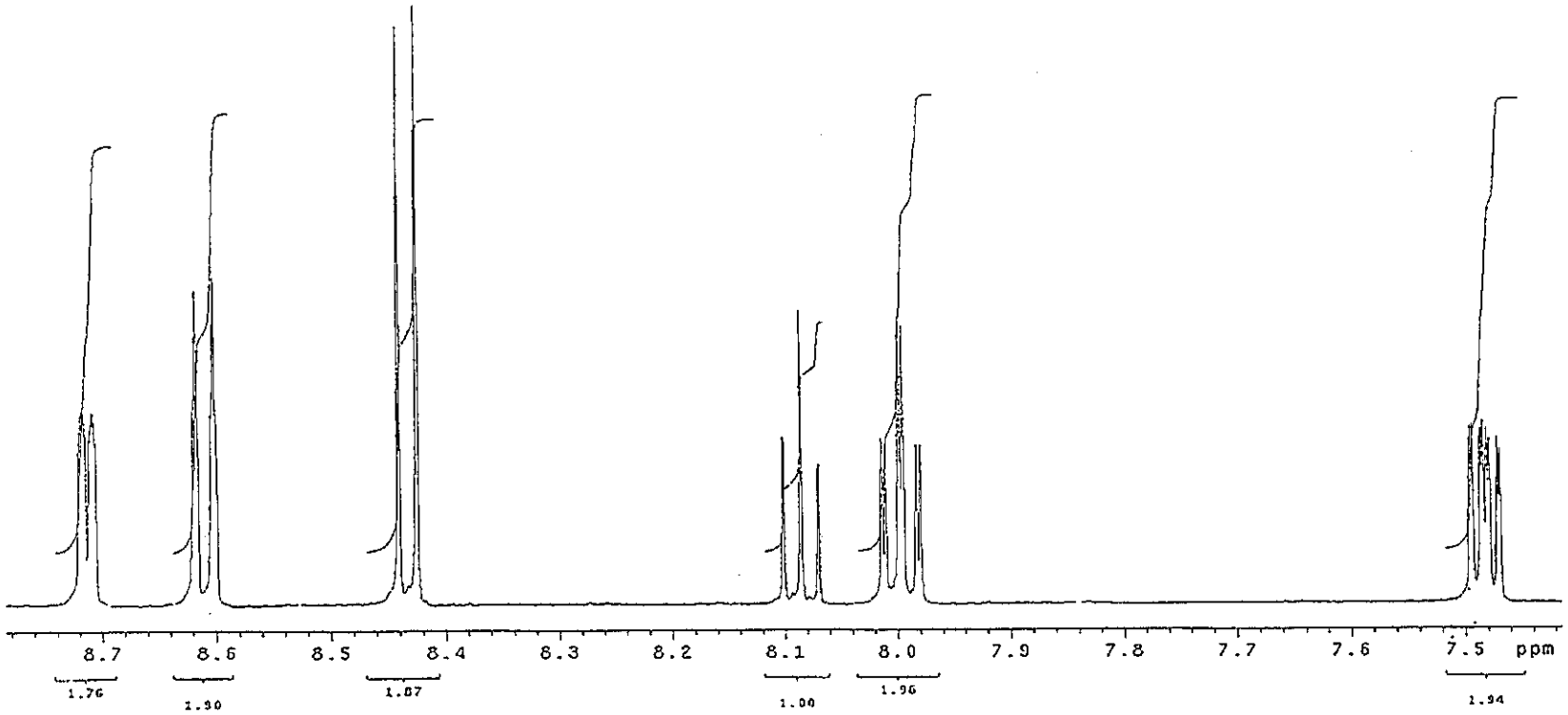

Figure 20 ^{1}H NMR spectrum of 2,2':6',2"-terpyridine ligand in d_6-DMSO.

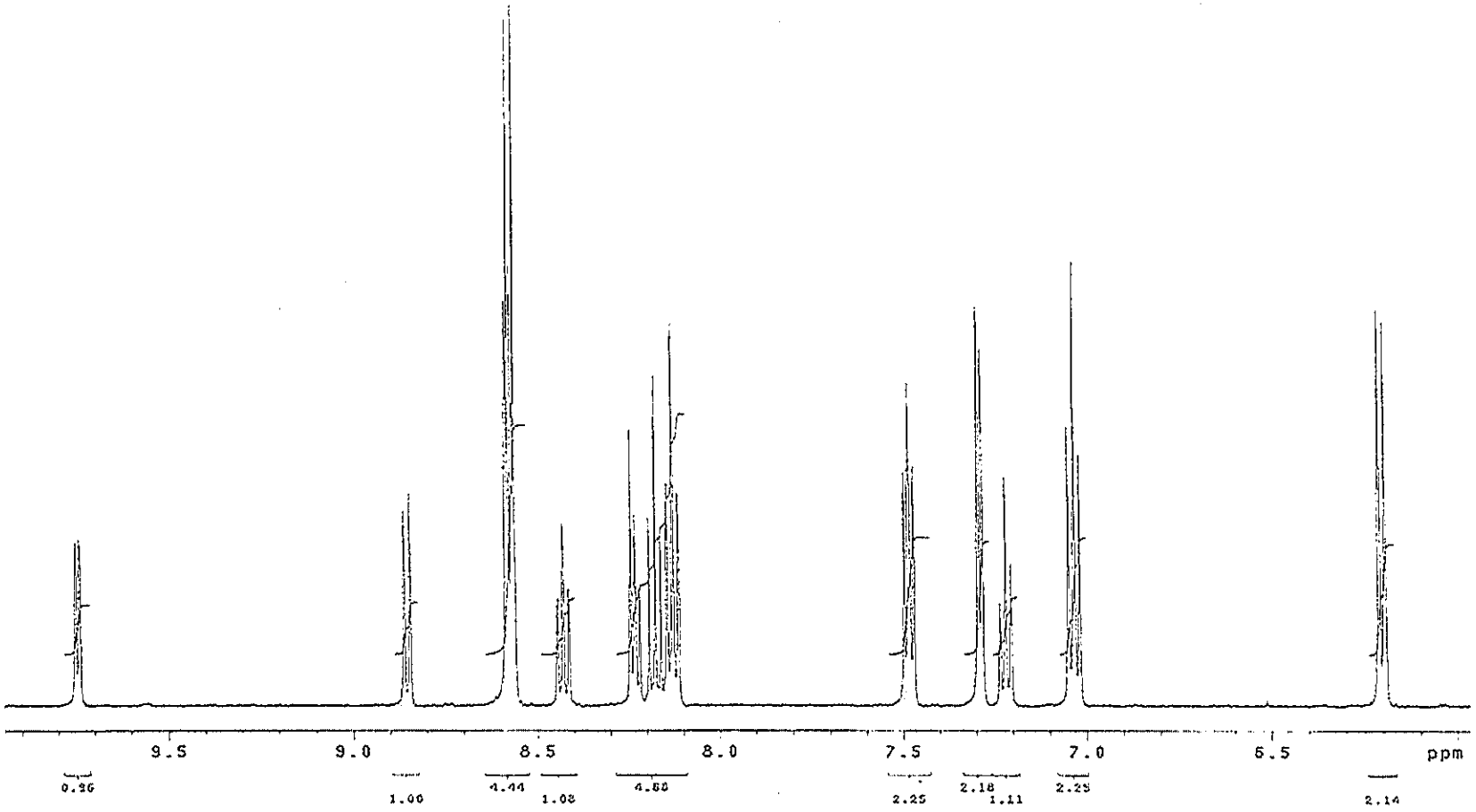

Figure 21 ^{1}H NMR spectrum of [Ru(tpy)(azpy)(Cl)](BF_4) complex in d_6-DMSO.

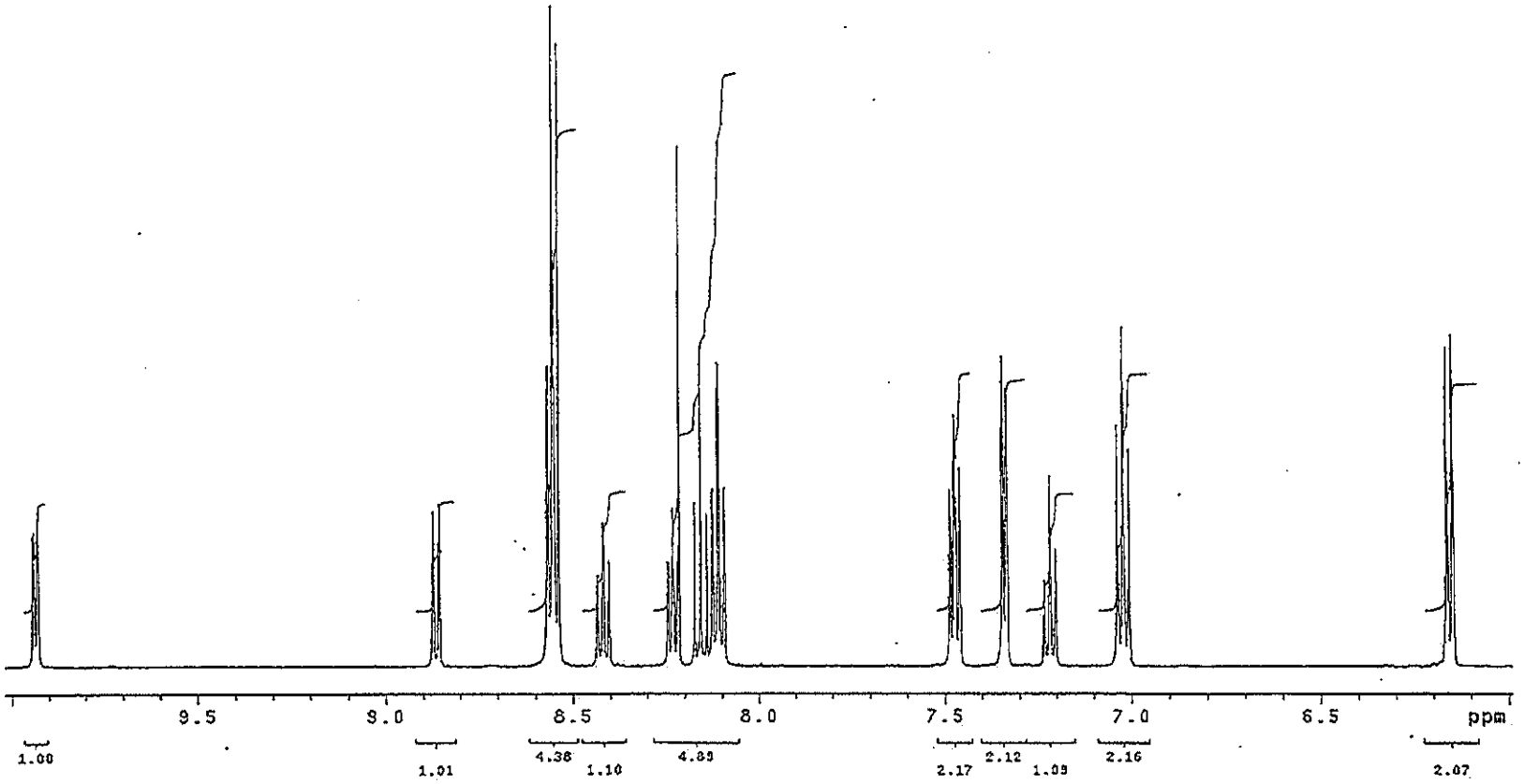

Figure 22 ^{1}H NMR spectrum of [Ru(tpy)(azpy)(Br)](BF$_4$) complex in d$_6$-DMSO.

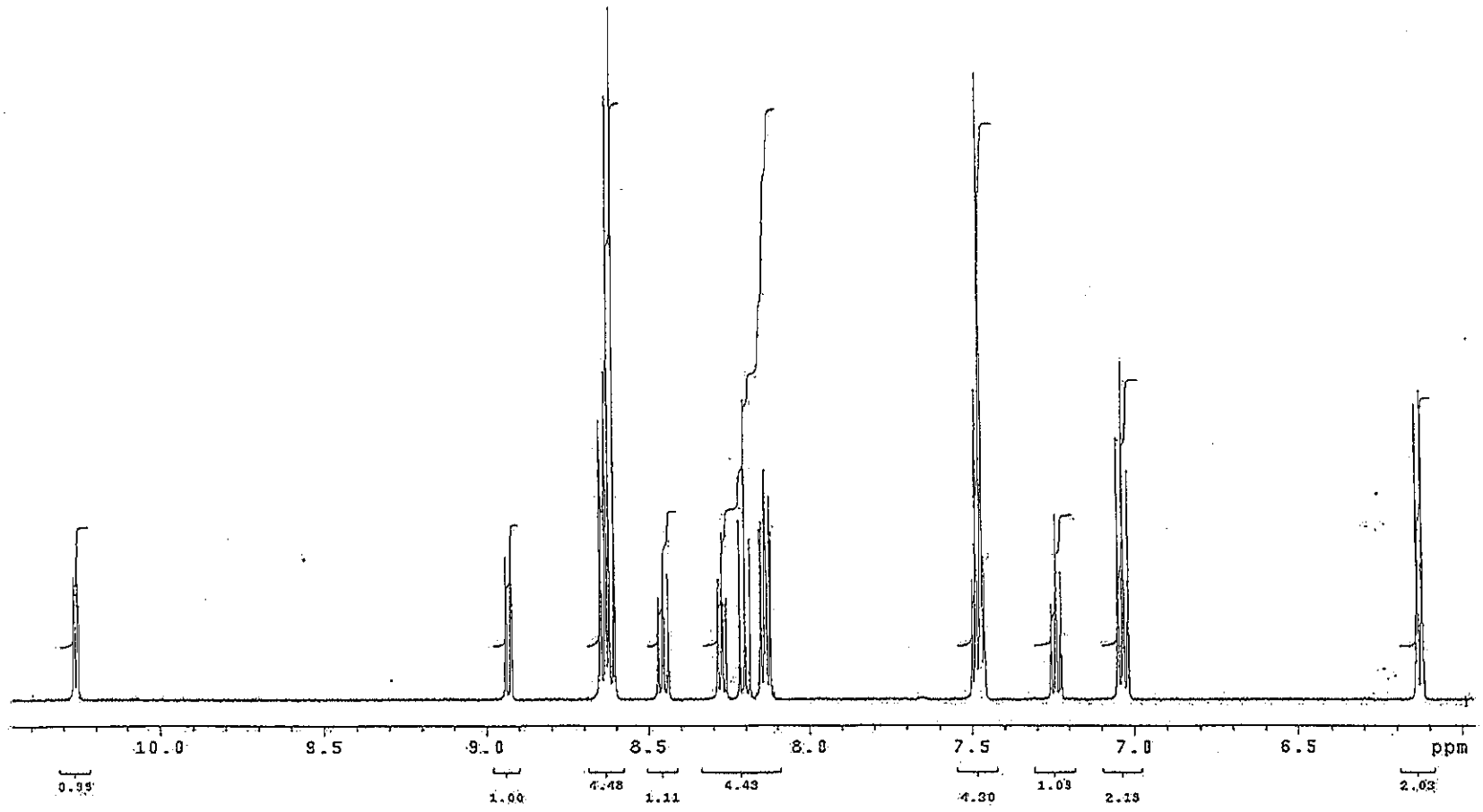

Figure 23 ^{1}H NMR spectrum of [Ru(tpy)(azpy)(I)](BF$_4$) complex in d$_6$-DMSO.

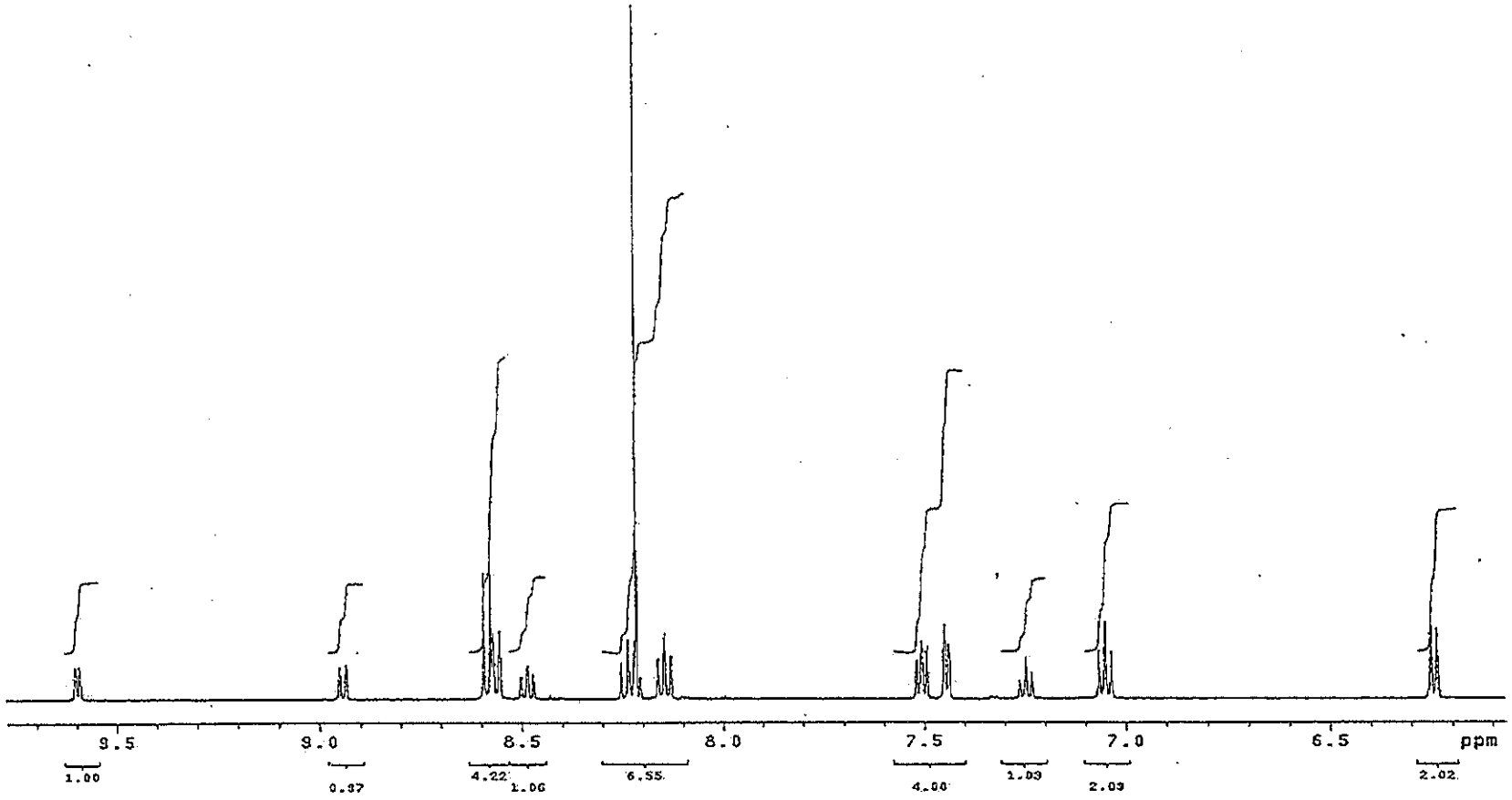

Figure 24 ^{1}H NMR spectrum of $[Ru(tpy)(azpy)(NO_2)](BF_4)$ complex in d_6-DMSO.

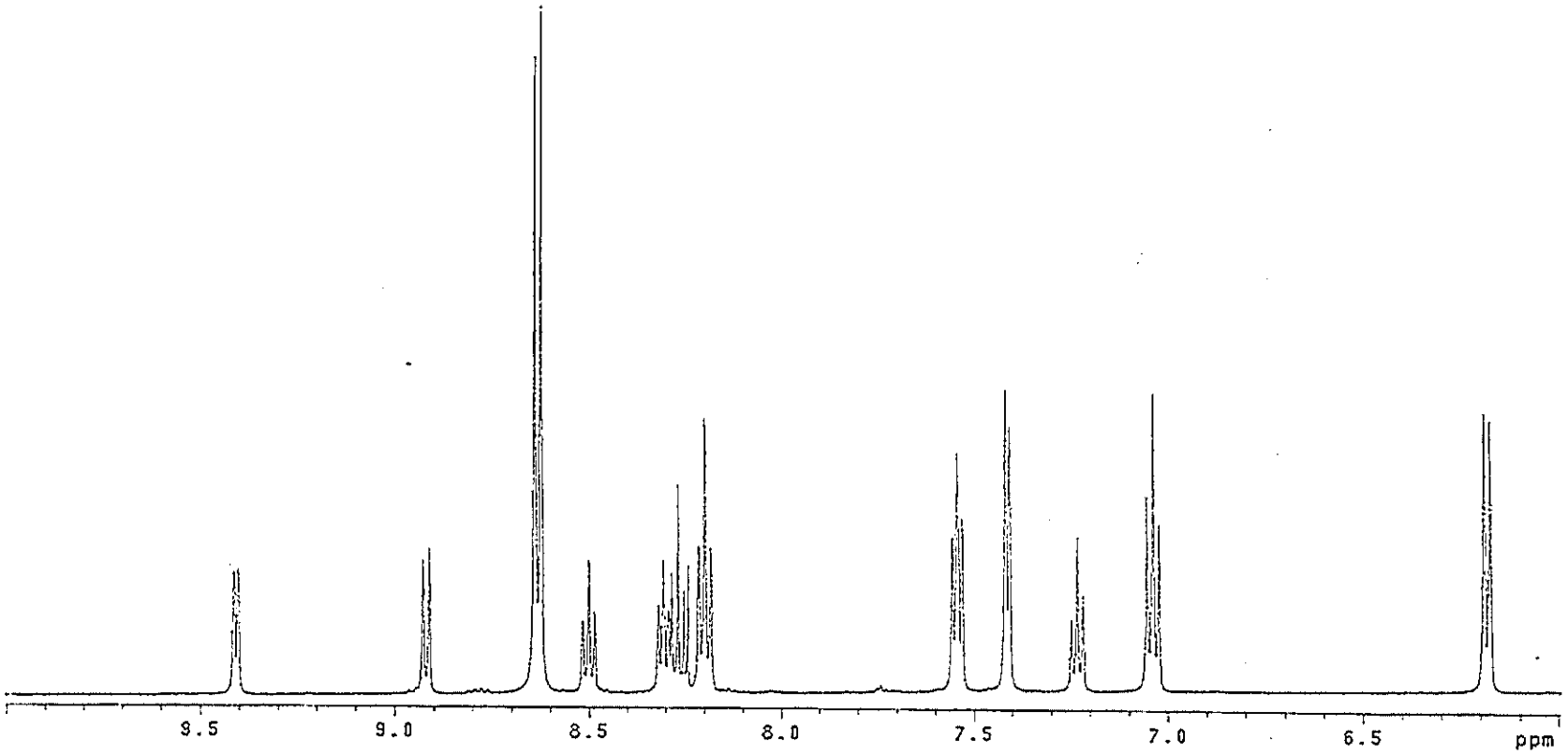

Figure 25 ^{1}H NMR spectrum of [Ru(tpy)(azpy)(NCS)](BF$_4$) complex in d$_6$-DMSO.

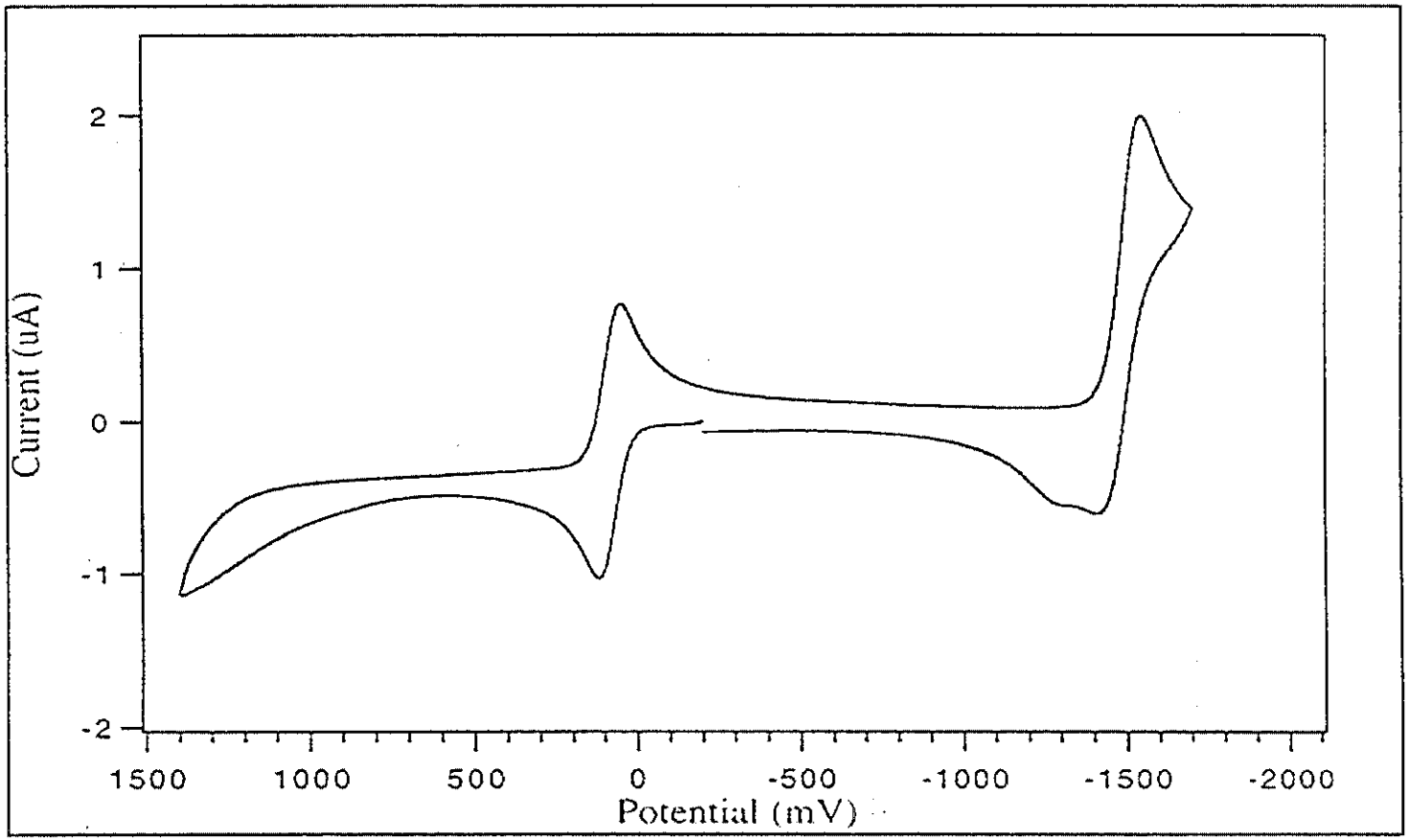

Figure 26 Cyclic voltammogram of 2-(phenylazo)pyridine in acetonitrile. (scan rate 50 mV/s)

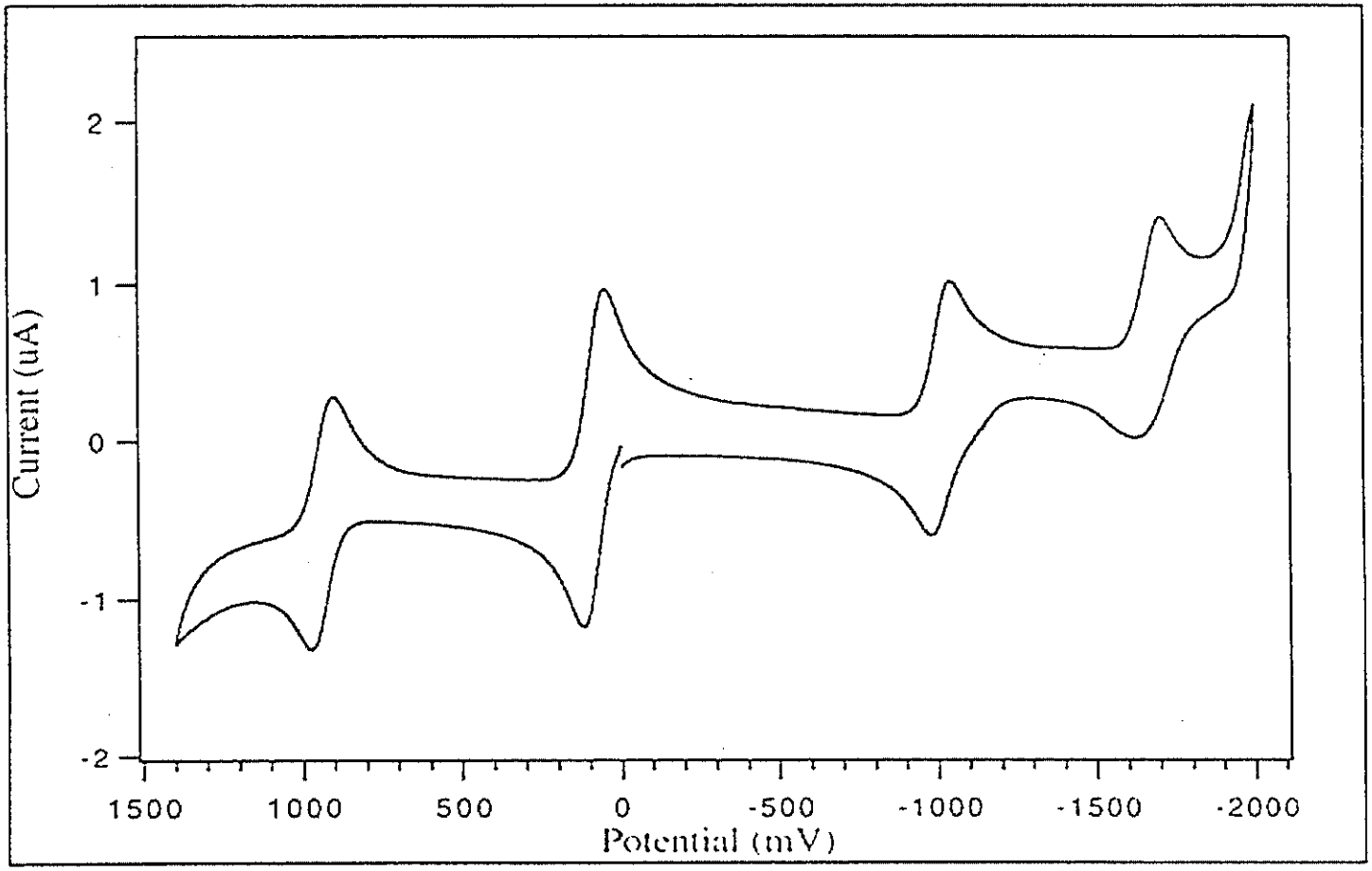

Figure 27 Cyclic voltammogram of [Ru(tpy)(azpy)(Cl)](BF_4) in acetonitrile. (scan rate 50 mV/s)

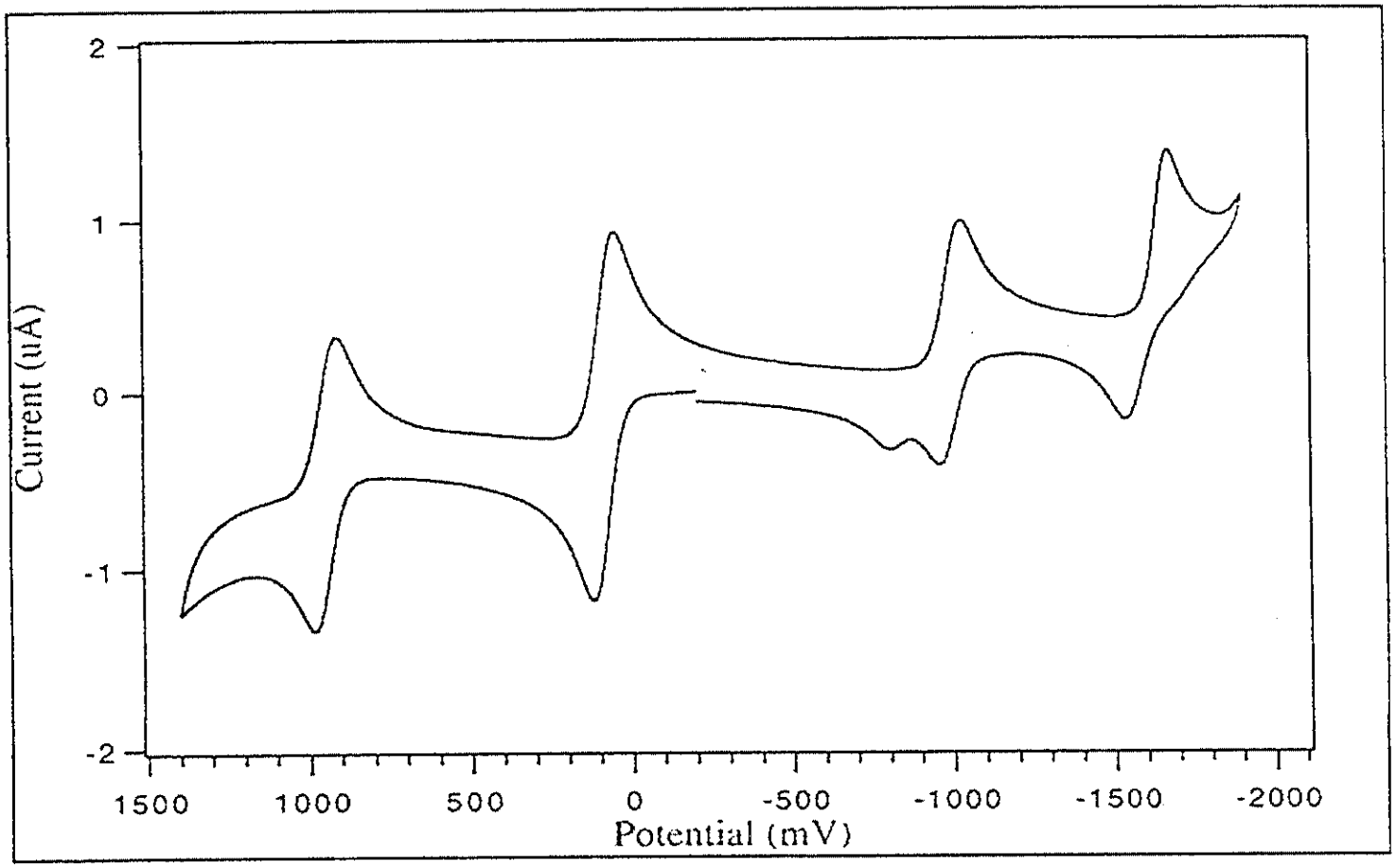

Figure 28 Cyclic voltammogram of [Ru(tpy)(azpy)(Br)](BF_4) in acetonitrile. (scan rate 50 mV/s)

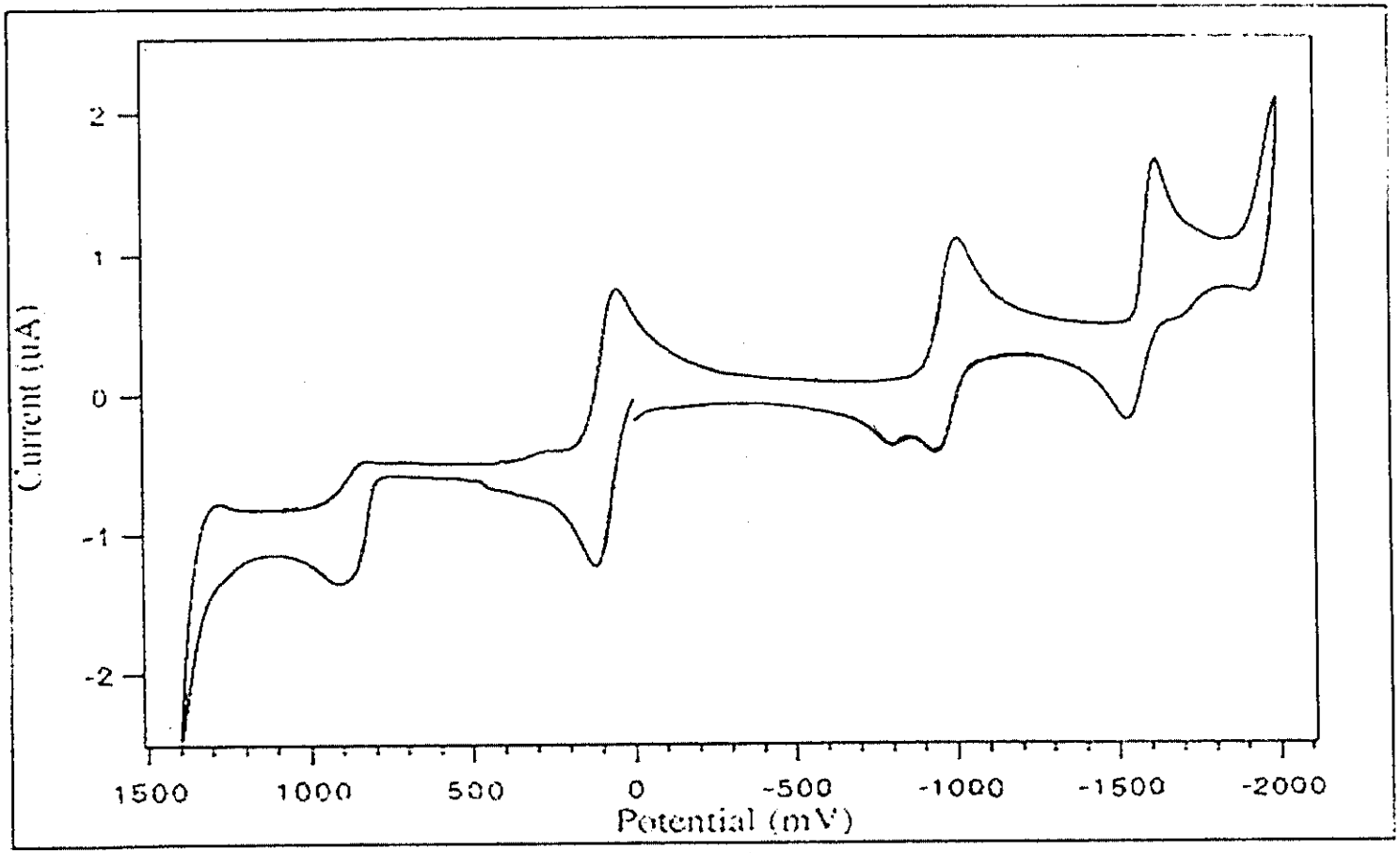

Figure 29 Cyclic voltammogram of [Ru(tpy)(azpy)(I)](BF_4) in acetonitrile. (scan rate 50 mV/s)

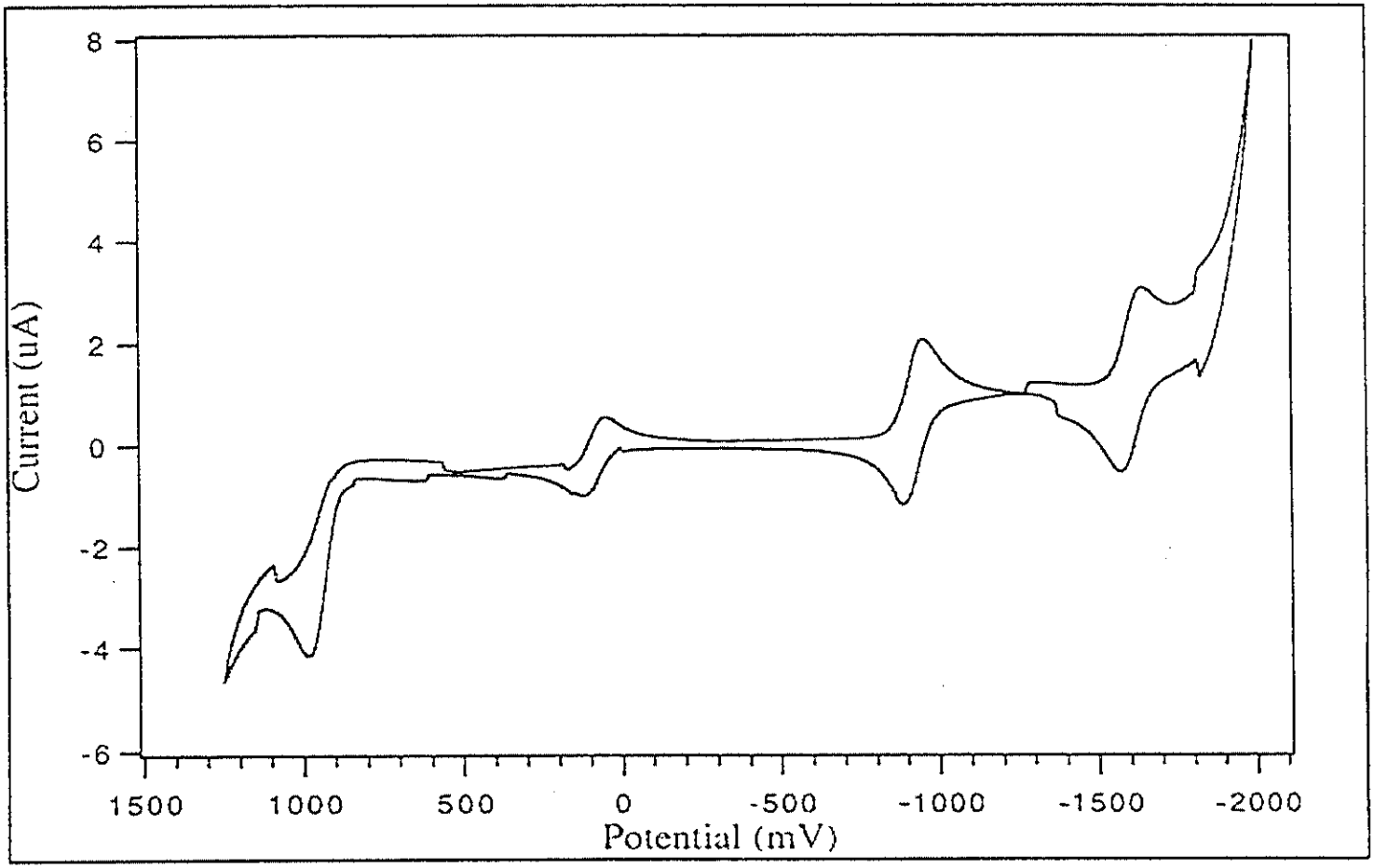

Figure 30 Cyclic voltammogram of [Ru(tpy)(azpy)(NCS)](BF_4) in acetonitrile. (scan rate 50 mV/s)

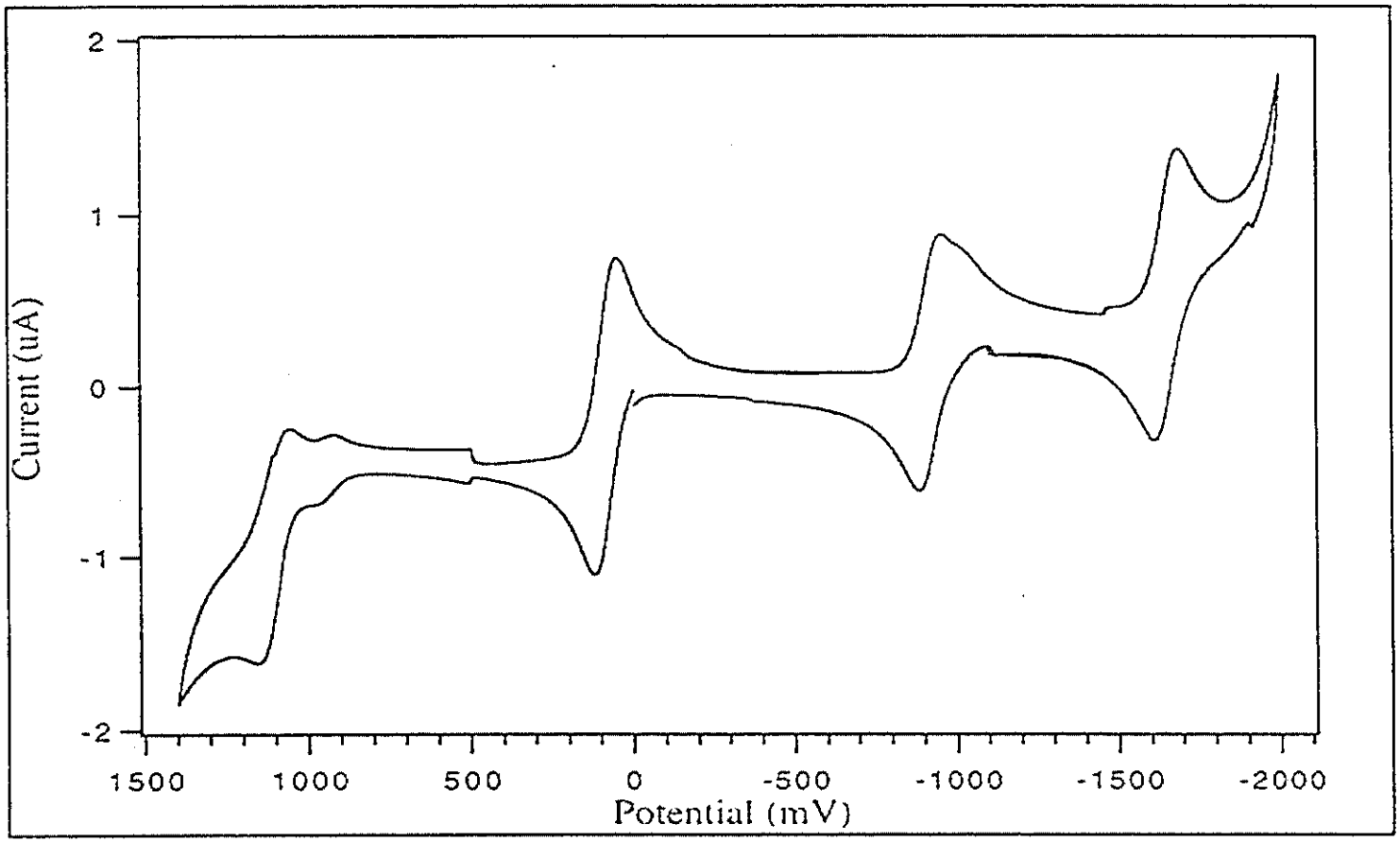

Figure 31 Cyclic voltammogram of $[Ru(tpy)(azpy)(NO_2)](BF_4)$ in acetonirile. (scan rate 50 mV/s)

3.2 Single Crystal X-ray Diffraction

Crystal structure

The X-ray crystallography is the most important technique to identify the geometry of the complexes.

The crystal structures of 4 complexes, [Ru(tpy)(azpy)Cl]Cl (1), [Ru(tpy)(azpy)-(Cl/I)](BF_4) (2), [Ru(tpy)(azpy)(NO_2)](BF_4) (3) and [Ru(tpy)(azpy)(NCS)](BF_4) (4), are shown in Figure 32-35, respectively. The crystallographic data are listed in Table 3-14. These complexes have two isomer, 1 and 2 isomer (Figure 36), the crystals of (1) are 1 isomer and the crystals of (2)-(4) are 2 isomer.

Table 3 The crystallographic data for [Ru(tpy)(azpy)Cl]Cl.

Identical code	my16m	
Empirical formula	$C_{26}H_{20}N_6Cl_2Ru$	
Formula weight	588.45	
Temperature	295(2) K	
Wavelength	0.71073	
Crystal system	monoclinic	
Space group	P2(1)/n	
Unit cell dimensions	a = 8.7780(9) Å	$\alpha = 90^\circ$
	b = 22.607(2) Å	$\beta = 99.755(2)^\circ$
	c = 12.8686(14) Å	$\gamma = 90^\circ$
Volume	2516.8(5) $Å^3$	
Z	4	
Density (calculated)	1.553 mg/m^3	

Absorption coefficient	0.862 mm^{-1}
F(000)	1184
Crystal size	0.50 x 0.40 x 0.20 mm
Theta range for data collection	1.80 to 28.28
Index ranges	$-11 \leq h \leq 11, -30 \leq k \leq 25, -16 \leq l \leq 17$
Reflections collected	16145
Observed reflection [$I > 2\sigma(I)$]	4429
Independent reflections	6033 [R(int) = 0.0411]
Refinement method	Full-matrix least-squares on F^2
Data / restraints / parameters	6033 / 0 / 327
Goodness-of-fit on F^2	0.937
Final R indices [$I > 2\sigma(I)$]	R1 = 0.0524, wR2 = 0.1439
R indices (all data)	R1 = 0.0772, wR2 = 0.1575
Largest diff. Peak and hole	1.492 and -0.585 e. $Å^3$

Table 4 Non-hydrogen interatomic distances of [Ru(tpy)(azpy)Cl]Cl.

Atom	Distance (Å)
Ru-N(5)	1.990(4)
Ru-N(3)	1.999(4)
Ru-N(1)	2.019(4)
Ru-N(6)	2.073(4)
Ru-N(4)	2.076(4)
Ru-Cl(1)	2.4107(12)
N(1)-C(1)	1.344(6)
N(1)-C(5)	1.357(6)
C(1)-C(2)	1.362(7)
C(2)-C(3)	1.374(8)
C(3)-C(4)	1.377(8)
C(4)-C(5)	1.389(7)
C(5)-N(2)	1.384(6)
N(2)-N(3)	1.300(5)
N(3)-C(6)	1.434(6)
C(6)-C(7)	1.380(7)
C(6)-C(11)	1.388(7)
C(7)-C(8)	1.384(7)
C(8)-C(9)	1.382(9)
C(9)-C(10)	1.380(9)
C(10)-C(11)	1.366(8)
N(4)-C(25)	1.348(7)

Table 4 (continued)

Atom	Distance (Å)
N(4)-C(16)	1.361(6)
C(12)-C(24)	1.379(8)
C(12)-C(26)	1.390(8)
C(13)-C(25)	1.364(8)
C(13)-C(14)	1.396(8)
C(14)-C(15)	1.376(8)
C(15)-C(16)	1.385(7)
C(16)-C(17)	1.465(7)
N(5)-C(21)	1.348(6)
N(5)-C(17)	1.351(6)
C(17)-C(18)	1.392(7)
C(18)-C(19)	1.380(8)
C(19)-C(20)	1.383(8)
C(20)-C(21)	1.389(7)
C(21)-C(22)	1.479(7)
N(6)-C(26)	1.339(6)
N(6)-C(22)	1.365(6)
C(22)-C(23)	1.388(7)
C(23)-C(24)	1.385(8)

Table 5 Non-hydrogen interbond angles of [Ru(tpy)(azpy)Cl]Cl.

Atom	Angle (°)
N(5)-Ru-N(3)	172.90(15)
N(5)-Ru-N(1)	97.20(15)
N(3)-Ru-N(1)	76.70(15)
N(5)-Ru-N(6)	78.82(16)
N(3)-Ru-N(6)	104.82(16)
N(1)-Ru-N(6)	92.37(15)
N(5)-Ru-N(4)	78.57(16)
N(3)-Ru-N(4)	97.59(16)
N(1)-Ru-N(4)	89.76(15)
N(6)-Ru-N(4)	157.38(17)
N(5)-Ru-Cl(1)	86.77(11)
N(3)-Ru-Cl(1)	99.26(11)
N(1)-Ru-Cl(1)	175.85(11)
N(6)-Ru-Cl(1)	89.58(11)
N(4)-Ru-Cl(1)	89.84(11)
C(1)-N(1)-C(5)	118.1(4)
C(1)-N(1)-Ru	128.4(3)
C(5)-N(1)-Ru	113.5(3)
N(1)-C(1)-C(2)	122.7(5)
C(1)-C(2)-C(3)	119.6(5)
C(2)-C(3)-C(4)	119.0(5)

Table 5 (continued)

Atom	Angle (°)
C(3)-C(4)-C(5)	119.1(5)
N(1)-C(5)-N(2)	118.0(4)
N(1)-C(5)-C(4)	121.5(5)
N(2)-C(5)-C(4)	120.6(5)
N(3)-N(2)-C(5)	111.3(4)
N(2)-N(3)-C(6)	112.3(4)
N(2)-N(3)-Ru	120.2(3)
C(6)-N(3)-Ru	127.0(3)
C(7)-C(6)-C(11)	120.4(5)
C(7)-C(6)-N(3)	119.4(4)
C(11)-C(6)-N(3)	120.2(5)
C(6)-C(7)-C(8)	119.4(5)
C(9)-C(8)-C(7)	119.9(5)
C(10)-C(9)-C(8)	120.1(5)
C(11)-C(10)-C(9)	120.2(6)
C(10)-C(11)-C(6)	119.8(6)
C(25)-N(4)-C(16)	117.7(4)
C(25)-N(4)-Ru	127.8(4)
C(16)-N(4)-Ru	114.5(3)
C(24)-C(12)-C(26)	119.6(5)
C(25)-C(13)-C(14)	118.5(5)

Table 5 (continued)

Atom	Angle (°)
C(15)-C(14)-C(13)	119.0(5)
C(14)-C(15)-C(16)	119.5(5)
N(4)-C(16)-C(15)	121.7(5)
N(4)-C(16)-C(17)	114.7(4)
C(15)-C(16)-C(17)	123.5(5)
C(21)-N(5)-C(17)	122.4(4)
C(21)-N(5)-Ru	119.1(3)
C(17)-N(5)-Ru	118.5(3)
N(5)-C(17)-C(18)	119.4(5)
N(5)-C(17)-C(16)	113.6(4)
C(18)-C(17)-C(16)	127.1(5)
C(19)-C(18)-C(17)	118.7(5)
C(18)-C(19)-C(20)	121.4(5)
C(19)-C(20)-C(21)	118.1(5)
N(5)-C(21)-C(20)	120.1(5)
N(5)-C(21)-C(22)	112.7(4)
C(20)-C(21)-C(22)	127.2(5)
C(26)-N(6)-C(22)	118.3(4)
C(26)-N(6)-Ru	127.6(4)
C(22)-N(6)-Ru	114.1(3)
N(6)-C(22)-C(23)	121.9(5)

Table 5 (continued)

Atom	Angle (°)
N(6)-C(22)-C(21)	115.2(4)
C(23)-C(22)-C(21)	122.9(5)
C(24)-C(23)-C(22)	119.2(5)
C(12)-C(24)-C(23)	118.9(5)
N(4)-C(25)-C(13)	123.6(5)
N(6)-C(26)-C(12)	122.2(5)

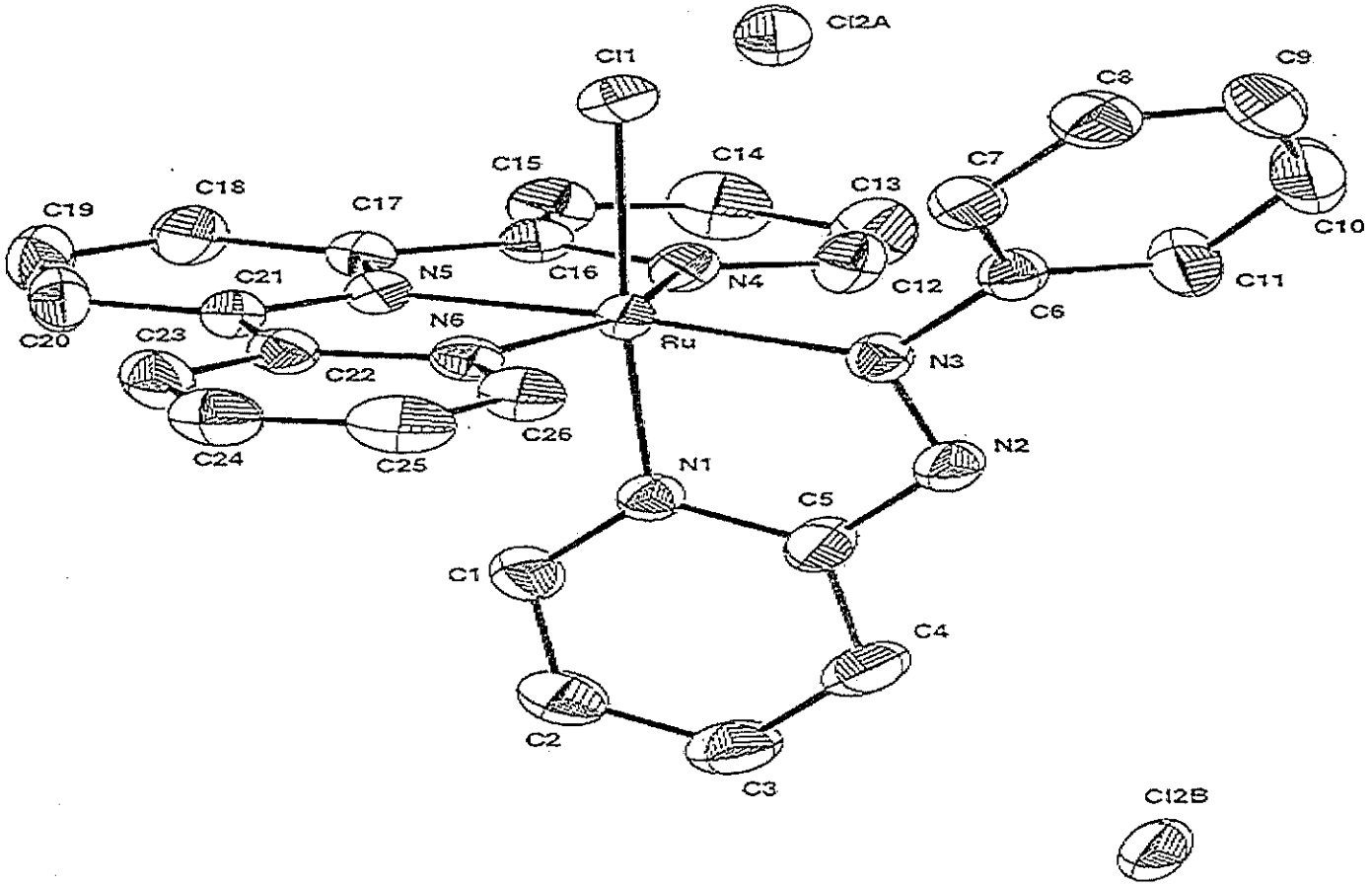

Figure 32 The structure of [Ru(tpy)(azpy)(Cl)]Cl. (H-atoms omitted)

Table 6 The crystallographic data for [Ru(tpy)(azpy)(Cl/I)](BF_4).

Identical code	runovos
Empirical formula	C26 H20 B Cl0.69 F4 I0.31 N6 Ru
Formula weight	668.16
Temperature	293(2) K
Wavelength	0.71073
Crystal system	monoclinic
Space group	P2(1)/n
Unit cell dimensions	a = 8.586(2) Å $\alpha = 90^\circ$
	b = 15.745(4) Å $\beta = 99.825(15)^\circ$
	c = 19.469(4) Å $\gamma = 90^\circ$
Volume	2593.4(10) $Å^3$
Z	4
Density (calculated)	1.711 mg/m^3
Absorption coefficient	1.102 mm^{-1}
F(000)	1325
Theta range for data collection	1.67 to 27.55
Index ranges	$-11 \leq h \leq 9, -14 \leq k \leq 20, -25 \leq l \leq 25$
Reflections collected	5977
Independent reflections	4362
Refinement method	Full-matrix least-squares on F^2
Data / restraints / parameters	5977 / 3 / 356
Goodness-of-fit observed	1.074
Final R indices [$I > 2\sigma(I)$]	R1 = 0.0348, wR2 = 0.0847
R indices (all data)	R1 = 0.0549, wR2 = 0.0898

Table 7 Non-hydrogen interatomic distances of [Ru(tpy)(azpy)(Cl/I)](BF_4).

Atom	Distance (Å)
Ru-N(4)	1.959(3)
Ru-N(2)	1.970(3)
Ru-N(6)	2.057(3)
Ru-N(1)	2.067(3)
Ru-N(3)	2.072(3)
Ru-Cl(1)	2.428(4)
Ru-I(1)	2.691(2)
N(1)-C(11)	1.359(4)
N(1)-C(15)	1.365(5)
N(2)-C(21)	1.349(4)
N(2)-C(25)	1.355(4)
N(3)-C(35)	1.339(4)
N(3)-C(31)	1.376(4)
N(4)-N(5)	1.298(3)
N(4)-C(41)	1.437(4)
N(5)-C(51)	1.383(4)
N(6)-C(55)	1.341(4)
N(6)-C(51)	1.363(4)
C(11)-C(12)	1.369(5)
C(12)-C(13)	1.347(6)
C(13)-C(14)	1.395(6)

Table 7 (continued)

Atom	Distance (Å)
C(14)-C(15)	1.391(5)
C(15)-C(21)	1.487(5)
C(21)-C(22)	1.378(5)
C(22)-C(23)	1.384(6)
C(23)-C(24)	1.388(6)
C(24)-C(25)	1.391(5)
C(25)-C(31)	1.467(5)
C(31)-C(32)	1.381(5)
C(32)-C(33)	1.374(5)
C(33)-C(34)	1.368(5)
C(34)-C(35)	1.388(5)
C(41)-C(42)	1.385(4)
C(41)-C(46)	1.388(5)
C(42)-C(43)	1.384(4)
C(43)-C(44)	1.372(5)
C(44)-C(45)	1.379(6)
C(45)-C(46)	1.391(5)
C(51)-C(52)	1.404(4)
C(52)-C(53)	1.378(5)
C(53)-C(54)	1.373(6)
C(54)-C(55)	1.384(5)

Table 7 (continued)

Atom	Distance (Å)
B(1)-F(1)	1.325(4)
B(1)-F(4)	1.325(4)
B(1)-F(3)	1.354(4)
B(1)-F(2)	1.378(4)

Table 8 Non-hydrogen interbond angles of [Ru(tpy)(azpy)(Cl/I)](BF_4).

Atom	Angle (°)
N(5)-Ru-N(3)	172.90(15)
N(5)-Ru-N(1)	97.20(15)
N(4)-Ru-N(2)	101.05(11)
N(4)-Ru-N(6)	76.58(11)
N(2)-Ru-N(6)	177.43(10)
N(4)-Ru-N(1)	95.82(11)
N(2)-Ru-N(1)	79.59(12)
N(6)-Ru-N(1)	99.56(11)
N(4)-Ru-N(3)	87.85(10)
N(2)-Ru-N(3)	79.49(11)
N(6)-Ru-N(3)	101.33(10)
N(1)-Ru-N(3)	159.08(11)
N(4)-Ru-Cl(1)	173.23(15)
N(2)-Ru-Cl(1)	85.07(14)
N(6)-Ru-Cl(1)	97.35(14)
N(1)-Ru-Cl(1)	88.1(2)
N(3)-Ru-Cl(1)	90.46(14)
N(4)-Ru-I(1)	169.09(10)
N(2)-Ru-I(1)	89.84(10)
N(6)-Ru-I(1)	92.54(10)
N(1)-Ru-I(1)	86.54(10)

Table 8 (continued)

Atom	Angle (°)
N(3)-Ru-I(1)	93.74(10)
C(11)-N(1)-C(15)	118.5(3)
C(11)-N(1)-Ru	127.7(2)
C(15)-N(1)-Ru	113.8(2)
C(21)-N(2)-C(25)	122.7(3)
C(21)-N(2)-Ru	118.7(2)
C(25)-N(2)-Ru	118.4(2)
C(35)-N(3)-C(31)	118.4(3)
C(35)-N(3)-Ru	127.5(2)
C(31)-N(3)-Ru	113.6(2)
N(5)-N(4)-C(41)	113.8(2)
N(5)-N(4)-Ru	122.1(2)
C(41)-N(4)-Ru	123.2(2)
N(4)-N(5)-C(51)	111.2(3)
C(55)-N(6)-C(51)	117.8(3)
C(55)-N(6)-Ru	130.1(2)
C(51)-N(6)-Ru	112.1(2)
N(1)-C(11)-C(12)	122.7(4)
C(13)-C(12)-C(11)	118.5(4)
C(12)-C(13)-C(14)	121.3(4)
C(15)-C(14)-C(13)	118.1(4)

Table 8 (continued)

Atom	Angle (°)
N(1)-C(15)-C(14)	120.7(4)
N(1)-C(15)-C(21)	114.7(3)
C(14)-C(15)-C(21)	124.5(4)
N(2)-C(21)-C(22)	120.1(4)
N(2)-C(21)-C(15)	112.8(3)
C(22)-C(21)-C(15)	127.1(4)
C(21)-C(22)-C(23)	118.3(4)
C(22)-C(23)-C(24)	121.3(3)
C(23)-C(24)-C(25)	118.6(4)
N(2)-C(25)-C(24)	119.0(3)
N(2)-C(25)-C(31)	113.7(3)
C(24)-C(25)-C(31)	127.3(3)
N(3)-C(31)-C(32)	120.8(3)
N(3)-C(31)-C(25)	114.4(3)
C(32)-C(31)-(C2)	124.7(3)
C(33)-C(32)-C(31)	119.4(3)
C(34)-C(33)-C(32)	120.4(3)
C(33)-C(34)-C(35)	118.3(4)
N(3)-C(35)-C(34)	122.6(3)
C(42)-C(41)-C(46)	120.6(3)
C(42)-C(41)-N(4)	119.8(3)

Table 8 (continued)

Atom	Angle (°)
C(46)-C(41)-N(4)	119.3(3)
C(43)-C(42)-C(41)	119.8(3)
C(44)-C(43)-C(42)	120.0(4)
C(43)-C(44)-C(45)	120.3(4)
C(44)-C(45)-C(46)	120.7(4)
C(41)-C(46)-C(45)	118.5(3)
N(6)-C(51)-N(5)	117.7(3)
N(6)-C(51)-C(52)	122.3(3)
N(5)-C(51)-C(52)	120.0(3)
C(53)-C(52)-C(51)	118.2(4)
C(54)-C(53)-C(52)	119.5(3)
C(53)-C(54)-C(55)	119.7(4)
N(6)-C(55)-C(54)	122.4(3)
F(1)-B(1)-F(4)	114.6(3)
F(1)-B(1)-F(3)	110.2(3)
F(4)-B(1)-F(3)	104.6(4)
F(1)-B(1)-F(2)	112.9(3)
F(4)-B(1)-F(2)	106.5(3)
F(3)-B(1)-F)(2)	107.4(3)

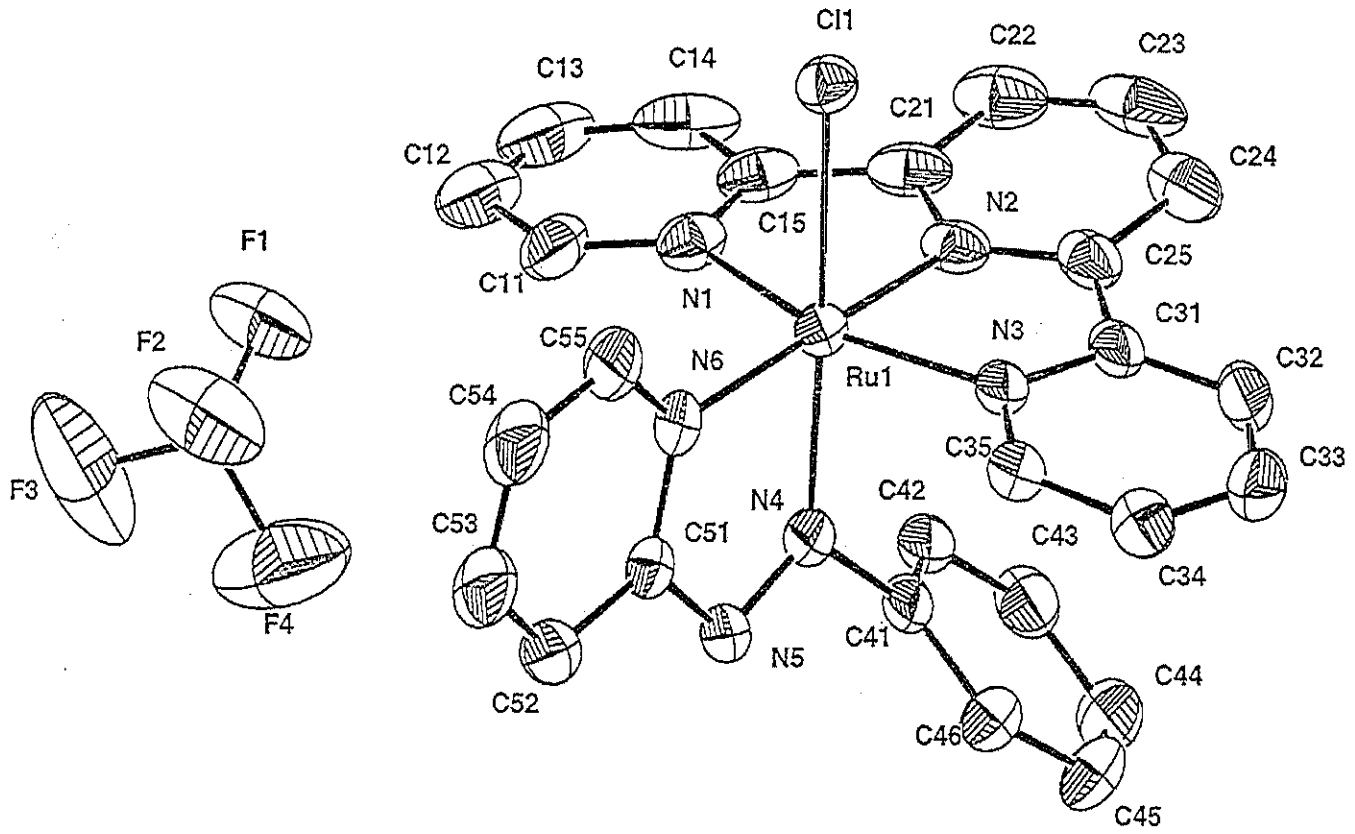

Figure 33 The structure of [Ru(tpy)(azpy)(Cl/I)](BF_4). (H-atoms omitted)

Table 9 The crystallographic data for $[Ru(tpy)(azpy)(NO_2)](BF_4)$.

Identical code	au07m
Empirical formula	$C_{26} H_{20} B F_4 N_7 O_2 Ru$
Formula weight	650.37
Temperature	296(2) K
Wavelength	0.71073
Crystal system	monoclinic
Space group	Pc
Unit cell dimensions	a = 9.2347(13) Å $\alpha = 90^\circ$
	b = 9.6814(13) Å $\beta = 95.948(2)^\circ$
	c = 14.588(2) Å $\gamma = 90^\circ$
Volume	1297.2(3) $Å^3$
Z	2
Density (calculated)	1.665 mg/m^3
Absorption coefficient	0.673 mm^{-1}
F(000)	652
Crystal size	0.36 x 0.30 x 0.15 mm
Theta range for data collection	2.10 to 28.32
Index ranges	$-10 \leq h \leq 12, -12 \leq k \leq 12, -18 \leq l \leq 18$
Reflections collected	7966
Independent reflections	4727 [R(int) = 0.0355]
Completeness to theta = 28.32	95.4 %
Refinement method	Full-matrix least-squares on F^2
Data / restraints / parameters	4727 / 2 / 370
Goodness-of-fit on F^2	0.656

Final R indices [I > 2σ(I)]	R1 = 0.0271, wR2 = 0.0740
R indices (all data)	R1 = 0.0292, wR2 = 0.0766
Absolute structure parameter	-0.06(2)
Largest diff. Peak and hole	0.437 and –0.374 e. $Å^3$

Table 10 Non-hydrogen interatomic distances of [Ru(tpy)(azpy)(NO_2)](BF_4).

Atom	Distance (Å)
Ru-N(5)	1.982(3)
Ru-N(2)	2.038(3)
Ru-N(6)	2.066(3)
Ru-N(4)	2.073(4)
Ru-N(1)	2.065(4)
Ru-N(3)	2.082(4)
O(1)-N(6)	1.238(4)
O(2)-N(6)	1.243(4)
N(1)-C(11)	1.349(5)
N(1)-C(12)	1.361(5)
N(2)-N(7)	1.262(5)
N(2)-C(22)	1.454(4)
N(3)-C(32)	1.338(6)
N(3)-C(31)	1.367(5)
N(4)-C(42)	1.342(6)
N(4)-C(41)	1.368(5)
N(5)-C(52)	1.345(5)
N(5)-C(51)	1.348(5)
N(7)-C(11)	1.399(5)
C(11)-C(13)	1.396(5)
C(12)-C(14)	1.384(5)

Table 10 (continued)

Atom	Distance (Å)
C(13)-C(15)	1.366(6)
C(14)-C(15)	1.380(6)
C(21)-C(25)	1.403(5)
C(21)-C(22)	1.395(5)
C(22)-C(23)	1.373(6)
C(23)-C(24)	1.396(6)
C(24)-C(26)	1.368(8)
C(25)-C(26)	1.358(8)
C(31)-C(34)	1.389(5)
C(31)-C(52)	1.467(5)
C(32)-C(33)	1.374(8)
C(33)-C(35)	1.376(9)
C(34)-C(35)	1.369(7)
C(41)-C(44)	1.385(5)
C(41)-C(51)	1.471(5)
C(42)-C(45)	1.363(7)
C(43)-C(45)	1.382(8)
C(43)-C(44)	1.393(7)
C(51)-C(55)	1.390(5)
C(52)-C(53)	1.400(5)
C(53)-C(54)	1.360(7)

Table 10 (continued)

Atom	Distance (Å)
C(54)-C(55)	1.392(6)
B-F(3)	1.343(6)
B-F(2)	1.344(6)
B-F(1)	1.361(7)
B-F(4)	1.369(9)

Table 11 Non-hydrogen interbond angles of $[Ru(tpy)(azpy)(NO_2)](BF_4)$.

Atom	Angle (°)
N(5)-Ru-N(2)	103.18(13)
N(5)-Ru-N(6)	84.99(15)
N(2)-Ru-N(6)	171.79(14)
N(5)-Ru-N(4)	79.31(14)
N(2)-Ru-N(4)	94.25(13)
N(6)-Ru-N(4)	87.92(12)
N(5)-Ru-N(1)	176.29(16)
N(2)-Ru-N(1)	75.43(13)
N(6)-Ru-N(1)	96.45(13)
N(4)-Ru-N(1)	97.30(15)
N(5)-Ru-N(3)	79.18(15)
N(2)-Ru-N(3)	92.57(14)
N(6)-Ru-N(3)	88.23(14)
N(4)-Ru-N(3)	158.40(12)
N(1)-Ru-N(3)	104.25(16)
C(11)-N(1)-C(12)	117.0(4)
C(11)-N(1)-Ru	113.5(2)
C(12)-N(1)-Ru	129.2(3)
N(7)-N(2)-C(22)	112.7(3)
N(7)-N(2)-Ru	120.6(3)
C(22)-N(2)-Ru	126.5(3)

Table 11 (continued)

Atom	Angle (°)
C(32)-N(3)-C(31)	118.4(4)
C(32)-N(3)-Ru	128.5(3)
C(31)-N(3)-Ru	112.9(3)
C(42)-N(4)-C(41)	118.5(4)
C(42)-N(4)-Ru	127.8(3)
C(41)-N94)-Ru	113.7(3)
C(52)-N(5)-C(51)	122.3(3)
C(52)-N(5)-Ru	118.9(3)
C(51)-N(5)-Ru	118.3(2)
O(2)-N(6)-O(1)	118.4(3)
O(2)-N(6)-Ru	119.7(2)
O(1)-N(6)-Ru	121.8(3)
N(2)-N(7)-C(11)	112.9(3)
N(1)-C(11)-C(13)	123.9(3)
N(1)-C(11)-N(7)	117.2(3)
C(13)-C(11)-N(7)	118.8(3)
C(14)-C(12)-N(1)	121.5(4)
C(15)-C(13)-C(11)	118.1(3)
C912)-C(14)-C(15)	120.4(4)
C(13)-C(15)-C(14)	119.2(3)
C(25)-C(21)-C(22)	117.3(4)

Table 11 (continued)

Atom	Angle (°)
C(23)-C(22)-C(21)	121.3(3)
C(23)-C(22)-N(2)	120.0(3)
C(21)-C(22)-N(2)	118.7(3)
C(22)-C(23)-C(24)	119.7(4)
C(23)-C(24)-C(26)	119.4(5)
C(26)-C(25)-C(21)	121.3(4)
C(25)-C(26)-C(24)	121.0(4)
N(3)-C(31)-C(34)	120.9(4)
N(3)-C(31)-C(52)	116.0(3)
C(34)-C(31)-C(52)	123.0(4)
N(3)-C(32)-C(33)	122.7(5)
C(32)-C(33)-C(35)	119.0(5)
C(35)-C(34)-C(31)	119.4(4)
C(34)-C(35)-C(33)	119.5(4)
C(44)-C(41)-N(4)	121.2(4)
C(44)-C(41)-C(51)	123.8(3)
N(4)-C(41)-C(51)	115.0(3)
N(4)-C(42)-C(45)	123.1(4)
C(45)-C(43)-C(44)	119.4(4)
C(41)-C(44)-C(43)	118.8(4)
C(42)-C(45)-C(43)	119.0(4)

Table 11 (continued)

Atom	Angle (°)
N(5)-C(51)-C(55)	120.0(4)
N(5)-C(51)-C(41)	113.5(3)
C(55)-C(51)-C(41)	126.5(3)
N(5)-C(52)-C(53)	119.2(4)
N(5)-C(52)-C(31)	112.9(3)
C(53)-C(52)-C(31)	127.8(3)
C(54)-C(53)-C(52)	119.1(4)
C(53)-C(54)-C(55)	121.3(4)
C(54)-C(55)-C(51)	118.0(4)
F(3)-B-F(2)	109.9(5)
F(3)-B-F(1)	110.7(5)
F(2)-B-F(1)	109.9(5)
F(3)-B-F(4)	108.7(6)
F(2)-B-F(4)	107.9(6)
F(1)-B-F(4)	109.8(5)

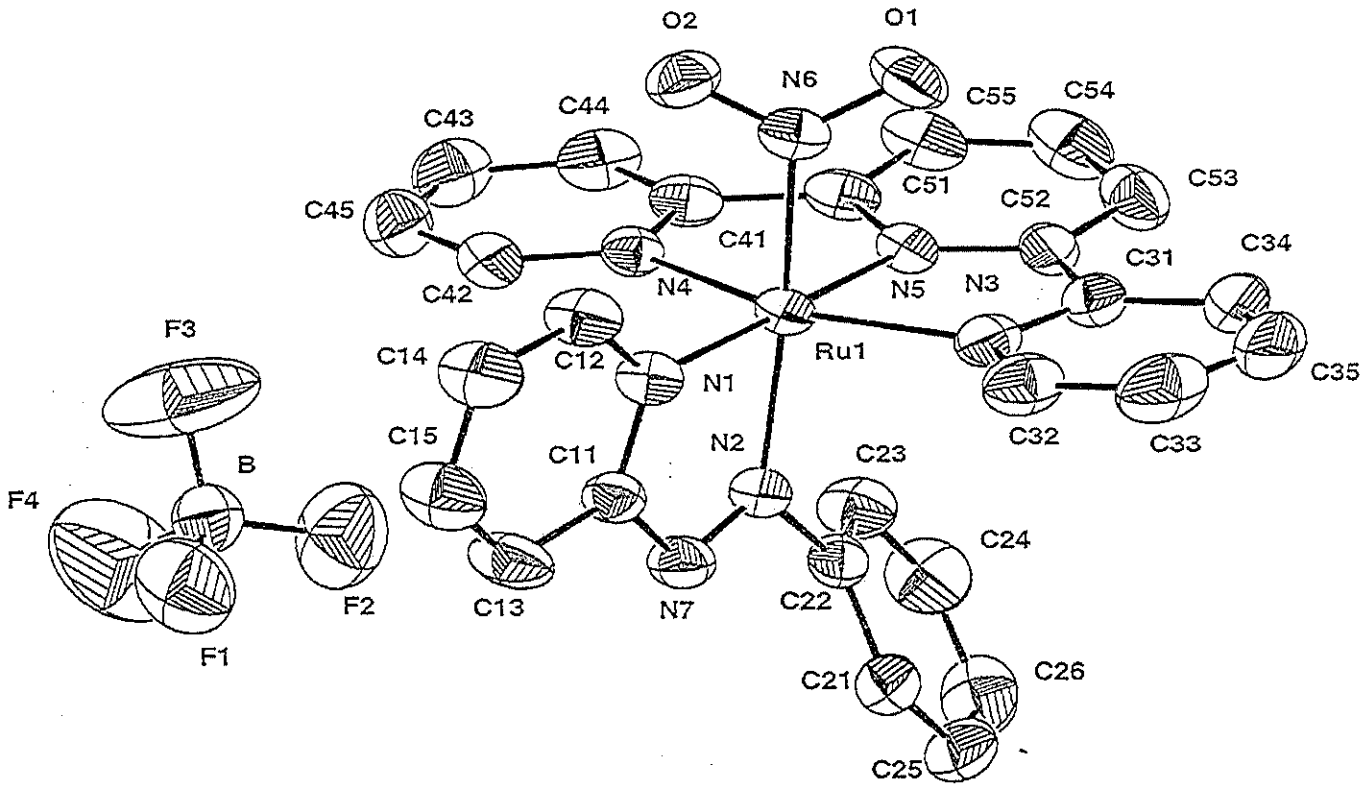

Figure 34 The structure of $[Ru(tpy)(azpy)(NO_2)](BF_4)$. (H-atoms omitted)

Table 12 The crystallographic data for [Ru(tpy)(azpy)(NCS)](BF$_4$).

Identical code	k57_00
Empirical formula	C28 H23 B F4 N7 O0.50 S Ru
Formula weight	685.47
Temperature	123(2) K
Wavelength	0.7107
Crystal description	Tabular
Crystal colour	Green
Crystal size	0.15 x 0.08 x 0.05 mm
Crystal system	monoclinic
Space group	P 21/c
Unit cell dimensions	a = 16.1481(2) Å $\alpha = 90^\circ$
	b = 11.0176(1) Å $\beta = 104.2683(5)^\circ$
	c = 16.4298(2) Å $\gamma = 90^\circ$
Volume	2832.91(5) Å^3
Z	4
Density (calculated)	1.607 mg/m^3
Absorption coefficient	0.688 mm^{-1}
F(000)	1380.00
Wavelength (Mo-Kα)	0.7107
2θ range ($^\circ$)	1.59 to 28.29
Index ranges	$-21 \leq h \leq 21$, $-14 \leq k \leq 14$, $-21 \leq l \leq 21$
Reflections collected	7331
Observed reflection [$I > 2\sigma(I)$]	4743 [R(int) = 0.04514]
Data / restraints / parameters	4743 / 0 / 382

Final R indices [$I > 2\sigma(I)$]	R1 = 0.0334, wR2 = 0.0413
R indices (all data)	R1 = 0.0681, wR2 = 0.0461

Table 13 Non-hydrogen interatomic distances of [Ru(tpy)(azpy)(NCS)](BF_4).

Atom	Distance (Å)
Ru-N(1)	2.048(3)
Ru-N(2)	2.075(3)
Ru-N(3)	1.981(3)
Ru-N(4)	2.082(3)
Ru-N(5)	2.005(3)
Ru-N(7)	2.051(3)
S(1)-C(1)	1.635(4)
F(1)-B(1)	1.395(5)
F(2)-B(1)	1.340(6)
F(3)-B(1)	1.385(6)
F(4)-B(1)	1.359(6)
O(1)-C(28)	1.46(1)
O(1)-C(28)	1.51(1)
N(1)-C(1)	1.155(4)
N(2)-C(2)	1.349(4)
N(2)-C(6)	1.370(5)
N(3)-C(7)	1.341(5)
N(3)-C(11)	1.358(4)
N(4)-C(12)	1.373(4)
N(4)-C(16)	1.337(5)
N(5)-N(6)	1.299(4)

Table 13 (continued)

Atom	Distance (Å)
N(5)-C(17)	1.447(5)
N(6)-C(23)	1.380(4)
N(7)-C(23)	1.359(4)
N(7)-C(27)	1.348(5)
C(2)-C(3)	1.379(6)
C(3)-C(4)	1.372(6)
C(4)-C(5)	1.389(5)
C(5)-C(6)	1.383(5)
C(6)-C(7)	1.485(5)
C(7)-C(8)	1.380(5)
C(8)-C(9)	1.403(5)
C(9)-C(10)	1.387(6)
C(10)-C(11)	1.388(5)
C(11)-C(12)	1.467(5)
C(12)-C(13)	1.387(5)
C(13)-C(14)	1.384(6)
C(14)-C(15)	1.379(6)
C(15)-C(16)	1.389(5)
C(17)-C(18)	1.381(6)
C(17)-C(22)	1.393(5)
C(18)-C(19)	1.390(5)

Table 13 (continued)

Atom	Distance (Å)
C(19)-C(20)	1.383(6)
C(20)-C(21)	1.379(6)
C(21)-C(22)	1.383(5)
C(23)-C(24)	1.391(5)
C(24)-C(25)	1.375(5)
C(25)-C(26)	1.390(5)
C(26)-C(27)	1.381(5)
C(28)-C(28)	1.38(2)
C(28)-C(29)	1.14(1)

Table 14 Non-hydrogen interbond angles of [Ru(tpy)(azpy)(NCS)](BF_4).

Atom	Angle (°)
N(1)-Ru-N(2)	86.1(1)
N(1)-Ru-N(3)	86.9(1)
N(1)-Ru-N(4)	87.0(1)
N(1)-Ru-N(5)	170.6(1)
N(1)-Ru-N(7)	94.5(1)
N(2)-Ru-N(3)	79.2(1)
N(2)-Ru-N(4)	157.6(1)
N(2)-Ru-N(5)	96.8(1)
N(2)-Ru-N(7)	100.4(1)
N(3)-Ru-N(4)	79.2(1)
N(3)-Ru-N(5)	102.4(1)
N(3)-Ru-N(7)	178.5(1)
N(4)-Ru-N(5)	93.5(1)
N(4)-Ru-N(7)	101.3(1)
N(5)-Ru-N(7)	76.2(1)
C(28)-O(1)-C(28)	55.5(7)
Ru-N(1)-C(1)	178.1(3)
Ru-N(2)-C(2)	127.9(3)
Ru-N(2)-C(6)	113.8(2)
C(2)-N(2)-C(6)	118.1(3)
Ru-N(3)-C(7)	119.1(2)

Table 14 (continued)

Atom	Angle (°)
Ru-N(3)-C(11)	118.7(3)
C(7)-N(3)-C(11)	121.9(3)
Ru-N(4)-C(12)	113.4(3)
Ru-N(4)-C(16)	127.8(3)
C(12)-N(4)-C(16)	118.6(3)
Ru-N(5)-N(6)	120.3(2)
Ru-N(5)-C(17)	128.7(2)
N(6)-N(5)-C(17)	110.8(3)
N(5)-N(6)-C(23)	112.6(3)
Ru-N(7)-C(23)	113.5(2)
Ru-N(7)-C(27)	128.6(2)
C(23)-N(7)-C(27)	117.9(3)
S(1)-C(1)-N(1)	179.5(4)
N(2)-C(2)-C(3)	122.0(4)
C(2)-C(3)-C(4)	119.9(3)
C(3)-C(4)-C(5)	119.2(4)
C(4)-C(5)-C(6)	118.8(4)
N(2)-C(6)-C(5)	121.9(3)
N(2)-C(6)-C(7)	114.8(3)
C(5)-C(6)-C(7)	123.3(4)
N(3)-C(7)-C(6)	113.2(3)

Table 14 (continued)

Atom	Angle (°)
N(3)-C(7)-C(8)	121.0(3)
C(6)-C(7)-C(8)	125.8(4)
C(7)-C(8)-C(9)	118.0(4)
C(8)-C(9)-C(10)	120.2(4)
C(9)-C(10)-C(11)	119.2(3)
N(3)-C(11)-C(10)	119.4(4)
N(3)-C(11)-C(12)	113.3(3)
C(10)-C(11)-C(12)	127.2(3)
N(4)-C(12)-C(11)	115.4(3)
N(4)-C(12)-C(13)	120.9(4)
C(11)-C(12)-C(13)	123.7(4)
C(12)-C(13)-C(14)	119.8(4)
C(13)-C(14)-C(15)	119.2(4)
C(14)-C(15)-C(16)	118.9(4)
N(4)-C(16)-C(15)	122.7(4)
N(5)-C(17)-C(18)	120.1(4)
N(5)-C(17)-C(22)	119.3(4)
C(18)-C(17)-C(22)	120.7(4)
C(17)-C(18)-C(19)	119.5(4)
C(18)-C(19)-C(20)	119.9(4)
C(19)-C(20)-C(21)	120.4(4)

Table 14 (continued)

Atom	Angle (°)
C(20)-C(21)-C(22)	120.3(4)
C(17)-C(22)-C(21)	119.3(4)
N(6)-C(23)-N(7)	117.4(3)
N(6)-C(23)-C(24)	119.8(3)
N(7)-C(23)-C(24)	122.7(3)
C(23)-C(24)-C(25)	118.6(3)
C(24)-C(25)-C(26)	119.1(3)
C(25)-C(26)-C(27)	119.6(4)
N(7)-C(27)-C(26)	122.0(3)
O(1)-C(28)-O(1)	124.5(7)
O(1)-C(28)-C(28)	63.8(8)
O(1)-C(28)-C(29)	120(1)
O(1)-C(28)-C(28)	60.7(8)
O(1)-C(28)-C(29)	116(1)
C(28)-C(28)-C(29)	175(1)
F(1)-B(1)-F(2)	106.4(5)
F(1)-B(1)-F(3)	107.4(4)
F(1)-B(1)-F(4)	106.5(4)
F(2)-B(1)-F(3)	109.8(4)
F(2)-B(1)-F(4)	115.7(5)
F(3)-B(1)-F(4)	110.5(4)

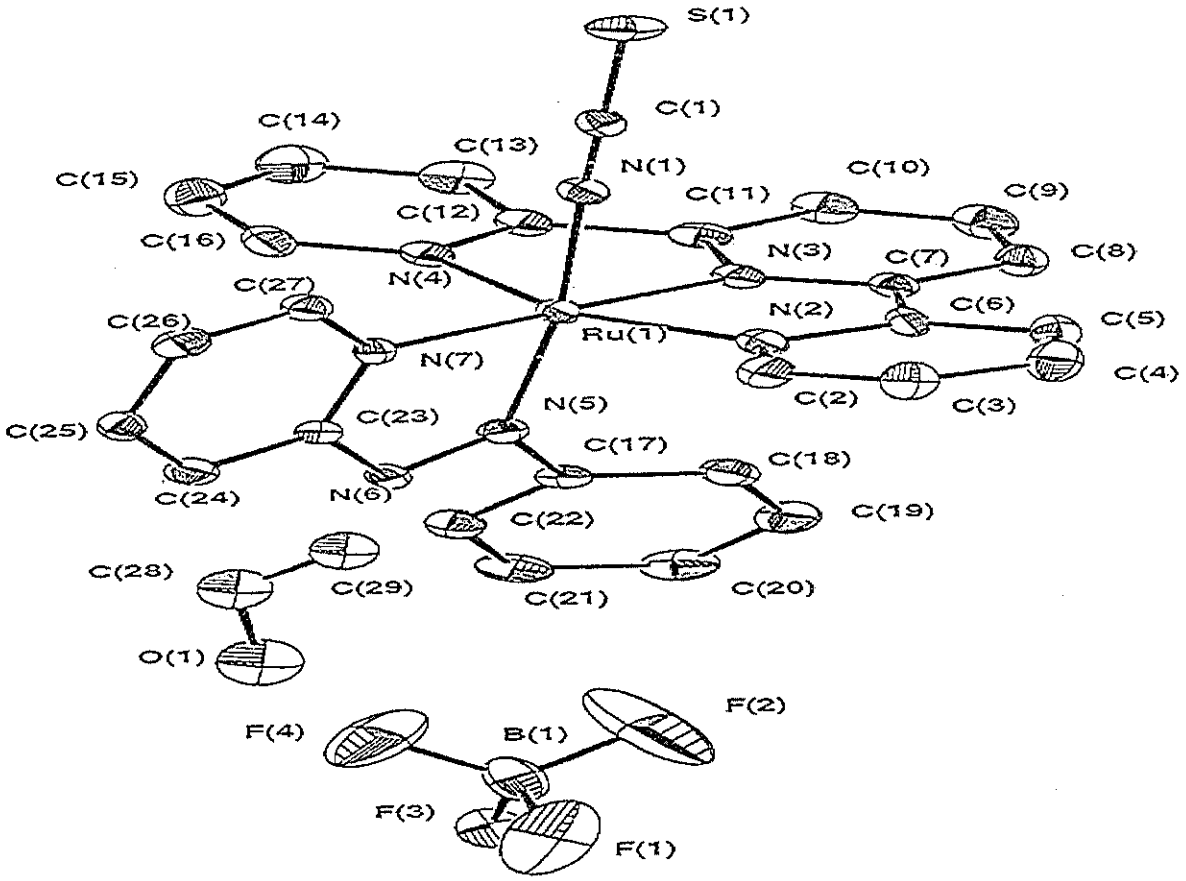

Figure 35 The structure of [Ru(tpy)(azpy)(NCS)](BF_4). (H-atoms omitted)

Chapter 4

DISCUSSION

4.1 Preparation of Complexes

The $Ru(tpy)Cl_3$ was used as a precursor to prepare ruthenium(II) complexes, $[Ru(tpy)(azpy)(X)]^+$ (where $X = Cl^-$, Br^-, I^-, NO_2^-, and NCS^-). All complexes in this series with general formula $[Ru(tpy)(azpy)(X)]^+$, were synthesized by following the general route shown in eq. (1)-(3). It is interesting to note that ruthenium(III) was reduced to ruthenium(II) in a synthetic reaction.

$$[Ru^{III}(tpy)Cl_3] + azpy \xrightarrow[LiCl\ ,\ reflux]{NEt_3\ ,\ EtOH/H_2O\ (3:1)} [Ru^{II}(tpy)(azpy)Cl]Cl \qquad (1)$$

Triethylamine, which also functions as a base, is the probable reductant (Pramanik, *et al.*, 1998). The role of LiCl is to prevent any possible dissociation of the coordinated chloride ion and thus to increase the yield of the desired product.

Each ruthenium complex containing various ligands other than Cl were prepared by replacement of chloride with other anions in the presence of Ag^+ as shown in eq. (2) and eq. (3) to give $[Ru(tpy)(azpy)(X)]^+$ complexes, where $X = Br^-$, I^-, NO_2^-, and NCS^-.

$$[Ru(tpy)(azpy)Cl]Cl \xrightarrow[AgNO_3\ ,\ reflux]{Acetone/H_2O} [Ru(tpy)(azpy)(OH_2)]^+ + AgCl \qquad (2)$$

$$[Ru(tpy)(azpy)(H_2O)]^+ \xrightarrow[EtOH/H_2O,\ reflux]{X = LiBr,\ NaI,\ NaNO_2 \text{ or } KSCN} [Ru(tpy)(azpy)(X)]^+ \quad (3)$$

Since azpy is an unsymmetrical bidentate ligand, then the $[Ru(tpy)(azpy)Cl]^+$ complexes may exist in two isomeric forms, 1 and 2, as shown in Figure 36. For all the complexes the structure of the 2 isomer is less steric hindrance than that in the 1 isomer, then the 2 isomer is obtained in much greater yield. Herein, this research is restricted only to the 2 isomer of each complex.

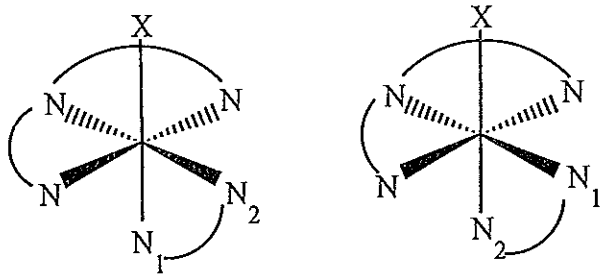

1 isomer 2 isomer

Figure 36 The two isomeric forms of $[Ru(tpy)(azpy)(X)]^+$.

This work is concentrated on the varying of monodentate ligands (X) because they have different properties. The halide ligands, Cl^-, Br^-, and I^-, when engaged in σ bonding to metal atoms, have electrons in essentially nonbonding $p\pi$ orbitals which can interact with appropriate $d\pi$ orbitals of the metal atoms. The t_{2g} orbitals of the metal can interact with t_{2g} ligand group orbitals constructed from the halide p orbitals to form π-bonding and antibonding molecular orbitals. Since halide are more electronegative than metal, the halide $p\pi$ orbitals lie at a lower energy than the corresponding metal $d\pi$ orbitals. Under these circumstances, the bonding π

molecular orbitals will resemble the halide orbitals more than that of the metal orbitals. Since the $p\pi$ orbitals on the halide ligands are filled, these electrons will fill the resultant molecular t_{2g} π orbitals. The electrons from the $d(t_{2g})$ orbitals of the metal are therefore in π antibonding orbital (π^*) at a higher energy than they would be if π bonding had not taken place. Since the level of the e_g^* orbitals is unaffected by the π interaction, 10 Dq is reduced as a result of the π bonding. It is felt that this is the source of the position of halides at the weak field extreme in the spectrochemical series (weaker than most σ-only ligands). However, π-acceptor ligand such as NCS^- and NO_2^- ligands have empty π^* orbitals lying low enough in energy that they can receive electron density from the metal. These orbitals have fairly low electronegativities (compared to the metal orbitals), and so the t_{2g} ligand group orbitals formed from them will lie at a higher energy than the corresponding metal orbitals. Although the t_{2g} orbitals of the complex are lowered and the t_{2g}^* raised in a manner almost identical to that of the previous case, the fact that the ligand t_{2g} orbitals are empty allows the t_{2g}^* orbitals to rise with no cost of energy while the bonding t_{2g} orbitals are stabilized. So that the quantity 10 Dq is increased. Pi bonding of this type thus can stabilize a complex by increasing the bond energy. In addition, the resulting t_{2g} π orbital is delocalized over both metal and ligands as opposed to being a nonbonding t_{2g} orbital localized on the metal, which would have been the case in the absense of π bonding. The former type of ligands with empty π^* orbitals (such as NO_2^- and NCS^-) can experience back-donation of electron density from the metal into the π^* orbitals. In this sense, the π^* orbitals play the role of acceptor orbitals. The latter type of ligands that have only occupied π orbitals (such as halide) are called π-donor ligands because their π electrons are delocalized onto the metal. (Huheey, *et al.*, 1993 : 420-423)

4.2 Electrospray Mass Spectroscopy

Electrospray mass spectroscopy is one important technique to study the structure and molecular weight of the complexes. Therefore, the proposed molecular weight of the complexes will be confirmed by this method.

The electrospray mass spectra of $[Ru(tpy)(azpy)(X)](BF_4)$ complexes, where X = Cl^-, Br^-, I^-, NO_2^-, NCS^-, and Cl^-/I^-, are shown in Figure 2-7. The important electrospray mass spectroscopic data of these complexes, with corresponding relative abundance are shown in Table 15.

Table 15 Electrospray mass spectroscopic data of $[Ru(tpy)(azpy)(X)](BF_4)$ complexes, where X = Cl^-, Br^-, I^-, NO_2^-, and NCS^-.

m/z	Stoichiometry	Equivalent species	Rel. Abun.
555	$[Ru(tpy)(azpy)(Cl)+2H]^+$	$(MCl+2H)^+$	90
553	$[Ru(tpy)(azpy)(Cl)]^+$	$(MCl)^+$	100
552	$[Ru(tpy)(azpy)(Cl)-H]^+$	$(MCl-H)^+$	50
551	$[Ru(tpy)(azpy)(Cl)-2H]^+$	$(MCl-2H)^+$	40
599	$[Ru(tpy)(azpy)(Br)]^+$	$(MBr)^+$	100
288	$[Ru(azpy)+4H]^+$	$(M-(tpy)(Br)+4H)^+$	68
645	$[Ru(tpy)(azpy)(I)]^+$	$(MI)^+$	100
288	$[Ru(azpy)+4H]^+$	$(M-(tpy)(I)+4H)^+$	23
566	$[Ru(tpy)(azpy)(NO_2)+2H]^+$	$(MNO_2+2H)^+$	53
564	$[Ru(tpy)(azpy)(NO_2)]^+$	$(MNO_2)^+$	100
563	$[Ru(tpy)(azpy)(NO_2)-H]^+$	$(MNO_2-H)^+$	40
562	$[Ru(tpy)(azpy)(NO_2)-2H]^+$	$(MNO_2-2H)^+$	34

m/z	Stoichiometry	Equivalent species	Rel. Abun.
578	$[Ru(tpy)(azpy)(NCS)+2H]^+$	$(MNCS+2H)^+$	53
576	$[Ru(tpy)(azpy)(NCS)]^+$	$(MNCS)^+$	100
575	$[Ru(tpy)(azpy)(NCS)-H]^+$	$(MNCS-H)^+$	48
573	$[Ru(tpy)(azpy)(NCS)-3H]^+$	$(MNCS-3H)^+$	32
647	$[Ru(tpy)(azpy)(I)+2H]^+$	$(MI+2H)^+$	50
645	$[Ru(tpy)(azpy)(I)]^+$	$(MI)^+$	100
643	$[Ru(tpy)(azpy)(I)-H]^+$	$(MI-H)^+$	47
642	$[Ru(tpy)(azpy)(I)-2H]^+$	$(MI-2H)^+$	35
555	$[Ru(tpy)(azpy)Cl+2H]^+$	$(MCl+2H)^+$	43
553	$[Ru(tpy)(azpy)Cl]^+$	$(MCl)^+$	60
551	$[Ru(tpy)(azpy)Cl-H]^+$	$(MCl-H)^+$	26
551	$[Ru(tpy)(azpy)Cl-2H]^+$	$(MCl-2H)^+$	17
102	$[Ru+H]^+$	$(Ru+H)^+$	57

M = {Ru(tpy)(azpy)X} , such as $(MCl)^+$ is $[Ru(tpy)(azpy)(Cl)]^+$.

The parent peak, which gives 100% relative abundance, is molecular weight of each complex. This data can be used to confirm the molecular structure and molecular weight of these complexes as expected.

The molecular weight of $[Ru(tpy)(azpy)(Cl)]^+$ is 553 g/mol and the electrospray mass spectrum shows the parent peak at $m/z = 553$. It means that the $m/z = 553$ was used to confirm the molecular weight of chloro complex. Electrospray mass spectra of $[Ru(tpy)(azpy)(Br)]^+$ and $[Ru(tpy)(azpy)(I)]^+$ exhibit two particularly peaks, the parent peaks at $m/z = 599$ for bromo complex and $m/z = 645$ for iodo complex, and another peak at $m/z = 288$, is attributed to the splitting of tpy and iodo/bromo ligands followed by protonation of four in the structure.

The electrospray mass spectrum of $[Ru(tpy)(azpy)(Cl/I)]^+$ mixed complex shows three intense peaks, the parent peaks at *m/z* = 553 for chloro complex , *m/z* = 645 for iodo complex, and *m/z* = 102 for protonated ruthenium. Results from electrospray mass spectrum of this mixed complex shows that it is mixed of 2 compounds, chloro and iodo complexes.

Besides the parent peak, other peaks are the protonated and deprotonated structure of complexes as described in Table 15.

4.3 UV-Visible Absorption Spectroscopy

UV-Visible absorption spectroscopy is the technique to study the electronic transitions of the ligands and complexes. In the UV region, the absorption spectra show very intense bands which belong to the electronic transitions of the azpy and tpy ligands. In the visible region, each complex exhibits intense band (log ε = 4.07 – 4.34), which referred to charge transfer transition. The log ε value in visible region greater than three, is assigned to charge transfer transition (Shriver, 1994 : 595-600). In this work, the complexes of $[Ru(tpy)(azpy)(X)](BF_4)$, where $X = Cl^-$, Br^-, I^-, NO_2^-, and NCS^-, display metal-to-ligand charge transfer transition, d(Ru) → π^*(azpy), because the π^* orbital of azpy ligand is lower than that in tpy ligand (Krause and Krause, 1980).

Electronic spectra of $[Ru(tpy)(azpy)(X)](BF_4)$ complexes, where $X = Cl^-$, Br^-, I^-, NO_2^-, and NCS^-, were recorded in 5 solvents, acetone, acetonitrile, methanol, *N,N*-dimethylformamide (DMF) and dimethylsulfoxide (DMSO), show similar intense absorption bands in visible region as shown in Figure 7 - 11 and Table 16.

The absorption spectra of azpy ligand in this series of solvents show intense bands at 314-318 nm (log $\varepsilon > 3$) in UV region which referred to $\pi \rightarrow \pi^*$ transition,

and the broad bands at 440-446 nm (log ε < 3) in visible region which belong to n → π^* transition.

The complexes exhibit characteristic d(Ru) → π^*(azpy) MLCT transitions, (λ_{max}) in the 506-520 nm range of visible spectrum, and ligand π → π^* stransitions in the UV region. In order to study the effect of solvent to the excited state π^* orbital of azpy ligand, the solvents have been varied. Absorption spectra show that the intense MLCT bands in visible region are not changed with the solvent (no solvent effect). Results from this study indicate that the excited state π^* orbital of azpy ligand is not sensitive to the polarity of solvent. These may also results from the solubility of complexes. Most of solvents, which have been used, are not much different in the polarity because of the limited solubility of these complexes.

Table 16 UV-Visible absorption spectroscopic data of $[Ru(tpy)(azpy)(X)](BF_4)$ complexes, where X = Cl^-, Br^-, I^-, NO_2^-, and NCS^-.

Complex	Solvent	λ_{max}, nm (log ε)	
		UV region	Visible region
$[Ru(tpy)(azpy)(Cl)](BF_4)$	DMF	274 (4.32), 316 (4.52)	512 (4.15)
	DMSO	274 (4.24), 286 (4.20), 318 (4.47)	512 (4.08)
	MeCN	204 (4.95), 272 (4.47), 314 (4.53)	510 (4.17)
	Acetone	210 (4.43), 328 (4.42)	512 (4.12)
	MeOH	206 (4.76), 272 (4.45), 314 (4.55)	506 (4.18)
$[Ru(tpy)(azpy)(Br)](BF_4)$	DMF	274 (4.42), 316 (4.42), 330 (4.38)	512 (4.07)
	DMSO	274 (4.45), 318 (4.46), 332 (4.43)	512 (4.10)
	MeCN	200 (4.82), 278 (5.14)	510 (4.14)
	Acetone	210 (4.38), 330 (4.51)	512 (4.22)
	MeOH	208 (4.75), 272 (4.49), 314 (4.49)	510 (4.13)
$[Ru(tpy)(azpy)(I)](BF_4)$	DMF	208 (4.79), 272 (4.55), 316 (4.55)	512 (4.19
	DMSO	262 (4.53), 276 (4.52), 318 (4.52)	520 (4.15)

Table 16 (continued)

Complex	Solvent	λ_{max}, nm (log ε)	
		UV region	Visible region
	MeCN	220 (4.76), 272 (4.52), 314 (4.52)	516 (4.17)
	Acetone	212 (4.42), 330(4.40)	518 (4.16)
	MeOH	220 (4.77), 272 (4.51), 314 (4.50)	518 (4.14)
[Ru(tpy)(azpy)(NO_2)](BF_4)	DMF	274 (4.21) , 318 (4.45) , 332 (4.45)	516 (4.06)
	DMSO	274 (4.31) , 318 (4.50) , 332 (4.50)	516 (4.07)
	MeCN	202 (4.82) , 270 (4.48) , 314 (4.49)	512 (4.10)
	Acetone	210 (4.52) , 330 (4.62)	514 (4.25)
	MeOH	206 (4.83) , 314 (4.57) , 330 (4.57)	510 (4.18)
[Ru(tpy)(azpy)(NCS)](BF_4)	DMF	276 (4.44) , 318 (4.51) , 334 (4.43)	512 (4.18)
	DMSO	276 (4.56) , 318 (4.48) , 334 (4.41)	512 (4.12)
	MeCN	202 (4.82) , 272 (4.47) , 314 (4.45)	510 (4.13)
	Acetone	210 (4.49) , 332 (4.26)	514 (4.21)
	MeOH	208 (4.93) , 272 (4.65) , 314 (4.67)	510 (4.34)

4.4 Infrared Spectroscopy

Infrared spectroscopy is also an important technique to study the molecular structure of the complexes, vibrational spectra in the region 4,000-400 cm^{-1}, can be used to determine the ligand geometry around a central metal atom. The vibrational spectra in the region 400-200 cm^{-1} referred to the vibrational frequencies of a central metal atom which coordinated to ligands (Ru-N and Ru-X).

Infrared spectra of azpy ligand and these complexes show many vibrations of different intensities below 1,600 cm^{-1}. The 2-substituted pyridine ring show C=N stretching vibration at 1,600 cm^{-1}. At 1,400 cm^{-1} is assigned to the C=C stretching vibration in monosubstituted benzene ring (Krause and Krause, 1980). The monosubstituted aromatic ring shows C-H out of plane bending ($\delta_{C\text{-}H}$ out of plane) at 690-710 and 730-770 cm^{-1}.

Furthermore, it is possible to use vibrational spectroscopy as a probe of more than molecular symmetry; in favourable cases the detailed molecular structure can be explored, such as, Krause reported that the N=N(azo) stretching modes of azpy can be use to be diagnostic of the coligand(AB) π-accepting behavior in $[Ru(azpy)_2(AB)]^{n+}$ (where AB = 2,2'-bipyridyl, 4,4'-bithiazole, 1,2-diaminoethane, 2,4-pentanedione anion and X_2 (X = NO_2^-, CN^-, Br^-, N_3^-, and thiourea)), which strong π-accepting coligands give the highest N=N(azo) stretching frequencies (Krause and Krause, 1982).

The infrared spectra of ruthenium(II) complexes, $[Ru(tpy)(azpy)(X)]^+$ (where X = Cl^-, Br^-, I^-, NO_2^- and NCS^-) were recorded. The N=N(azo) stretching modes of azpy in complexes occur in a spectral region (ca. 1,421-1,312 cm^{-1}) almost free from other features as shown in Table 18. The N=N(azo) stretching vibrations were varied with

the π-acceptor ability of the X ligand, this indicated that the N=N(azo) stretching frequencies acted as a π-bonding probe.

4.4.1 Infrared spectroscopy of 2-(phenylazo)pyridine, azpy.

Infrared spectrum of azpy is shown in Figure 13. Intense band at 1,421 cm^{-1} is assigned to the N=N(azo) stretching vibration ($\nu_{(N=N)}$). The intense band of C=N stretching mode in 2-substituted pyridine is at 1,581 cm^{-1}, and the C=C stretching mode in monosubstituted benzene appears at 1,464 cm^{-1}. The C-H out of plane bending in monosubstituted benzene is at 790 and 687 cm^{-1}. The results correspond to the previous work (Krause and Krause, 1980).

4.4.2 Infrared spectroscopy of [Ru(tpy)(azpy)(Cl)](Cl).

Infrared spectrum of [Ru(tpy)(azpy)(Cl)](Cl) is shown in Figure 14. The N=N (azo) vibrational frequency at 1,312 cm^{-1}, is shifted from free azpy ligand, ca. 109 cm^{-1}, because the π-back-bonding between azpy ligand and ruthenium(II) results in a decrease the vibrational energy of the N=N(azo) stretching mode. The strong band of Ru-Cl stretching mode is at 324 cm^{-1}. The Ru-N(azo) stretching mode of azpy and Ru-N(py) stretching vibration of tpy are at 380 and 355 cm^{-1}, respectively.

4.4.3 Infrared spectroscopy of [Ru(tpy)(azpy)(Br)](BF_4).

Infrared spectrum of [Ru(tpy)(azpy)(Br)](BF_4) is shown in Figure 15. Intense band at 1,316 cm^{-1} assigned to the N=N(azo) stretching vibration, is similar to that of the ruthenium(II) chloro complex. Broad intense vibrational frequency is observed at 1,080 cm^{-1} due to the presence of BF_4^- salt, then the Ru-N and Ru-X vibrational

frequencies in the region, 400-200 cm^{-1}, could not be observed because vibrational frequencies in this region are too complicated to be assigned.

4.4.4 Infrared spectroscopy of [Ru(tpy)(azpy)(I)](I).

Infrared spectrum of [Ru(tpy)(azpy)(I)](I) is shown in Figure 16. Intense band at 1,316 cm^{-1}, is attributed to the N=N(azo) stretching vibration, is similar to ruthenium (II) chloro complex. The Ru-N(azo) stretching vibration appears at 380 cm^{-1}. The other Ru-X and Ru-N stretching modes can not be observed clearly in this complex because they are too weak to be observed.

4.4.5 Infrared spectroscopy of [Ru(tpy)(azpy)(NCS)](BF_4).

Infrared spectrum of [Ru(tpy)(azpy)(NCS)](BF_4) is shown in Figure 17. Intense band at 1,331 cm^{-1}, is attributed to the N=N(azo) stretching frequencies, shifted from free azpy ligand about 90 cm^{-1}. The bonding modes of isothiocyanate ligand are three vibrationals mode, the C-N stretching [$\nu_{(C\equiv N)}$], the C-S stretching [$\nu_{(C\text{-}S)}$] and the N-C-S bending [$\delta_{(N\text{-}C\text{-}S)}$]. Sharp band at 2,108 cm^{-1} is assigned to the C≡N stretching vibrational and C-S stretching frequency appears at 822 cm^{-1} (medium). The N-C-S bending vibrational is not observed because it is too weak to be observed.

4.4.6 Infrared spectroscopy of [Ru(tpy)(azpy)(NO_2)](BF_4).

Infrared spectrum of [Ru(tpy)(azpy)(NO_2)](BF_4) is shown in Figure 18. Intense band at 1,356 cm^{-1}, is assigned to the N=N(azo) stretching frequencies, shifted from free azpy ligand about 65 cm^{-1}. The bonding mode of the nitro ligand are two vibrational modes, NO_2 assymetric stretching vibrational ($\nu_{as(N\text{-}O)}$) which appears at

1,327 cm^{-1} and the NO_2 symmetric stretching vibrational ($\nu_{s(N\text{-}O)}$) is at 1294 cm^{-1}. (Dovletoglou, *et al.*, 1996) However, the nitro ligand vibrational modes are not observed clearly in this complex because they were concealed by the N=N(azo) stretching vibration.

The summary of the infrared spectroscopic data are listed in Table 17.

Table 17 Summarized infrared spectroscopic data of azpy ligand and [Ru(tpy)(azpy)-(X)]$^+$, where X = Cl^-, Br^-, I^-, NO_2^- and NCS^-.

Complex	Wave number , cm^{-1}		
	$\nu_{(C=N)}$, $\nu_{(C=C)}$	$\nu_{(N=N)}$ azo	$\delta_{(C\text{-}H)}$ out of plane
$[Ru^{II}(tpy)(azpy)(Cl)]^+$	1600 , 1450	1312	773 , 699
$[Ru^{II}(tpy)(azpy)(Br)]^+$	1601 , 1450	1314	777 , 703
$[Ru^{II}(tpy)(azpy)(I)]^+$	1599 , 1448	1314	775 , 701
$[Ru^{II}(tpy)(azpy)(NCS)]^+$	1600 , 1450	1331	770 , 703
$[Ru^{II}(tpy)(azpy)(NO_2)]^+$	1602 , 1450	1356	770 , 699
Azpy	1581 , 1464	1421	790 , 687

As expected the N=N(azo) vibrational frequencies are varied with π-accepting behavior of X ligand. The N=N(azo) vibrational frequencies of the compounds are shifted from free azpy ligand, ca. 65-109 cm^{-1}. As the employed coligand, NO_2^- and NCS^-, are better π-acceptors than the halide ions, there is competition for the ruthenium t_{2g} electrons and less π back-donation to azpy, this gives rise to increase the azo bond order. Thus, with a very strong π-acid X ligand, the azo mode could approach the free ligand value. Ligands may be arranged in a series in the order of

their π-acceptor abilities as; NO_2^- > NCS^- > halide (Cl^-, Br^-, I^-). This order is corresponded to the order of their abilites to split d-orbital levels in spectrochemical series. The selected vibrational frequencies of $[Ru(tpy)(azpy)(X)]^+$ complexes are summarized in Table 18.

Table 18 Selected vibrational frequencies of azpy ligand and $[Ru(tpy)(azpy)(X)]^+$ complexes.

Compound	$\nu_{(N=N)}$, cm^{-1}
$[Ru(tpy)(azpy)(Cl)]^+$	1,312
$[Ru(tpy)(azpy)(Br)]^+$	1,314
$[Ru(tpy)(azpy)(I)]^+$	1,314
$[Ru(tpy)(azpy)(NCS)]^+$	1,331
$[Ru(tpy)(azpy)(NO_2)]^+$	1,356
Free azpy	1,421

4.5 Nuclear Magnetic Resonance Spectroscopy (^{1}H NMR)

NMR spectroscopy has developed to the point at which it is also important technique in chemistry to confirm molecular structure (the most important being X-ray diffraction). ^{1}H NMR spectroscopy is important technique to determine molecular structure because the different protons in the molecular structure will show the different chemical shifts. Furthermore, ^{1}H NMR spectra exhibit the proportionation of protons in each complex, and their chemical shifts are related to their position in

complexes. In addition, they show the number of protons in each peak corresponding to the formula structure.

The chemical shift of the pyridine ring is 8.50, 6.99, and 7.50 ppm for the proton in ortho-, meta- and para- position, respectively. The chemical shifts in 6.50-8.00 ppm range belong to the benzene ring. The ^{1}H NMR spectra of tpy, azpy ligand and [Ru(tpy)(azpy)(X)](BF_4) complexes, where X = Cl^-, Br^-, I^-, NCS^- and NO_2^-, are shown in Figure 19-25. The ^{1}H NMR spectroscopic data of these complexes are given in Table 19.

Table 19 ^{1}H NMR spectroscopic data of [Ru(tpy)(azpy)(X)](BF_4) complexes, where X = Cl^-, I^-, Br^-, NCS^- and NO_2^-.

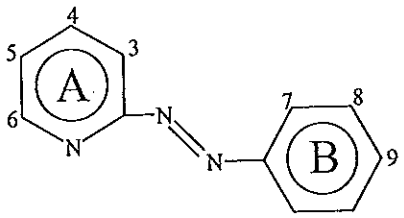

2-(Phenylazo)pyridine (azpy)

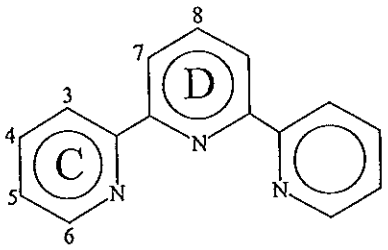

2,2':6',2"-Terpyridine (tpy)

Proton	Number of proton	Chemical shift, ppm				
		Ru-Cl	Ru-I	Ru-Br	Ru-NCS	Ru-NO_2
6A	1	9.75 (dd)	10.25 (dd)	9.93 (dd)	9.41 (dd)	9.60 (dd)
3A	1	8.86 (d)	8.93 (d)	8.87 (d)	8.92 (d)	8.94 (d)
6C	2	8.56 (d)	8.64 (d)	8.55 (d)	8.63 (d)	8.56 (d)
7D	2	8.58 (d)	8.62 (d)	(sharp)	(sharp)	8.58 (d)
5A	1	8.43 (dt)	8.45 (dt)	8.42 (dt)	8.50 (dt)	8.48 (dt)
8D	1	8.24 (t)	8.27 (t)	8.23 (t)	8.30 (t)	8.24 (t)

Proton	Number of proton	Chemical shift, ppm				
		Ru-Cl	Ru-I	Ru-Br	Ru-NCS	Ru-NO_2
4A	1	8.17 (t)	8.20 (t)	8.15 (t)	8.26 (t)	8.21 (m)
5C	2	8.13 (dt)	8.13 (dt)	8.11 (dt)	8.20 (dt)	8.15 (dt)
4C	2	7.48 (t)	7.47 (m)	7.47 (t)	7.54 (t)	7.51 (t)
3C	2	7.29 (d)		7.34 (d)	7.41 (d)	7.45 (d)
9B	1	7.22 (t)	7.24 (t)	7.22 (t)	7.23 (t)	7.25 (t)
8B	2	7.03 (t)	7.03 (t)	7.02 (t)	7.03 (t)	7.05 (t)
7B	2	6.19 (d)	6.12 (d)	6.16 (d)	6.17 (d)	6.24 (d)

Ru-X = $[Ru(tpy)(azpy)(X)](BF_4)$ where X = Cl^-, I^-, Br^-, NCS^- and NO_2^-.

d = doublet , t = triplet , m = multiplet , dd = doublet of doublet ,

dt = doublet of triplet

^1H NMR spectra of $[Ru(tpy)(azpy)(X)](BF_4)$ complexes (where X = Cl^-, I^-, Br^-, NCS^- and NO_2^-), recorded in d_6-DMSO, show many sharp resonances (Figure 19-25). In total thirteen resonances may be expected for twenty hydrogens present in the $[Ru(tpy)(azpy)(X)](BF_4)$ complexes, seven signals for nine hydrogens of azpy ligand and six signals for eleven hydrogens of tpy ligand, because a plane of symmetry splits the tpy ligand into two equal halves. Integration of the signals corresponds to twenty hydrogens present in the complex.

Table 19 shows the ^1H NMR spectroscopic data and the assignments for $[Ru(tpy)(azpy)(X)](BF_4)$. Major differences are expected in the chemical shifts to the proton of the azpy ligand. 6 position proton (H_{6A}) of ring A of azpy ligand in $[Ru(tpy)(azpy)(X)](BF_4)$ complexes shows a sole downfield chemical shift as a doublet of doublet. The proton H_{6A} of the azpy ligand lies in the outer ring currents

of tpy ligand from the molecular models and X-ray structural data. The resonance is shifted downfield accordingly.

Once again the doublet of doublet peak of H_{6A} in $[Ru(tpy)(azpy)(X)](BF_4)$ complexes shifted remarkably on changing ligand X in the Ru-X environment. H_{6A} peak also provides a valuable diagnostic tool for detecting changes in X at the Ru-X coordination site. Previous studies on the ^1H NMR spectra for $[Ru(bpy)_2(py)(X)]^{+/2+}$ complexes ($X = Cl^-, Br^-, NO^-, NO_2^-, OH_2$ etc.) showed that the chemical shift of 6 or 6' protons of the bipyridine appeared as an isolated doublet of doublet in the downfield in part of the spectrum, because it was out of ring current of the each bpy or py ligand (Dobson, *et al.*, 1989).

With the exception of the H_{6A} signal for $[Ru(tpy)(azpy)(X)](BF_4)$ complexes (where $X = Cl^-, Br^-, I^-$), the chemical shift to the particular proton uniformly increases as the ligand field strength increases upon substitution of the other ligand X for the chloride ligand in complexes. It is surprising that the chemical shift of the proton H_{6A} for $[Ru(tpy)(azpy)(halide)](BF_4)$ complexes move lower downfield than $[Ru(tpy)$-$(azpy)(X)](BF_4)$, where $X = NCS^-$, and NO_2^-, because the particular proton of the azpy moiety has short intramolecular contact with the adjacent electronegative Cl atom as was discovered in X-ray data. $[Ru(tpy)(azpy)(I)](BF_4)$ moves farthest downfield, because of the largest size of I atom in this series (halide). The summarized of H_{6A} NMR spectroscopic data are listed in Table 20. The large downfield shift is due to less effective shielding by electron density d_{xy} orbital (taking the z axis to lie along the Ru-X ($X = NCS^-, NO_2^-$)).

Table 20 Summarized H_{6A} NMR spectroscopic data of $[Ru(tpy)(azpy)(X)](BF_4)$ complexes, where X = Cl^-, I^-, Br^-, NCS^- and NO_2^-.

X	Chemical shift, ppm $[Ru(tpy)(azpy)(X)]^+$ (H_{6A})
Cl^-	9.75
Br^-	9.93
I^-	10.25
NCS^-	9.41
NO_2^-	9.60

4.6 Cyclic Voltammetry

Cyclic voltammetry is a method of studying the oxidation-reduction process in detail. This technique was quite useful and became popular in recent years for the measurement of redox potentials of compounds. The cyclic voltammetry is the important technique to study and to monitor the mechanism of the ligands and a central metal atom.

Cyclic voltammogram of $[Ru(tpy)(azpy)(X)](BF_4)$, where X = Cl^-, Br^-, I^-, NO_2^- and NCS^-, are shown in Figure 26-31. The summary of the cyclic voltammetric data are demonstrated in Table 21.

Table 21 Cyclic voltammetric data of $[Ru(tpy)(azpy)(X)](BF_4)$ complexes, where $X = Cl^-, Br^-, I^-, NO_2^-$ and NCS^-.

Compound	Scan rate , mV/s	Peak	E_{pa} , V	E_{pc} , V	ΔE_p , mV	$E_{1/2}$, V	Assignment
Azpy	50	1	0.119	0.050	69	0.085	Ferrocene
		2	-1.403	-1.541	138	-1.472	Azpy
Ru-Cl	50	1	0.971	0.903	68	0.937	Ru^{II}/Ru^{III}
		2	0.120	0.052	68	0.086	Ferrocene
		3	-0.976	-1.040	64	-1.008	Azpy
		4	-1.622	-1.699	77	-1.661	Azpy
Ru-Br	50	1	0.982	0.914	68	0.948	Ru^{II}/Ru^{III}
		2	0.119	0.052	67	0.086	Ferrocene
		3	-0.804	none	none	none	Impurity
		4	-0.958	-1.026	68	-0.992	Azpy
		5	-1.535	-1.670	135	-1.603	Azpy
Ru-I	50	1	0.901	none	none	none	Ru^{II}/Ru^{III}
		2	0.121	0.051	70	0.086	Ferrocene
		3	-0.803	none	none	none	Impurity
		4	-0.936	-1.008	72	-0.972	Azpy
		5	-1.531	-1.620	89	-1.576	Azpy
Ru-NCS	50	1	0.983	none	none	none	Ru^{II}/Ru^{III}
		2	0.120	0.049	71	0.085	Ferrocene
		3	-0.886	-0.952	66	-0.919	Azpy
		4	-1.572	-1.639	67	-1.606	Azpy

Compound	Scan rate , mV/s	Peak	E_{pa} , V	E_{pc} , V	ΔE_p , mV	$E_{1/2}$, V	Assignment
Ru-NO_2	50	1	1.152	1.054	98	1.103	Ru^{II}/Ru^{III}
		2	0.120	0.051	69	0.086	Ferrocene
		3	-0.882	-0.949	67	-0.916	Azpy
		4	-1.609	-1.684	75	-1.647	Azpy

Ru-X = $[Ru(tpy)(azpy)(X)](BF_4)$ where X = Cl^-, I^-, Br^-, NCS^- and NO_2^-.

E_{pa} = oxidation potential , E_{pc} = reduction potential

$\Delta E_p = E_{pa} - E_{pc}$, $E_{1/2} = (E_{pa}+E_{pc})/2$

The redox potentials of the various complexes were determined by cyclic voltammetry in acetonitrile solution. These complexes exhibit a single metal-centered oxidation in the positive potential region due to the Ru^{II}/Ru^{III} redox couple and successive ligand-based reduction in the negative potential region. These reductions correspond to the formation of radical anions as electrons are added to the π^* orbitals of the azpy and/or tpy ligands. It is noted that only oxidation peak was observed in $[Ru(tpy)(azpy)(X)](BF_4)$, where X = NCS^- or I^-, this could be result from the chemical reduction of Ru(III) → Ru(II) by other species, such as I^- or NCS^-. This occurred faster than the usual electrochemical reductions.

Goswami, Mukherjee and Chakravorty reported that the free 2-(phenylazo)-pyridine ligand, azpy, displays two quasireversible in the negative potential region, show that azpy accept two electrons in its lowest unoccupied molecular orbital (LUMO) which is primary azo in character (Goswami, *et al.*, 1983).

Polypyridine ligands were also capable of accepting electrons. However, it is well documented in literature that the azopyridine ligands are better acceptors and undergo easier reductions than the polypyridine ligands (Krause and Krause, 1980). Hence the first two reductions observed in the $[Ru(tpy)(azpy)(X)]^{+}$ complexes are assigned to azpy (eq. (4)-(5)) and the third one is assigned to tpy (eq. (6)), but the reduction potentials of tpy are too negative to be observed within the solvent window.

$$[Ru^{II}(tpy)(azpy)(X)]^{+} + e^{-} \rightleftharpoons [Ru^{II}(tpy)(azpy^{\cdot-})(X)]^{0} \quad (4)$$

$$[Ru^{II}(tpy)(azpy^{\cdot-})(X)]^{0} + e^{-} \rightleftharpoons [Ru^{II}(tpy)(azpy^{\cdot-\cdot-})(X)]^{-} \quad (5)$$

$$[Ru^{II}(tpy)(azpy^{\cdot-\cdot-})(X)]^{-} + e^{-} \rightleftharpoons [Ru^{II}(tpy^{\cdot-})(azpy^{\cdot-\cdot-})(X)]^{2-} \quad (6)$$

The Ru^{II}/Ru^{III} oxidation potential in these complexes is observed to be sensitive to the nature of X ligand. The geometries of these complexes show that the changing monodentate ligand (X) are *trans* to N-azo of the azpy ligand, while all three rings of the terpyridine are in a *cis* orientation with respect to X ligand. Thus, azpy should feel any electronic variations due to the changing ligand (X) to a greater extent than tpy. As the π-electron accepting nature of the monodentate increased, there is an increased stabilization of Ru(II) and an increased effective nuclear charge. The extent of π-back-donation to the other ligands is then reduced, thus decreasing the destabilization of their π^* orbitals.

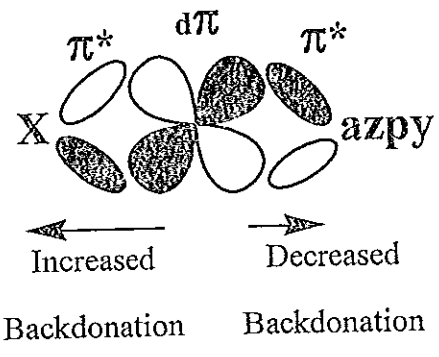

Therefore, as the π-accepting ability increases in the order ; halide < NCS^- < NO_2^-, the azpy 1st reduction potentials decrease to less negative potentials. The summarized reduction potentials data are listed in Table 22.

Table 22 Summarized reduction potentials data of $[Ru(tpy)(azpy)(X)](BF_4)$ complexes, where X = Cl^-, Br^-, I^-, NO_2^- and NCS^-.

Assigned	$E_{1/2}$, V				
	Ru-Cl	Ru-Br	Ru-I	Ru-NCS	Ru-NO_2
1st reduction	-1.008	-0.992	-0.972	-0.919	-0.916
2nd reduction	-1.661	-1.603	-1.576	-1.606	-1.647

Because of the differing σ-donating/π-accepting abilities of monodentate ligands (X), the ruthenium oxidative couple is shifted to the more positive potential with the stronger π-acceptor X ligands as shown in Table 23.

Table 23 Summarized Ru^{II}/Ru^{III} oxidation potential data of $[Ru(tpy)(azpy)(X)(BF_4)$ complexes, where X = Cl^-, Br^-, I^-, NO_2^- and NCS^-.

Assigned	$E_{1/2}$, V				
	Ru-Cl	Ru-Br	Ru-I	Ru-NCS	Ru-NO_2
Ru^{II}/Ru^{III} couple	0.937	0.948	-	-	1.103
E_{pa}	0.971	0.982	0.901	0.983	1.152

Thus, the Ru^{II}/Ru^{III} oxidation potential of $[Ru(tpy)(azpy)(NO_2)]^+$ complex is the highest in this series, it is indicated that NO_2^- ligand is the better π-acceptor than NCS^- and halide to stabilize Ru(II) center.

Comparison the Ru^{II}/Ru^{III} redox potential of $[Ru(tpy)(azpy)Cl]^+$ with a series of related complexes $[Ru(tpy)(N\text{-}N)Cl]^+$, where N-N = 2,2'-bipyridine (bpy) and 1,10-phenanthroline (phen), are listed in Table 24.

Table 24 Summarized Ru^{II}/Ru^{III} oxidation potential data of $[Ru(tpy)(N\text{-}N)(Cl)](BF_4)$ complexes, where N-N = 2,2'-bipyridine (bpy) and 1,10-phenanthroline (phen).

Compounds	Ru^{II}/Ru^{III} oxidation potential, V
$[Ru(tpy)(azpy)Cl]^+$	0.94
$[Ru(tpy)(bpy)Cl]^+$	0.83[a]
$[Ru(tpy)(phen)Cl]^+$	0.80[b]

[a] Vs Ag/AgCl. All measurements were made in a 0.1 M $(TBA)PF_6$ acetonitrile solution. (Reedijk, *et al.*, 1995)

[b] Vs Ag/AgCl. All measurements were made in a 0.1 M $(TBA)PF_6$ acetonitrile solution. (Thorp, *et al.*, 1993)

The following data give the Ru^{II}/Ru^{III} oxidation potential in the order: azpy > bpy > phen. It indicates that the azpy ligand is the most capable N-N donor ligand to stabilize Ru(II) center in this series. These data also support that the azpy ligand has the potential to be better π-acceptor than bpy and phen. The Ru^{II}/Ru^{III} oxidation

potential in $[Ru(tpy)(azpy)(Cl)]^+$ appears to be the highest among the $[Ru(tpy)(N\text{-}N)(Cl)]^+$ complexes reported so far.

4.7 Single Crystal X-ray Diffraction

Undoubtedly the most important method of structure determination at present time is the X-ray crystallographic technique. Results from X-ray crystallography give the valuable data, such as the metal-ligand bond distances and angles, and the geometry of the complexes.

To obtain crystals suitable for X-ray diffraction studies, solids were dissolved in organic solvent (acetone, ethanol) and H_2O. The crystallization of these complexes were obtained by slow solvent evaporation.

The crystal structures of 4 complexes, [Ru(tpy)(azpy)Cl]Cl (1), $[Ru(tpy)(azpy)(Cl/I)](BF_4)$ (2), $[Ru(tpy)(azpy)(NO_2)](BF_4)$ (3) and $[Ru(tpy)(azpy)(NCS)](BF_4)$ (4), were reported. There are two isomer, 1 and 2 isomer as shown in Figure 36, the crystals of (1) are 1 isomer and the crystals of (2)-(4) are 2 isomer. Here we describe structure results from the crystal of each complex.

4.7.1 [Ru(tpy)(azpy)Cl]Cl (1)

A perspective view of the complex is shown in Figure 32 and non-hydrogen interatomic distances and interbond angles are listed in Table 4-5. The coordination sphere around ruthenium is octahedron with varying Ru-N distances. The tpy ligand exhibits the meridional disposition of the planar ligands around the metal center with the central nitrogen (N5) *trans* to the chloro ligand. The Ru-N3(azo), 1.959(3) Å, is shorter than the Ru-N1(py) distance, 2.019(4) Å, which is attributed to the better

π-back-bonding ($d\pi(Ru) \rightarrow \pi^*(azo)$) power of the azo function. The azo N2-N3 distance, 1.300(5) Å, is longer than that in the free ligand, 1.248(4) Å (Panneerselvam, *et al.*, 2000).

4.7.2 [Ru(tpy)(azpy)(Cl/I)](BF_4) (2)

The perspective view of the structure of the complex is shown in Figure 33. Non-hydrogen interatomic distances and interbond angles are given in Table 7-8. The coordination sphere of this complex show asymmetric bond distances to the varying ligands. The azo nitrogen (N4) is coordinated closest to ruthenium, 1.959(3) Å. The azo nitrogen (N4) is coordinated to ruthenium *trans* to the coordinated Cl^-/I^-. It is interesting that crystals of this complex show two coordination spheres, one with 2.428(4) Å of Cl and the other with 2.691(2) Å of I. In azpy, the Ru-N4(azo) bond distance is shorter than the Ru-N6(py) bond distance, 2.057(3) Å, which is attributed to the better π-back-bonding of the azo function ($d\pi(Ru) \rightarrow \pi^*(azo)$). The azo N4-N5 distance, 1.298(3) Å, is longer than that in the free ligand.

4.7.3 [Ru(tpy)(azpy)(NO_2)](BF_4) (3)

The X-ray crystal structure of [Ru(tpy)(azpy)(NO_2)](BF_4) is shown in Figure 34. Non-hydrogen interatomic distances and interbond angles are listed in Table 10-11. The ruthenium(II) ion is coordinated to a tridentate tpy ligand, a bidentate azpy ligand and unidentate NO_2^- ligand, with Ru-N bond distance varying considerably from 1.982-2.082 Å (Table 10). The central nitrogen (N5) of tpy ligand is coordinated closest to ruthenium. The ruthenium is coordinated to azpy ligand with the azo nitrogen (N2) *trans* to the coordinated NO_2^-. In azpy, the Ru-N2(azo), 2.038(3) Å, is shorter than the Ru-N1(py), 2.065(4) Å, distance which is attributed to the better

π-back-bonding ($d\pi(Ru) \rightarrow \pi^*(azo)$) power of the azo function. The azo N2-N7 distance, 1.262(5) Å, is longer than that in the uncoordinated ligand.

4.7.4 $[Ru(tpy)(azpy)(NCS)](BF_4)$ (4)

The X-ray structure of the $[Ru(tpy)(azpy)(NCS)](BF_4)$ complex is shown in Figure 35. Non-hydrogen interatomic distances and interbond angles are given in Table 13-14. The coordination sphere of this complex shows asymmetric bond distances to varying ligands. Most noticeable is the short Ru-N distance to the central nitrogen of the tpy ligand, 1.981(3) Å. The azpy ligand is bound to ruthenium with the azo nitrogen (N5) *trans* to the coordinated NCS^-. The Ru-N(azo) and N5-N6(azo) is similar to the X-ray structure of $[Ru(tpy)(azpy(Cl/I)](BF_4)$ and $[Ru(tpy)(azpy)-(NO_2)](BF_4)$ complexes mentioned above.

In the case of **2** isomer, it is interesting that the Ru-N(azo) bond distance is varied with the nature of X ligand, the better π-acceptor X ligand result in elongation of Ru-N(azo) bond distance, in series; $NO_2^- > NCS^- > Cl^-/I^-$. The summarized selected bond distances of three of **2** isomer are given in Table 25. Because the NO_2^- ligand is bound to ruthenium with better π-back-bonding than NCS^- and Cl^-/I^-, the Ru-N(azo) distance of nitro complex is the longest in this series.

Table 25 Selected bond distances of $[Ru(tpy)(azpy)(X)]^{+}$, where X = Cl^{-}, Cl^{-}/I^{-}, NO_2^{-} and NCS^{-}.

Complex	Bond distance , Å						
	N=N	Ru-X	Ru-N(1)	Ru-N(2)	Ru-N(3)	Ru-N(4)	Ru-N(5)
$[Ru(tpy)(azpy)(Cl)]Cl$ [a]	1.300(5)	2.4107(12)	1.999(4)	2.019(4)	2.073(4)	1.990(4)	2.076(4)
$[Ru(tpy)(azpy)(Cl/I)](BF_4)$ [b]	1.298(3)	2.428(4)/2.691(2)	1.959(3)	2.057(3)	2.072(3)	1.970(3)	2.067(3)
$[Ru(tpy)(azpy)(NO_2)](BF_4)$ [b]	1.262(5)	2.066(3)	2.038(3)	2.065(4)	2.073(4)	1.982(3)	2.082(4)
$[Ru(tpy)(azpy)(NCS)](BF_4)$ [b]	1.299(4)	2.048(3)	2.005(3)	2.051(3)	2.075(3)	1.981(3)	2.082(3)

[a] 1 isomer

[b] 2 isomer

Ru-N(1) = Ru-N(azo) (azpy)

Ru-N(2) = Ru-N(py) (azpy)

Ru-N(3) = Ru-N(py) (tpy (right))

Ru-N(4) = Ru-N(py) (tpy (central))

Ru-N(5) = Ru-N(py) (tpy (left))

Chapter 5

CONCLUSION

Five ruthenium(II) complexes, $[Ru(tpy)(azpy)(X)]^+$ (X = Cl^-, Br^-, I^-, NO_2^- and NCS^-), were prepared and characterized by spectroscopic and electrochemical methods. Since azpy is an asymmetric ligand, then there are two possible isomers. In 1 isomer, the N(py) is *trans* to the X ligand. In 2 isomer, the N(azo) is *trans* to the X ligand. Some of them were studied by X-ray diffraction. Results from the X-ray structure confirm these two configuration of complexes. Because the 1 isomer give lower yield, the characterization with spectroscopic and electrochemistry techniques are then restricted only to the 2 isomer of each complex. The chemistries of $[Ru(tpy)(azpy)(X)]^+$ complexes are varied with the nature of X ligand and confirmed by spectroscopic and electrochemical methods. Visible spectra of the complexes give similar intense d(Ru) → π*(ligand) MLCT bands and show no solvent effect. Infrared spectra show the azpy azo stretching mode is sensitive to the nature of X ligand and this can be diagnostic of the X ligand. The X ligand with π-accepting behavior results in increasing the azpy $\nu_{(N=N)}$ vibration frequencies. The highest N=N(azo) stretching vibration frequency belongs to $[Ru(tpy)(azpy)(NO_2)]^+$ complex. The cyclic voltammogram show that the NO_2^- ligand is the greatest coligand in this series to stabilize ruthenium(II) center, because the $[Ru(tpy)(azpy)(NO_2)]^+$ complex give the highest Ru^{II}/Ru^{III} oxidation potential. Then, ligands may be arranged in a series of their π-acceptor abilities as; NO_2^- > NCS^- > halide (Cl^-, Br^-, I^-). Results from this study are consistent with the ligand field strength of ligand (X) in the spectrochemical series, which the ligand field of NO_2^- ligand is the strongest.

A knowledge from this work is one of the fundamental aims of chemistry and is essential for a proper understanding of the physical and chemical properties of the materials.

Bibliography

Bardwell, D. A., Cargill-Thompson, A. M. W., Jeffery, J. C., McCleverty, J. A. and Ward, M. D. 1996. "New tricks for an old ligand: cyclometallated and didentate co-ordination of 2,2':6',2"-terpyridine to ruthenium(II)" J. Chem. Soc., Dalton Trans. (1996), 873-878.

Berger, R. M., McMillin, D. R. 1988. "Localized States in Reduced and Excited-State Ruthenium(II) Terpyridyls" Inorg. Chem. 27(1988), 4245-4249.

Boelrijk, A. E. M., Jorna, A. M. J. and Reedijk, J. 1995. "Oxidation of octyl α-D-glucuronic acid, catalyzed by several ruthenium complexes, containing a 2-(phenyl)azopyridine or a 2-(nitrophenyl)azopyridine ligand" J. Mol. Catal. A 103(1995), 73-85.

Coe, B. J., Thompson, D. W., Culbertson, C. T., Schoonover, J. R. and Meyer, T. J. 1995. "Synthesis and Photophysical Properties of Mono(2,2',2"-terpyridine) Complexes of Ruthenium(II)" Inorg. Chem. 34(1995), 3385-3395.

Dobson, J. C., Helms, J. H., Doppelt, P., Sullivan, P. B., Hatfield, W. E. and Meyer, T. J. 1989 "Electronic Structure of the Oxidation Catalyst *cis*-$[Ru^{IV}(bpy)_2(py)(O)](ClO_4)_2$" Inorg. Chem. 28(1989), 2200-2204.

Dovletoglou, A., Adeyemi S. A. and Meyer, T. J. 1996. "Coordination and Redox Chemistry of Substituted-Polypyridyl Complexes of Ruthenium" Inorg. Chem. 35(1996), 4120-4127.

Gerli, A., Reedijk, J., Lakin, M. T. and Spek, A. L. 1995. "Redox Properties and Electrocatalytic Activity of the Oxo/Aqua System $[Ru(terpy)(bpz)(O)]^{2+}$/$[Ru(terpy)(bpz)(H_2O)]^{2+}$. X-ray Crystal Structure of $[Ru(terpy)(bpz)Cl]PF_6 \bullet$ MeCN (terpy = 2,2',2"-Terpyridine; bpz = 2,2'-Bipyrazine)" Inorg. Chem. 34(1995), 1836-1843.

Goswami, S., Chakravarty, A. R. and Chakravorty, A. 1983. "Chemistry of Ruthenium. 7. Aquo Complexes of Isomeric Bis[2-(phenylazo)pyridine]-ruthenium(II) Moieties and Their Reactions: Solvolysis, Protic Equilibria, and Electrochemistry" Inorg. Chem. 22(1983), 602-609.

Goswami, S., Mukherjee, R. and Chakravorty, A. 1983. "Chemistry of Ruthenium. 12.[1] Reactions of Bidentate Ligands with Diaquabis[2-(arylazo)pyridine]-ruthenium(II) Cation. Stereoretentive Synthesis of Tris Chelates and Their Characterization: Metal Oxidation, Ligand Reduction, and Spectroelectrochemical Correlation" Inorg. Chem. 22(1983), 2825-2832.

Goswami, S., Chakravarty, A. R. and Chakravorty, A. 1982. "Chemistry of Ruthenium. 5.[1] Reaction of *trans*-Dihalobis[2-(phenylazo)pyridine] ruthenium(II) with Tertiary Phosphines: Chemical, Spectroelectrochemical, and Mechanistic Characterization of Geometrically Isomerized Substitution Products" Inorg. Chem. 21(1982), 2737-2742.

Grover, N., Welch, T. W., Fairley, T. A., Cory, M. and Thorp, H. H. 1994. "Covalent Binding of Aquaruthenium Complexes to DNA" Inorg. Chem. 33(1994), 3544-3548.

Grover, N. and Thorp, H. H. 1994. "Efficient Electrocatalytic and Stoichiometric Oxidative Cleavage of DNA by Oxoruthenium(IV)" J. Am. Chem. Soc. 113 (1991), 7030-7031.

Gulyas, P. T., Hambley, T. W. and Lay, P. A. 1996. "The Crystal Structure of (2,2'-bipyridine)(pyrazine)(2,2';6',2"-terpyridine)ruthenium(II) Hexafluorophosphate" Aust. J. Chem. 49(1996), 527-532.

Gupta, N., Grover, N., Neyhart, G. A., Singh, P. and Thorp, H. H. 1993. "Synthesis and Properties of New DNA Cleavage Agents Based on Oxoruthenium-(IV)" Inorg. Chem. 32(1993), 310-316.

Hecker, C. R., Fanwick, P. E. and McMillin, D. R. 1991. "Evidence for Dissociative Photosubstitution Reactions of $[Ru(trpy)(bpy)(NCCH_3)]^{2+}$. Crystal and Molecular Structure of $[Ru(trpy)(bpy)(py)](PF_6)_2 \cdot (CH_3)_2CO$ " Inorg. Chem. 30(1991), 659-666.

Huheey, E. J., Keiter, E. A. and Keiter, R. L. 1993. Inorganic Chemistry : Principle of Structure and Reactivity. 4th ed., New York : HarperCollins College Publishers.

Krause, R. A. and Krause K. 1982. "Chemistry of Bipyridyl-like Ligands. 2 Mixed Complexes of Ruthenium(II) with 2-(phenylazo)pyridine; A new π-Bonding Probe[1]", Inorg. Chem. 21(1982), 1714-1720.

Krause, R. A. and Krause K. 1980. "Chemistry of Bipyridyl-like Ligands. Isomeric Complexes of Ruthenium(II) with 2-(phenylazo)pyridine", Inorg. Chem. 19(1980), 2600-2603.

Nazeeruddin, M. K., Kay, A., Rodicio, I., Humphry-Baker, R., Muller, E., Liska, P., Vlachopoulos, N. and Gratzel, M. 1993. "Conversion of Light to Electricity by *cis*-X_2Bis(2,2'-bipyridyl-4,4'-dicarboxylate)ruthenium(II) Charge-Transfer Sensitizers (X= Cl^-, Br^-, I^-, CN^-, and SCN^-) on Nanocrystalline TiO_2 electrodes" J. Am. Chem. Soc. 115(1993), 6382-6390.

Panneerselvam, K., Hansongnern, K., Rattanawit, N., Liao, F-L. and Lu, T-H. 2000. "Crystal Structure of the [Protonated 2-(Phenylazo)pyridine and Protonated 2-(4-hydroxyphenylazo)pyridine (3:1)]tetrafluoroborate", Anal. Sci. 16 (2000), 1107-1108.

Pramanik, N. C., Pramanik, K., Ghosh, P. and Bhattacharya, S. 1998. "Chemistry of $[Ru(tpy)(pap)(L')]^{n+}$ (tpy = 2,2',6',2"-terpyridine; pap = 2-(phenylazo)pyridine ; L' = Cl^-, H_2O, CH_3CN, 4-picoline, N_3^- ; n = 1,2). X-ray crystal structure of $[Ru(tpy)(pap)(CH_3CN)](ClO_4)_2$ and catalytic oxidation of water to dioxygen by $[Ru(tpy)(pap)(H_2O)]^{2+}$" Polyhedron 17(1998), 1525-1534.

Ramussen, S. C., Ronco, S. E., Mlsna, D. A., Billadeau, M. A., Pennington, W. T., Kolis, J. W. and Petersen, J. D. 1995. "Ground- and Excited-State Properties of Ruthenium(II) Complexes Containing Tridentate Azine Ligands, Ru(tpy)-(bpy)L^{2+} , Where L Is a Polymerizable Acetylene" Inorg. Chem. 34 (1995), 821-829.

Seok, W. K., Moon, S. W. and Kim, M. Y. 1998. "NMR Study on Ru(II) Complexes Containing 2,2':6',2"-terpyridine" Bull. Korean Chem. Soc. 19(1998), 1207-1210.

Shriver, D. F., Atkins, P. W. and Langford, C. H. 1994. Inorganic Chemistry. 2nd ed., Oxford : Oxford University Press.

Sullivan, P. B., Calvert, J. M. and Meyer, T. J. 1980. "Cis-Trans Isomerism in (trpy)-(PPh_3)$RuCl_2$. Comparison between the Chemical and Physical Properties of a Cis-Trans Isomeric Pair" Inorg. Chem. 19(1980), 1404-1407.

Takeuchi, K. J., Thompson, M. S., Pipes, D. W. and Meyer, T. J. 1984. "Redox and Spectral Properties of Monooxo Polypyridyl Complexes of Ruthenium and Osmium in Aqueous Media" Inorg. Chem. 23(1984), 1845-1851.

Thummel, R. and Jahng, Y. 1986. "Polyaza Cavity-Shaped Molecules. 9. Ruthenium-(II) Complexes of Annelated Derivatives of 2,2':6',2"-terpyridine and Related Systems: Synthesis, Properties, and Structure" Inorg. Chem. 25(1986), 2527-2534.

Tokel-Takvoryan, N. E., Hemingway, R. E. and Bard, A. J. 1973. " Electrogenerated Chemiluminescence. XIII. Electrochemical and Electrogenerated Chemiluminescence Studies of Ruthenium Chelates " J. Am. Chem. Soc. 95(1973), 6582-6589.

Vogler, L. M., Jones, S. W., Jensen, G. E., Brewer, G. R. and Brewer, K. J. 1996. "Comparing the Spectroscopic and Electrochemical Properties of Ruthenium and Osmium Complexes of the Tridentate Polyazine Ligands 2,2':6',2"-terpyridine and 2,3,5,6-tetrakis(2-pyridyl)pyrazine" Inorg. Chim. Acta. 250 (1996), 155-162.

Appendix

Appendix A

Electrochemical cell

Electrochemical experiments were performed using a CS-2000 (Cypress). A standard three-electrode configuration was used, with platinum wire working , platinum gauze counter and a $Ag/AgNO_3$ reference electrode. Electrochemical measurements were done in CH_3CN and 10 mM tetra-n-butylammonium-hexafluorophosphate ($[NBu_4]PF_6$) was used as the supporting electrolyte. Ferrocene was added at the end of each experiment as an internal standard; all potentials are quoted vs the ferrocene/ferrocenium couple (Fc/Fc^+). The solvent was used as receive. N_2 was bubbled through the solutions prior to measurement. The electrochemical cell is shown in Figure 37.

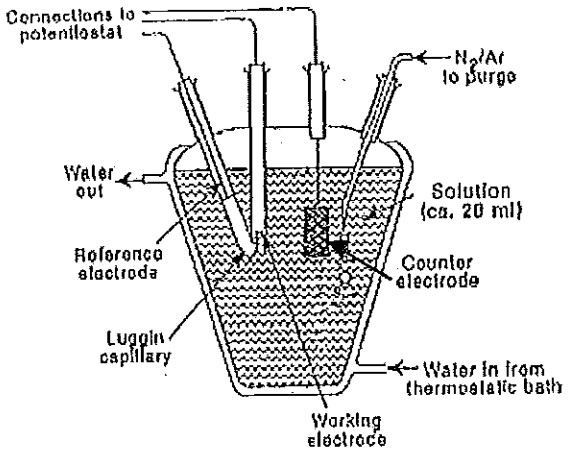

Figure 37 Schematic diagram of a general electrochemical cell.

Vitae

Name Miss Uraiwan Saeteaw

Birth date 12 March 1975

Educational Attainment

Degree	Name of Institution	Year of Graduation
Bachelor of Science (Chemistry)	Prince of Songkla University	1996

Scholarship Awards during Enrolment

The scholarship of Ministry of University Affairs, the Royal Thai Government. (June 1999 to May 2000)

Postgraduate Education and Research Program in Chemistry. (June 2000 to October 2000)

Publication from Master Thesis

Hansongnern, K., Saeteaw, U., Mostafa, G., Jiang, Y-C and Lu, T-H. 2001 . "Crystal Structure of Chloro(2,2':6',2"-terpyridine)(2-(phenyazo)pyridine)ruthenium(II) Chloride" Anal. Sci. 17(2001), 683-684.